UNIVERSIDAD COMPLUTENSE DE MADRID

FACULTAD DE CIENCIAS ECONÓMICAS Y EMPRESARIALES

Departamento de Fundamentos del Análisis Económico II (Economía Cuantitativa)

VALUATION OF DERIVATIVE ASSETS UNDER CYCLICAL MEAN-REVERSION PROCESSES FOR SPOT PRICES

MEMORIA PARA OPTAR AL GRADO DE DOCTOR
PRESENTADA POR

Federico Daniel Platania

Bajo la dirección de los doctores

Alfonso Novales Cinca
Manuel Moreno Fuentes

MADRID, 2013

UNIVERSIDAD COMPLUTENSE
MADRID

Facultad de Ciencias Económicas y Empresariales

Departamento de Economía Cuantitativa

Valuation of derivative assets under cyclical mean-reversion processes for spot prices

Federico Daniel Platania

Madrid 2013

UNIVERSIDAD COMPLUTENSE
MADRID

Facultad de Ciencias Económicas y Empresariales

Departamento de Economía Cuantitativa

Valuation of derivative assets under cyclical mean-reversion processes for spot prices

Tesis doctoral presentada por
Federico Daniel Platania

Dirigida por los doctores
Alfonso Novales Cinca
Manuel Moreno Fuentes

Madrid 2013

Resumen

El comportamiento estocástico de ciertos productos financieros, como el tipo de interés y el precio de los commodities, ha sido objeto de importantes estudios académicos y constituye un tema de especial relevancia para profesionales del sector. En la literatura académica podemos encontrar una gran variedad de modelos que abordan este problema, en su gran mayoría asumiendo que el activo financiero sigue un proceso con reversión a la media.

En el primer capitulo de esta tesis proponemos un nuevo modelo en tiempo continuo para la estructura temporal de tipos de interés, donde hemos asumido que el tipo de interés instantáneo converge a cierto tipo asintótico que varia de forma cíclica con el tiempo según una serie de Fourier, es decir

$$\begin{aligned} dr_t &= \kappa(f(t) - r_t)dt + \sigma dW_t \\ f(t) &= \sum_{n=0}^{\infty} Re\left[A_n e^{in\omega t}\right] \end{aligned}$$

donde $\kappa, \sigma \in \mathbb{R}^+$, W_t es un proceso de Wiener, y donde solo consideramos la parte real de la serie de Fourier puesto que es la parte que tiene sentido económico. Esta representación del tipo de interés instantáneo nos permite capturar numerosos cambios en la curvatura de la estructura temporal de tipos, y nos permite obtener soluciones analíticas para el precio de derivados y medidas del riesgo financiero.

Dado que un buen ajuste de la estructura temporal de tipos de interés sugiere que el modelo es potencialmente adecuado para ajustar el precio de bonos y derivados, utilizaremos observaciones diarias de la US Treasury yield curve rates desde el 31 de Julio del 2001 hasta el 21 de Septiembre del 2012 para analizar el comportamiento empírico de nuestro modelo frente a dos modelos de referencia, a saber Vasicek (1977) y Nelson Siegel (1987).

Los resultados de la estimación dentro de la muestra revelan que, nuestro modelo de Fourier en su más simple representación, es decir $n = 1$, supera a ambos modelos de referencia, reduciendo un 24% la suma total de residuos cuadrados del modelo de Nelson Siegel, y un 82% la del modelo de

Vasicek. Estos resultados son muy interesantes puesto que no es necesario incrementar los términos en la serie de Fourier para obtener un buen ajuste. Sin embargo, dado que la estructura temporal de tipos de interés pertenece a un espacio de Hilbert $L^2([t,T])$, incrementando el numero de términos en la serie de Fourier nos permitiría ajustar arbitrariamente bien la curva de tipos observada, derivando en un modelo de no arbitraje.

Durante el periodo muestral la curva de tipos ha adoptado diferentes formas. En este trabajo consideraremos tres periodos, de aproximadamente un año, para analizar el poder de predicción del modelo considerando un horizonte temporal de un día, una semana, y un mes.

El primer periodo, desde el 3 de Agosto del 2004 al 2 de Agosto del 2005, presenta un escenario muy interesante, donde la curva de tipos tiene pendiente positiva al principio de la muestra y se vuelve relativamente plana al final. Para un horizonte de predicción de un día, el modelo de Fourier mejora ampliamente las predicciones de ambos modelos de referencia. Para horizontes de estimación más largos, nuestro modelo proporciona mejores resultados pero la brecha se estrecha para algunos vencimientos. En este periodo, y considerando todos los horizontes de predicción, nuestro modelo proporciona la suma de residuos cuadrados más baja en 23 de las 33 predicciones.

El segundo periodo va desde el 2 de Agosto del 2006 al 31 de Julio del 2007, y corresponde a un periodo donde la curva de tipos es muy errática, con abruptas subidas y bajadas en el nivel de tipos de interés. Bajo estas condiciones ningún modelo proporciona buenos resultados, lo que nos indica que no es posible anticipar un comportamiento tan caótico.

El tercer periodo corresponde a la muestra más reciente, desde el 20 de Septiembre del 2001 al 21 de Septiembre del 2012. En este periodo los tipos a corto presentan niveles extremadamente bajos, provocando una gran diferencia entre el nivel de tipos con distintos vencimientos. En promedio, nuestro modelo de Fourier mejora las predicciones de sus competidores, obteniendo la suma de residuos cuadrados más baja para 25 de las 33 predicciones.

Considerando los tres periodos, podemos ver que hay ciertos momentos donde el modelo de Vasicek y Nelson Siegel producen errores de predicción muy grandes. Sin embargo, cuando el modelo de Fourier es vencido por sus competidores, la diferencia en los errores de perdición es muy estrecha.

En el segundo capitulo, proponemos un nuevo modelo del tipo CIR donde el tipo de interés instantáneo converge a cierto tipo asintótico que varia de forma cíclica con el tiempo según un oscilador armónico. Se puede demostrar que los procesos de este tipo siguen una distribución chi-cuadrado con δ grados de libertad. Cuando la dimensión del sistema no es un numero entero positivo la distribución del tipo instantáneo es desconocida. Feller (1951) ha demostrado que cuando $\delta \geq 2$ el tipo instantáneo permanece positivo, si $\delta < 2$ se puede anular, pero nunca puede ser negativo. Con estas premisas y teniendo en cuenta que δ depende de los parámetros del sistema, la volatilidad del tipo instantáneo también se asume dependiente del tiempo y la caracterizamos con un oscilador

armónico con la misma fase que la del nivel de reversión. En particular

$$\begin{aligned} dr_t &= \kappa(\theta_t - r_t)dt + \sigma_t\sqrt{r_t}dW_t \\ \theta_t &= A_\theta \sin^2(\varphi - \omega t) \\ \sigma_t^2 &= A_\sigma \sin^2(\varphi - \omega t) \end{aligned}$$

donde $\kappa \in \mathbb{R}^+$, y $\delta = \frac{4\theta_t\kappa}{\sigma_t^2}$. Como ambos osciladores están en fase, la dimensión del modelo se puede representar como $\delta = \frac{4A_\theta\kappa}{A_\sigma} > 0$.

Bajo este marco teórico, obtenemos expresiones analíticas para el precio del bono cupón cero y de diferentes productos derivados.

En el tercer capitulo, proponemos un nuevo modelo en tiempo continuo asumiendo que el logaritmo del precio spot del commodity converge a cierto nivel dependiente del tiempo que caracterizamos con una serie de Fourier, es decir

$$\begin{aligned} dS_t &= \kappa\left(f(t) - \ln(S_t)\right) S_t dt + \sigma S_t dW_t \\ f(t) &= \sum_{n=0}^{\infty} Re\left[A_n e^{inwt}\right] \end{aligned}$$

donde $\kappa,\ \sigma \in \mathbb{R}^+$, W_t es un proceso de Wiener, y solo consideramos la parte real de la serie puesto que es la parte que tiene sentido económico.

La idea que subyace detrás de este supuesto se basa en que las fuerzas de mercado dominan el proceso de valoración del commodity, y por tanto esta sujeto a una fuerte componente estacional. Bajo esta premisa, obtenemos formulas de valoración analíticas para el precio de contratos de futuros, opciones Europeas sobre el commodity, y opciones Europeas sobre contratos de futuros.

Los mercados de energía proporcionan el marco perfecto para estudiar el comportamiento de este tipo de modelos. En particular, centraremos nuestra atención en el mercado de gas natural, tomando la serie de precios contado y futuros de Henry Hub. Consideramos la serie de precios desde el 2 de Febrero de 1998 hasta el 3 de Julio del 2011, para los contratos Ng 5, Ng 8, y Ng 12, donde Ng 5 es el quinto contrato más próximo al vencimiento, y así sucesivamente. En este análisis evaluaremos la capacidad de ajuste de dos representaciones de nuestro modelo frente a dos modelos de referencia. En particular, consideramos el modelo propuesto en Schwartz (1997), donde el autor asume un proceso con reversión a la media con parámetros constantes. Además, consideramos el modelo propuesto en Lucia y Schwartz (2002), donde los autores asumen un proceso con reversión a la media igual a cero, incorporando una función trigonométrica con frecuencia anual para abordar el comportamiento estacional. Un ADF test de las series de precios spot y futuros pone de manifiesto

la existencia de una raíz unitaria, por lo que ambas series son no estacionarias. En consecuencia, el análisis espectral de las series presenta un máximo de densidad que corresponde a una frecuencia igual a cero. Sin embargo, en este estudio necesitamos obtener el espectro de la componente del precio del futuro que no este explicada por los movimiento del precio spot. Para ello, creamos una red de frecuencias y ajustamos nuestro modelo a la serie temporal observada para cada valor de la red. De esta manera obtenemos un mínimo error de ajuste bien definido para una frecuencia corta, que debemos interpretar como la frecuencia fundamental, indicándonos un periodo de entre 15 y 16 años. Además, podemos ver que para la serie Ng 5 y Ng 8, la segunda frecuencia más relevante es la anual. Sin embargo, la importancia de esta frecuencia decrece con con el tiempo al vencimiento, desapareciendo completamente del espectro de la serie con vencimiento a un año, Ng 12. Los resultados de la estimación nos muestran que, ambas representaciones de nuestro modelo mejoran ampliamente los resultados de los modelos de referencia. El modelo con un término en la expansión de Fourier, reduce la suma de residuos cuadrados del modelo de Lucia y Schwartz en un 28%, 54%, y 79% para la serie Ng 5, 8, y 12, respectivamente. Comparando con el modelo de Schwartz, la mejora es del 48%, 61%, y 79% para la serie Ng 5, 8, y 12, respectivamente. Podemos ver que, para el futuro con vencimiento a un año, el modelo de Lucia y Schwartz no proporciona ninguna ventaja frente al modelo sin componente estacional, este resultado no debería sorprendernos puesto que la frecuencia anual desaparece completamente del espectro de la serie Ng 12.

Aunque la principal mejora proviene de incorporar la frecuencia fundamental, agregando un segundo y tercer término en la expansión de Fourier proporciona mejoras que no son en absoluto despreciables. Cabe destacar que, incrementar el numero de términos en la serie nos permitiría ajustar arbitrariamente bien la serie observada.

Los resultados obtenidos en este trabajo sugieren que, cada uno de nuestros modelos proporciona una valiosa herramienta para la gestión de cartera, gestión de riesgo y la valoración de derivados.

Summary

The stochastic behaviour of interest rates and commodity prices have been thoroughly analysed in the academic literature and constitutes an issue of special relevance for practitioners in financial markets. Previous studies have proposed numerous processes to model the stochastic component of these assets, most of them assuming a mean reverting process.

The first chapter of this work introduces a new continuous-time model for the term structure of interest rates where the instantaneous spot rate is assumed to converge to a long-term level that changes over time according to a Fourier series, that is

$$\begin{aligned} dr_t &= \kappa(f(t) - r_t)dt + \sigma dW_t \\ f(t) &= \sum_{n=0}^{\infty} Re\left[A_n e^{in\omega t}\right] \end{aligned}$$

where $\kappa, \sigma \in \mathbb{R}^+$ and W_t is a standard Wiener process, and where we only consider the real part of the Fourier series since it is the only one that makes economic sense. This representation of the spot rate allows us to capture a number of changes in the curvature of the term structure maintaining the analytical tractability and allowing us to compute closed-form expressions for the prices of numerous interest rate derivatives and risk management measures.

Since a good fit of the term structure should suggest a potentially good fit of bond and derivative prices, we use daily US Treasury yield curve rates from July 31, 2001 up to September 21, 2012 to empirically analyse the performance of the simplest expression of our proposed Fourier model, versus two benchmarks, Vasicek (1977) and Nelson and Siegel (1987).

The in-sample fitting results reveal that our Fourier model outperforms both alternative benchmarks, reducing the aggregate sum of squares by 24% relative to the Nelson Siegel model, and by 82% relative to the Vasicek model. This is an interesting result since we are estimating the simplest representation of the Fourier model, that is $n = 1$. However, since the yield curve function belongs to a Hilbert space $L^2([t, T])$, increasing the number of terms in the Fourier expansion would eventually allow for fitting arbitrarily well the observed yield curve, eventually leading to a no-arbitrage model of the term structure.

During the sample period from July 31, 2001 up to September 21, 2012, the yield curve adopted very different shapes. Hence, we consider three different moments in time to asses the forecasting power of each model. Each forecasting period covers approximately one year and three forecast horizons, that is one day, one week, and one month ahead.

The first forecasting period, from August 3, 2004 to August 2, 2005, presents an interesting scenario, where the term structure is upward sloping at the beginning of the sample and quite flat at the end. The Fourier model consistently beats its competitors in the one-day ahead forecasting. For larger forecasting horizons of 5 or 21-days ahead, the Fourier model still provides better predictions than its competitors although the gap narrows at some maturities. Over this period, the Fourier model has the lowest sum of squared forecast errors in 23 of the 33 comparisons over maturity and forecasting horizon.

The second forecasting period, from August 2, 2006 to July 31, 2007, corresponds to a erratic yield curve, with several ups and downs in yield levels. Under this scenario no model can anticipate such chaotic behaviour providing poor predictions.

The third forecasting period, from September 20, 2011 to September 21, 2012, is the most recent sample where shortest maturities are extremely low and yield levels drastically differ with maturity. On average, the Fourier model again outperforms both competitors, achieving the lowest sum of squared forecast errors in 25 of the 33 comparisons.

An interesting fact arises considering the three forecasting periods all together, we have found instances in which the Vasicek and the Nelson-Siegel models produce forecast errors much higher than their competitors. However, when the Fourier model is beaten by the Vasicek and Nelson-Siegel models, the difference in forecasting performance is usually quite narrow.

In chapter 2 we propose a new square-root model where the instantaneous interest rate is pulled back to a certain time-dependent long term level characterized by an harmonic oscillator. Square-root process of this type follows a rescaled non-central chi-square distribution with δ degrees of freedom. Whenever the dimension of the process is not a positive integer the spot rate distribution is unknown. Feller (1951) has demonstrated that whenever $\delta \geq 2$ the spot rate remains positive, if $\delta < 2$ it can become null but never negative. Under that assumption and considering that δ depends on the model parameters, we also propose a time-dependent spot rate volatility characterized by another harmonic oscillator in phase with the reverting level function. In more detail,

$$\begin{aligned} dr_t &= \kappa(\theta_t - r_t)dt + \sigma_t\sqrt{r_t}dW_t \\ \theta_t &= A_\theta \sin^2(\varphi - \omega t) \\ \sigma_t^2 &= A_\sigma \sin^2(\varphi - \omega t) \end{aligned}$$

where $\kappa \in \mathbb{R}^+$, and $\delta = \frac{4\theta_t \kappa}{\sigma_t^2}$. As both waves are in phase, the model's dimension can be represented as $\delta = \frac{4A_\theta \kappa}{A_\sigma} > 0$.

Under this framework, we compute closed-form expressions for the prices of zero-coupon bonds, Forward on a zero coupon-bond, European option on a zero-coupon bond, European option on a coupon bond, European bond forward option, Forward Rate Agreement, Interest rate swap and swaption, Caps, floors, and collars.

The third chapter introduces a new continuous-time model based on an Ornstein-Uhlenbeck process for the logarithm of the commodity spot price, with a reversion to a time dependent long-run level, the time variation of the long-run price level being characterized by a Fourier series. In more detail,

$$\begin{aligned} dS_t &= \kappa \left(f(t) - \ln(S_t) \right) S_t dt + \sigma S_t dW_t \\ f(t) &= \sum_{n=0}^{\infty} Re \left[A_n e^{inwt} \right] \end{aligned}$$

where $\kappa,\ \sigma \in \mathbb{R}^+$ and W_t is a standard Wiener process, and it is only considered the real part of the series since it is the part that makes economic sense.

The underlying idea behind this assumption is that the pricing process is driven by market forces and dominated by a strong seasonal component. Under that assumption, we compute closed-form expressions for the prices of Futures contract, European option on the commodity, and European option on the forward commodity.

Energy and power markets present a perfect framework to analyse the suitability of this kind of models with a seasonal component. We focus our analysis on natural gas as a source of energy, taking Henry Hub as the pricing point for natural gas futures contracts. We analyse the time-series from 02/02/1998 to 07/03/2011 for futures contract Ng 5, Ng 8, and Ng 12, where Ng 5 is the fifth contract closest to maturity, and so on. We compare the fitting ability of two different representations of our model, that is considering one and two terms in the Fourier expansion, to market data against two alternative benchmarks. In particular, we use the one factor model proposed in Schwartz (1997), which assumes a mean reverting process with constant parameters. And the model proposed in Lucia and Schwartz (2002), which assumes a zero level mean reverting process, incorporating a trigonometric function with annual frequency in order to cope with the seasonal behaviour of the commodity price. An Augmented Dickey-Fuller test of the Spot and futures price series reveals the existence of a unit root, meaning that both, the spot and futures price series are nonstationary. Hence, a spectral analysis of these series presents a maximum spectral density corresponding to the zero frequency. Nevertheless, in this study we need to obtain the spectrum of the component of futures prices which is not explained by spot prices. Then using a grid of frequencies and fitting

our model to the observed time series for each value of the frequency in the grid will exposed those frequencies. Indeed, we obtain a well defined minimum fitting error at a short frequency, which should be interpreted as the fundamental frequency, indicating an underlying long run period of 15 to 16 years. Another interesting result arises, the second relevant term in the Fourier series for the Ng 5 and Ng 8 is the annual frequency. However, the importance of the annual frequency decreases with maturity, completely disappearing beyond the futures expiring in one year, Ng 12. Compared with the benchmark models, both representations of our model dramatically improve the in-sample fit of every observed futures time series. The model with just one term in the Fourier expansion, reduces the aggregate sum of squares of Lucia and Schwartz model by 28%, 54% and 79%, for Ng 5, 8 and 12, respectively. Compared with Schwartz model, the improvement is of 48%, 61% and 79% for Ng 5, 8 and 12, respectively. For the futures contract expiring in one year, Lucia and Schwartz model provides no further improvement from the model with no seasonal component, not surprising at all since the annual frequency has completely disappear from the Ng 12 spectrum.

Although the main improvement comes with the incorporation of the fundamental frequency, adding a second and a third term in the model still provide further improvements. On this regard, it is interesting to point out that increasing the number of terms in the Fourier expansion would eventually allow for fitting arbitrarily well the observed time series.

The results of each chapter are very relevant, suggesting that our proposed models provide a simple and powerful tool for portfolio management, risk management and derivative pricing on interest rates and commodities.

Contents

Chapter 1

A Term Structure Model with Cyclical Mean Reversion: Pricing and Risk Management

1.1 Introduction

The term structure of interest rates has been thoroughly analysed in many academic papers and constitutes an issue of special relevance for practitioners in financial markets. This chapter introduces a new continuous-time model for the term structure of interest rates where the instantaneous spot rate is assumed to converge to a long-term level that changes over time according to a Fourier series. That specification allows us to capture a number of changes in the curvature of the term structure, an attractive feature which is also incorporated in the Nelson-Siegel and Svensson models through exponential functions, providing these two models with a good fit to market interest rates.

Table 1.1 shows some of the models proposed in the academic literature, classified in two categories: endogenous and exogenous. Endogenous models assume that changes in interest rates are affected by one or more factors and propose a certain stochastic behaviour for the factors. Under those assumptions, the current term structure can be derived as an implication from the model. Popular examples of one-factor models are Vasicek (1977), Brennan and Schwartz (1980), or Cox *et al.* (1985). The downside of these models is the lack of an appropriate fit to observed interest rate data. To mitigate this drawback some multi-factor models have been proposed. See, for instance, Brennan and Schwartz (1979), Schaefer and Schwartz (1984), Longstaff and Schwartz (1992), Duffie and Kan (1996), or Chen (1996).

In contrast, exogenous models consider the current term structure as an input and aim to prevent arbitrage opportunities considering interest rates with different maturities. A pioneer work in this area was made by Ho and Lee (1986) who proposed a model consistent with observed data. As this model implies a Gaussian distribution and no mean reversion for interest rates, several papers have specified and analysed alternative model specifications such as Black *et al.* (1990), Hull and White (1990, 1993), Black and Karasinski (1991), Heath *et al.* (1992), and Mercurio and Moraleda (2000). For a complete survey on term structure models see, for instance, Webber and James (2001), Brigo and Mercurio (2006), or Filipović (2009).

In our model, the instantaneous spot rate completely characterizes the evolution in time of interest rates at different maturities. Under this framework, we compute closed-form expressions for the prices of zero-coupon bonds and different derivatives such as bond forwards, European options on zero-coupon and coupon-bearing bonds, European bond forward options, swaps, swaptions, caps, floors, and collars. Additionally, we compute several risk management measures for bonds, like Greeks for European bond options, and perform a sensitivity analysis on the model parameters. Finally, we dig a bit deeper analyzing the in- and out-of-sample performance of this model for the term structure of interest rates, comparing the results with two benchmark models: Vasicek(1977) and Nelson and Siegel (1987). We show that, for the data set used in this analysis, the proposed model outperforms its competitors both, in- and out-of-sample, providing a more precise adjustment

to actual market values as well as better forecasts.

This chapter is organized as follows. Section 1.2 introduces the posited model, its main features, the general pricing partial differential equation and derives the bond pricing equation. Sections 1.3 and 1.4 provide closed-form expressions for prices of different derivatives and some risk management measures, respectively. Section 1.5 and 1.6 present the empirical analysis. Finally, Section 1.7 summarizes the main findings and make some concluding comments. A final Appendix includes the mathematical proofs.

1.2 A New Model for the Term Structure

In this section we introduce the model, present the partial differential equation that must be satisfied by the price of any derivative asset, obtain the bond pricing equations, and characterize the term structure of interest rates.

1.2.1 The Model

Let r_t denote the instantaneous interest rate available at time t. We assume that the time evolution of r_t is given by the Ornstein-Uhlenbeck process, defined by a stochastic differential equation

$$dr_t = \kappa(f(t) - r_t)dt + \sigma dW_t \tag{1.1}$$

where $\kappa, \sigma \in \mathbb{R}^+$ and W_t is a standard Wiener process. In addition, we assume that the mean-reversion level, $f(t)$, follows a time-dependent process driven by a Fourier series:

$$f(t) = \sum_{n=0}^{\infty} Re\left[A_n e^{in\omega t}\right]$$

where we only consider the real part of the Fourier series since it is the only one that makes economic sense. Note that, $\forall n \mid A_n \in \mathbb{C}$, so that there is a phase factor contained in A_n. In more detail, $A_n = A_{n,x} + iA_{n,y}$ where $A_{n,x}, A_{n,y} \in \mathbb{R}$. Hence, $A_{n,x}$ and $A_{n,y}$ denote the amplitude and phase of the fluctuations in the instantaneous rate, respectively. Moreover, this model nests the model in Vasicek (1977) by taking $A_n = 0$, $\forall n \in \mathbb{N} - \{0\}$.

Now, let $\Lambda(r_t, t)$ denote the market price of risk, which is assumed constant, $\Lambda(r_t, t) = \lambda$. Then, the risk-neutral version of the process (1.1) is given by

$$dr_t = \mu_r dt + \sigma d\widetilde{W}_t \tag{1.2}$$

where

$$\mu_r = \kappa(\alpha + g(t) - r_t) \tag{1.3}$$

$$\alpha = A_0 - \frac{\lambda\sigma}{\kappa} \tag{1.4}$$

$$g(t) = \sum_{n=1}^{\infty} Re\left[A_n e^{in\omega t}\right] = f(t) - A_0 \tag{1.5}$$

where $A_0 \in \mathbb{R}$ and $\widetilde{W}_t = W_t + \lambda t$ is a standard Wiener process under the risk-neutral measure $\widetilde{P}$. The following Proposition establishes the solution of the stochastic differential equation (1.2).

Proposition 1 *The solution of the risk-neutral process followed by the instantaneous interest rate is given as*[1]

$$r_s = e^{-\kappa(s-t)} r_t + \left(1 - e^{-\kappa(s-t)}\right)\alpha + \sum_{n=1}^{\infty} Re\left[\frac{\kappa A_n}{\kappa + in\omega}\left(e^{in\omega s} - e^{-\kappa(s-t)+in\omega t}\right)\right] + \sigma\int_t^s e^{-\kappa(s-u)} d\widetilde{W}_u$$

■

From Proposition 23, it is clear that instantaneous interest rate follows a Normal distribution. Its first two statistical moments under $\widetilde{P}$ are given as

$$\widetilde{E}[r_T \mid r_t] = e^{-\kappa(T-t)} r_t + \left(1 - e^{-\kappa(T-t)}\right)\alpha + \sum_{n=1}^{\infty} Re\left[\frac{\kappa A_n}{\kappa + in\omega}\left(e^{in\omega T} - e^{-\kappa(T-t)+in\omega t}\right)\right] \tag{1.6}$$

$$\begin{aligned}\widetilde{V}[r_T \mid r_t] &= \widetilde{V}\left[\sigma\int_t^T e^{-\kappa(T-u)} d\widetilde{W}_u\right] = \left(\sigma\int_t^T e^{-\kappa(T-u)} d\widetilde{W}_u\right)^2 = \sigma^2\int_t^T e^{-2\kappa(T-u)} du \\ &= \frac{\sigma^2}{2\kappa}\left(1 - e^{-2\kappa(T-t)}\right)\end{aligned} \tag{1.7}$$

where we have applied the isometry property for stochastic integrals in the variance.

1.2.2 Bond Pricing and the Term Structure of Interest Rates

Let $P(r_t, t, T)$ denote the price at time t of a zero-coupon bond that pays \$1 at maturity T. Applying Itô's Lemma, standard no-arbitrage arguments and some trivial algebra, we get the following partial differential equation (PDE):

$$P_t(r_t, t, T) + (\mu_r - \Lambda(r_t, t)\sigma_r) P_r(r_t, t, T) + \frac{1}{2}\sigma_r^2 P_{rr}(r_t, t, T) - r_t P(r_t, t, T) = 0 \tag{1.8}$$

that must be verified by the price of any derivative.

[1] This result arises as $e^{-\kappa(s-t)}$ is square-integrable in $[t, s]$, so that it belongs to a Hilbert space.

Replacing expression (1.1) and the constant market price of risk λ into (2.10), we get the PDE for the bond price:

$$P_t + P_r\kappa\left(\alpha + g(t) - r_t\right) + P_{rr}\frac{\sigma^2}{2} - Pr_t = 0 \tag{1.9}$$

subject to the terminal condition $P(r_T, T, T) = 1,\ \forall\, r_T$.

Using probabilistic techniques, the solution of this PDE can be written as a risk-neutral conditional expectation, that is,

$$P(r_t, t, T) = \widetilde{E}\left[e^{-\int_t^T r_s ds} \mid r_t\right]$$

Looking at Proposition 23, it is clear that $\int_t^T r_s ds$ is a random Normal variable. Then, straightforward algebra leads to the solution of this PDE as given in the following Proposition.

Proposition 2 *The price at time t of a zero-coupon bond with maturity T and \$1 face value is given by*

$$P(r_t, t, T) = \exp\left\{-\widetilde{E}\left[\int_t^T r_s ds \mid r_t\right] + \frac{1}{2}\widetilde{V}\left[\int_t^T r_s ds \mid r_t\right]\right\}$$

where

$$\begin{aligned}
\widetilde{E}\left[\int_t^T r_s ds \mid r_t\right] &= \frac{1-e^{-\kappa(T-t)}}{\kappa} r_t - \left(\frac{1-e^{-\kappa(T-t)}}{\kappa} - (T-t)\right)\alpha \\
&+ \sum_{n=1}^{\infty} Re\left[\frac{A_n}{n\omega(\kappa + in\omega)}\left(e^{in\omega t}\left(n\omega e^{-\kappa(T-t)} + i\kappa - n\omega\right) - i\kappa e^{in\omega T}\right)\right] \qquad (1.10)\\
\widetilde{V}\left[\int_t^T r_s ds \mid r_t\right] &= \frac{\sigma^2}{\kappa^2}\left[(T-t) - 2\frac{1-e^{-\kappa(T-t)}}{\kappa} + \frac{1-e^{-2\kappa(T-t)}}{2\kappa}\right] \qquad (1.11)
\end{aligned}$$

■

Since all affine models provide an exponential-affine functional form for bond pricing, we can immediately rewrite the previous Proposition to obtain the next one.

Proposition 3 *The price at time t of a zero-coupon bond with maturity T and \$1 face value is given by*

$$P(r_t, t, T) = e^{A(t,T) - B(t,T) r_t}$$

where

$$\begin{aligned}
A(t,T) &= \frac{\sigma^2}{2\kappa^2}\left[(T-t) - 2B(t,T) + \frac{1-e^{-2\kappa(T-t)}}{2\kappa}\right] + \left(B(t,T) - (T-t)\right)\alpha \\
&- \sum_{n=1}^{\infty} Re\left[\frac{A_n}{n\omega(\kappa + in\omega)}\left(e^{in\omega t}\left(n\omega e^{-\kappa(T-t)} + i\kappa - n\omega\right) - i\kappa e^{in\omega T}\right)\right] \qquad (1.12)\\
B(t,T) &= \frac{1-e^{-\kappa(T-t)}}{\kappa} \qquad (1.13)
\end{aligned}$$

■

In Figure 1.1 we plot the term structure of bond prices for three different set of parameters in the Fourier model against the structure obtained with Vasicek's model. We can see the higher flexibility of our proposed model approach to fit different shapes of the term structure.

The following Corollary immediately arises.

Corollary 1 *As a coupon bond can be interpreted as a portfolio of zero-coupon bonds, the price of coupon bonds can be obtained applying Propositions 2 or 3.* ∎

Under this framework and considering the bond price $P(r_t, t, T)$ given by Proposition 3, the term structure of interest rates is fully characterized in the following Corollary.

Corollary 2 *The yield to maturity, $R(r_t, t, T)$, is given by*

$$R(r_t, t, T) = -\frac{1}{\tau} \ln P(r_t, t, T),\ \tau = T - t$$

The short-term interest rate is defined as the instantaneous interest rate at time t, that is,

$$r_t = \lim_{\tau \to 0} R(r_t, t, T) = R(r_t, t, t)$$

The instantaneous forward rate is given as

$$f(r_t, t, T) = -\frac{\partial \ln(P(r_t, t, T))}{\partial T}$$

∎

Figure 1.2 shows the yield curve for three different set of parameters in the Fourier model against Vasicek's model. Clearly, even for small number of terms (n) in the expansion, the Fourier model is capable of replicating different yield curve shapes such as upward sloping, downward sloping, humped, and inverted humped. On this respect, it is interesting to stress that our model should be able to replicate any yield curve shape as n goes to infinity, since the yield curve function belongs to a Hilbert space $L^2([t, T])$, and the Fourier series can be made to converge in quadratic mean to any function in such a space.

For illustrative purposes, Figures 1.3 and 1.4 show how the term structure of interest rates responds to different values of speed of reversion to the mean and the volatility parameter, respectively. Both models provide a similar pattern for the chosen parameters: the lower the speed of mean reversion, the lower the yield. Additionally, in the Fourier model, the lower the speed of mean reversion, the flatter the term structure. Moreover, Figure 1.4 shows that the yield decreases with volatility. Figure 1.5 compare how the term structure of interest rates responds in the Vasicek model and the Fourier model to different values of the common α parameter. Finally, Figure 1.6 displays how the

term structure under the Fourier model responds to changes in its parameters $A_{n,x}$, $A_{n,y}$ and ω. The most obvious effect is that of changes in the phase $A_{n,y}$. We can see how the position and height of the peak in the term structure occur in opposite places for different phases. All these representations confirm that our proposed model provides a great flexibility even for small number of terms in the Fourier expansion.

1.3 Derivatives Pricing

This section is devoted to the analytical computation of closed-form expressions for the prices of different derivative securities under this new model. In more detail, we price bond derivatives and derivatives on interest rates.

1.3.1 Pricing of Bond Derivatives

The bond pricing PDE (1.9) subject to the appropriate terminal condition allows us to obtain closed-form expressions for the price of any interest rate derivative. Then, considering a derivative whose pay-off at time T is given by $U_T(r_T)$,[2] the price at time t of this contract will read as:

$$U_t(r_t,t,T) = \widetilde{E}\left[e^{-\int_t^T r_s ds} U_T(r_T) \mid r_t\right]$$

Proposition 4 *The price at time t of any interest rate derivative with terminal pay-off $U_T(r_T)$ is given by*

$$U_t(r_t,t,T) = P(r_t,t,T)\widetilde{E}\left[U_T(w_T) \mid r_t\right]$$

where $P(r_t,t,T)$ is given by Proposition 2 and w_T follows a normal distribution with conditional moments

$$\widetilde{E}[w_T \mid r_t] = \widetilde{E}[r_T \mid r_t] - \widetilde{Cov}\left[r_T; \int_t^T r_s ds \mid r_t\right] \tag{1.14}$$

$$\widetilde{V}[w_T \mid r_t] = \widetilde{V}[r_T \mid r_t] \tag{1.15}$$

where $\widetilde{E}[r_T \mid r_t]$ and $\widetilde{V}[r_T \mid r_t]$ are given by equations (1.6)-(1.7), respectively, and

$$\widetilde{Cov}\left[r_T; \int_t^T r_s ds \mid r_t\right] = \frac{\sigma^2}{2}\left(\frac{1-e^{-\kappa(T-t)}}{\kappa}\right)^2 \tag{1.16}$$

■

Proof. See the Appendix. ■

After obtaining this general closed-form expression for the price of any interest rate derivative, we proceed to analyzing in detail several specific assets:

[2] Clearly, if $U_T(r_T) = 1$, the previous bond price expression is obtained.

1. **Forward on a zero coupon-bond**

Consider a forward contract expiring at time T_f written on a zero-coupon bond maturing at time $T_b > T_f$ and face value \$1. Under the risk neutral measure $\widetilde{P}$, the delivery price established at time t for this forward contract is given as

$$F(r_t, t, T_f, T_b) = \widetilde{E}\left[P(w_{T_f}, T_f, T_b) \mid r_t\right]$$

The value at time t of this forward is given by the next Proposition.

Proposition 5 *The value at time t of a bond forward contract maturing at time T_f written on a zero-coupon bond with maturity date T_b and face value \$1 is given by*

$$\begin{aligned} F(r_t, t, T_f, T_b) &= \widetilde{E}\left[P(w_{T_f}, T_f, T_b) \mid r_t\right] \\ &= \exp\left\{A(T_f, T_b) - B(T_f, T_b)\widetilde{E}\left[w_{T_f} \mid r_t\right] + \frac{1}{2}B^2(T_f, T_b)\widetilde{V}\left[w_{T_f} \mid r_t\right]\right\} \end{aligned}$$

where $A(T_f, T_b)$ and $B(T_f, T_b)$ are given by (1.12) and (1.13), respectively, and $\widetilde{E}\left[w_{T_f} \mid r_t\right]$ and $\widetilde{V}\left[w_{T_f} \mid r_t\right]$ as given by (1.14) and (1.15), respectively. ∎

2. **European option on a zero-coupon bond**

Consider a call option maturing at time T_c with strike K, written on a zero-coupon bond that matures at time $T_b > T_c$. Let $c_t(r_t, T_c, T_b, K)$ denote the price at time t of this call option.

Then, the boundary condition of the PDE (1.9) will be given by

$$c_{T_c}(r_{T_c}, T_c, T_b, K) = \max\left\{P(r_{T_c}, T_c, T_b) - K, 0\right\}$$

Hence, under the risk-neutral measure $\widetilde{P}$, the price at time t of this option will be given by

$$c_t(r_t, T_c, T_b, K) = \widetilde{E}\left[e^{-\int_t^{T_c} r_s ds}(P(r_{T_c}, T_c, T_b) - K)^+ \mid r_t\right]$$

The call option price is given by the following Proposition.

Proposition 6 *The price at time t of a European call option with maturity T_c written on a zero-coupon bond expiring at time T_b and \$1 face value is given by*

$$\begin{aligned} c_t(r_t, T_c, T_b, K) &= P(r_t, t, T_c)\widetilde{E}\left[(P(w_{T_c}, T_c, T_b) - K)^+ \mid r_t\right] \\ &= P(r_t, t, T_c)F(r_t, t, T_c, T_b)\Phi(d_1) - P(r_t, t, T_c)K\Phi(d_2) \end{aligned}$$

where the bond price $P(r_t, t, \cdot)$ is given by Proposition 2, the bond forward value $F(r_t, t, T_c, T_b)$ is given by Proposition 5, $\Phi(\cdot)$ denotes the standard normal distribution function, and

$$\begin{aligned} d_1 &= \frac{\ln\left(\frac{F(r_t,t,T_c,T_b)}{K}\right) + \frac{1}{2}B(T_c,T_b)^2\widetilde{V}[w_{T_c} \mid r_t]}{B(T_c,T_b)\sqrt{\widetilde{V}[w_{T_c} \mid r_t]}} \\ d_2 &= d_1 - B(T_c,T_b)\sqrt{\widetilde{V}[w_{T_c} \mid r_t]} \end{aligned}$$

with $B(T_c, T_b)$ as in (1.13), $\widetilde{V}[w_{T_c} \mid r_t]$ as given by (1.15), and $F(r_t, t, T_c, T_b)$ as in Proposition 5. ∎

3. **European option on a coupon bond**

Consider a European call option that matures at time T_c and strike K. The underlying asset is a coupon bond maturing at time T_b paying N coupons α_i at times $s_i,\ i = 1, 2, \cdots, N$ where $s_1 > T_c,\ s_N = T_b$. The price of this coupon bond at time T_c is given by the sum of the corresponding zero-coupon bonds, that is,

$$P(r_{T_c}, T_c, T_b) = \sum_{i=1}^{N} \alpha_i P(r_{T_c}, T_c, s_i) \tag{1.17}$$

where $P(r_{T_c}, T_c, s_i),\ i = 1, 2 \cdots, N$ is given by Proposition 3.

Let $c_t\left(r_t, T_c, \{s_i\}_{i=1}^N, K\right)$ denote the price at time t of this call option. Using (2.22), the boundary condition of the PDE (1.9) becomes now

$$c_{T_c}\left(r_{T_c}, T_c, \{s_i\}_{i=1}^N, K\right) = \max\left\{\sum_{i=1}^{N} \alpha_i P(r_{T_c}, T_c, s_i) - K, 0\right\}$$

Applying Proposition 4, the call option price is given as

$$\begin{aligned} c_t\left(r_t, T_c, \{s_i\}_{i=1}^N, K\right) &= P(r_t, t, T_c)\,\widetilde{E}\left[c_{T_c}\left(w_{T_c}, T_c, \{s_i\}_{i=1}^N, K\right) \mid r_t\right] \\ &= P(r_t, t, T_c)\,\widetilde{E}\left[\max\left\{\sum_{i=1}^{N} \alpha_i P(w_{T_c}, T_c, s_i) - K, 0\right\} \mid r_t\right] \end{aligned}$$

Since the bond price is lognormally distributed, the distribution of $\sum_{i=1}^N P(w_{T_c}, T_c, s_i)$ is unknown. Then, in line with Jamshidian (1989), we will find $K_i,\ i = 1, 2, \cdots, N$ such that

$$\max\left\{\sum_{i=1}^{N} \alpha_i P(w_{T_c}, T_c, s_i) - K, 0\right\} = \sum_{i=1}^{N} \alpha_i \max\{P(w_{T_c}, T_c, s_i) - K_i, 0\} \tag{1.18}$$

where $K_i = P(\varpi, T_c, s_i)$ and ϖ is the solution of $\sum_{i=1}^N \alpha_i P(\varpi, T_c, s_i) = K$.[3]

[3]Note that the existence of strikes K_i such that equation (2.23) has a solution is guaranteed as the bond price is a decreasing function of the instantaneous interest rate.

The European call option on a coupon bond can be interpreted as a portfolio of European call options on zero-coupon bonds with "appropriate" strikes K_i , which allows us to characterize its price in the following Proposition.

Proposition 7 *The price at time t of a European call option with maturity T_c on a coupon bond expiring at time T_b and paying coupons α_i at times s_i, $i = 1, 2, \cdots, N$ is given by*

$$c_t\left(r_t, T_c, \{s_i\}_{i=1}^N, K\right) = \sum_{i=1}^{N} \alpha_i \, c_t\left(r_t, T_c, s_i, K_i\right)$$

where $c_t\left(r_t, T_c, s_i, K_i\right)$ is given by Proposition 6. ∎

4. **European bond forward option**

Consider a European bond forward call option that matures at time T_c with strike K. If this option is exercised, the call-holder pays K and receives a forward maturing at time T_f on a bond that expires at time $T_b > T_f > T_c$. Let $c_t\left(r_t, T_c, T_f, T_b, K\right)$ denote the price at time t of this option.

The boundary condition of the PDE (1.9) is given as

$$c_{T_c}\left(r_{T_c}, T_c, T_f, T_b, K\right) = \max\left\{F(r_{T_c}, T_c T_f, T_b) - K, 0\right\}$$

Under the risk-neutral measure $\widetilde{P}$, the price at time t of this option is given as

$$c_t\left(r_t, T_c, T_f, T_b, K\right) = \widetilde{E}\left[e^{-\int_t^{T_c} r_s ds}\left(F(r_{T_c}, T_c, T_f, T_b) - K\right)^+ \mid r_t\right]$$

In short, we have the following Proposition.

Proposition 8 *The price at time t of a European bond forward call option with maturity T_c on a forward contract expiring at time T_f on a zero-coupon bond that matures at time T_b with a \$1 face value is given by*

$$\begin{aligned} c_t\left(r_t, T_c, T_f, T_b, K\right) &= P(r_t, t, T_c)\widetilde{E}\left[\left(F(w_{T_c}, T_c, T_f, T_b) - K\right)^+ \mid r_t\right] \\ &= P(r_t, t, T_c)\Theta(r_t, t, T_c, T_f, T_b)\Phi(d_1) - P(r_t, t, T_c)K\Phi(d_2) \end{aligned}$$

where $P\left(r_t, t, T_c\right)$ is given by Proposition 2, $\Phi(\cdot)$ denotes the standard normal distribution function, and

$$
\begin{aligned}
\Theta\left(r_t,t,T_c,T_f,T_b\right) &= \exp\left\{A(T_f,T_b)-B(T_f,T_b)\varrho\left(r_t,t,T_c,T_f,T_b\right)+\frac{1}{2}B\left(T_f,T_b\right)^2\widetilde{V}\left[w_{T_f}\mid r_t\right]\right\}\\
\varrho\left(r_t,t,T_c,T_f,T_b\right) &= \left(1-e^{-\kappa(T_f-T_c)}\right)\alpha+\widetilde{E}[w_{T_c}|r_t]e^{-\kappa(T_f-T_c)}-\widetilde{Cov}\left[r_{T_f},\int_{T_c}^{T_f}r_s ds|r_{T_c}\right]\\
&\quad+\sum_{n=1}^{\infty}Re\left[\frac{\kappa A_n}{\kappa+in\omega}\left(e^{in\omega T_f}-e^{-\kappa(T_f-T_c)+in\omega T_c}\right)\right]\\
d_1 &= \frac{v+\widetilde{V}\left[w_{T_c}\mid r_t\right]B(T_f,T_b)e^{-\kappa(T_f-T_c)}-\widetilde{E}\left[w_{T_c}\mid r_t\right]}{\sqrt{\widetilde{V}\left[w_{T_c}\mid r_t\right]}}\\
d_2 &= d_1-e^{-\kappa(T_f-T_c)}B(T_f,T_b)\sqrt{\widetilde{V}\left[w_{T_c}\mid r_t\right]}\\
v &= \frac{-\ln(K)+A(T_f,T_b)-B(T_f,T_b)\eta+\frac{1}{2}B(T_f,T_b)^2\widetilde{V}\left[w_{T_f}\mid r_{T_c}\right]}{B(T_f,T_b)e^{-\kappa(T_f-T_c)}}\\
\eta &= \left(1-e^{-\kappa(T_f-T_c)}\right)\alpha-\widetilde{Cov}\left[r_{T_f},\int_{T_c}^{T_f}r_s ds|r_{T_c}\right]\\
&\quad+\sum_{n=1}^{\infty}Re\left[\frac{\kappa A_n}{\kappa+in\omega}\left(e^{in\omega T_f}-e^{-\kappa(T_f-T_c)+in\omega T_c}\right)\right]
\end{aligned}
$$

where $A(T_f,T_b)$, $B(T_f,T_b)$, $\widetilde{E}[w_{T_x}\mid r_t]$, $\widetilde{V}\left[w_{T_x}\mid r_t\right]$, *and* $\widetilde{Cov}\left[r_y,\int_x^y r_s ds\mid r_x\right]$ *are given by equations (1.12)-(1.16), respectively.* ∎

Remark 1 *Note that* $P\left(r_t,t,T_c\right)\Theta\left(r_t,t,T_c,T_f,T_b\right)$ *should not be interpreted as the forward price at time* t *but rather, as the price at time* t *of an asset paying the forward price at time* T_c. ∎

Corollary 3 *For all the above cases, put option prices are directly obtained from application of put-call parity.* ∎

1.3.2 Interest Rate Derivatives

We now examine the pricing of derivative assets on a given interest rate: FRAs, swaps, caps, floors, and collars.

1. **Forward Rate Agreement**

Consider a FRA with maturity s and \$1 notional value, where the investor agrees to receive a floating rate with tenor $T_s - s$ and pay a fixed interest rate K. The floating rate is set at time s and the net cash-flow is received at time $T_r > s$.

Hence, under the risk-neutral measure $\widetilde{P}$, the FRA value at time t is given as

$$FRA_t(r_t, s, T_r, T_s, K) = \widetilde{E}\left[e^{-\int_t^{T_r} r_u du}\left(R(r_s, s, T_s) - K\right) \mid r_t\right]$$

The following Proposition provides a closed-form expression for the FRA value.

Proposition 9 *The value at time t of a FRA with maturity s and \$1 notional value, where it is agreed to pay a fixed rate K and receive a floating rate with tenor $T_s - s$, is given by*

$$\begin{aligned} FRA_t(r_t, s, T_r, T_s, K) &= P(r_t, t, T_r)\widetilde{E}[R(w_s, s, T_s) - K \mid r_t] \\ &= P(r_t, t, T_r)\left[\frac{B(s, T_s)\mu - A(s, T_s)}{T_s - s} - K\right] \end{aligned}$$

where $P(r_t, t, T_r)$ is given by Proposition 2 and $\mu = \widetilde{E}[w_s \mid r_t]$ is given by equation (1.14). ∎

2. **Interest rate swap and swaption**

An interest rate swap can be interpreted as either the difference between two coupon bonds or a portfolio of FRA's. Hence, valuing swaps arises directly by applying Proposition 2 or 9. Similarly, swaption valuation is an immediate consequence of Proposition 7.

3. **Caps, floors, and collars**

A cap (floor) contract guarantees its holder a pay-off if a certain floating interest rate is above (below) a specified rate, the cap (floor) level. Caps (floors) involve a series of regular payments, usually referred as caplets (floorlets). Hence, a cap (floor) can be interpreted as a portfolio of caplets (floorlets).

Consider a caplet contract written on the floating rate maturing at time s and with \$1 face value. If exercised, the investor pays a fixed interest rate K and receives a floating rate with tenor $T_s - s$. The floating rate is set at time s and the net cash-flow is received at time $T_r > s$. Hence, under the risk-neutral measure $\widetilde{P}$, the price at time t of this caplet is given by

$$Caplet_t(r_t, s, T_r, T_s, K) = \widetilde{E}\left[e^{-\int_t^{T_r} r_u du} \max\left\{R(r_s, s, T_s) - K, 0\right\} \mid r_t\right]$$

The caplet price is provided by the following Proposition.

Proposition 10 *The price at time t of a caplet contract written on the floating rate with \$1 face value and tenor $T_s - s$ is given as*

$$\begin{aligned} Caplet_t(r_t, s, T_r, T_s, K) &= P(r_t, t, T_r)\widetilde{E}\left[(R(w_s, s, T_s) - K)^+ \mid r_t\right] \\ &= P(r_t, t, T_r)\widetilde{E}\left[\left(\frac{B(s,T_s)w_s - A(s,T_s)}{T_s - s} - K\right)^+ \mid r_t\right] \\ &= P(r_t, t, T_r)\left[\left(\mu\frac{B(s,T_s)}{T_s - s} - \frac{A(s,T_s)}{T_s - s} - K\right)\Phi(d_1) - \sigma\phi(d_1)\right] \end{aligned}$$

where $P(r_t, t, T_r)$ is given by Proposition 2, $\phi(\cdot)$ and $\Phi(\cdot)$ denote the standard normal density and distribution functions, respectively, and $d_1 = \frac{\mu B(s,T_s) - A(s,T_s) - (T_s - s)K}{B(s,T_s)\sigma}$, and $\mu = \widetilde{E}[w_s \mid r_t]$ and $\sigma^2 = \widetilde{V}[w_s \mid r_t]$ are given by equations (1.14)-(1.15), respectively. ∎

Floorlet pricing arises from similar calculations as those in the above Proposition. Alternatively, we can use the caplet-floorlet parity.

Cap, floor, and collar prices are an immediate application of these results.

1.4 Risk Management

We now use the closed-form expressions we have obtained for the derivatives' prices to compute several risk measures for zero-coupon bonds, as well as Greeks and specific sensitivity measures for a European call option on a zero-coupon bond.

Firstly, consider a zero-coupon bond whose price is given by Proposition 3. As it is well known, the two major bond risk measures are duration and convexity. The duration measures the percentage change in the bond price with respect to changes in interest rates while the convexity measures the sensitivity of duration to changes in interest rates. The next Proposition provides mathematical expressions for both of them.

Proposition 11 *The duration and convexity for a zero-coupon bond are given as*

$$\begin{aligned} Duration &= -\frac{1}{P(r_t, t, T)}\frac{\partial P(r_t, t, T)}{\partial r_t} = B(t, T) \\ Convexity &= \frac{1}{P(r_t, t, T)}\frac{\partial^2 P(t_t, t, T)}{\partial r_t^2} = B^2(t, T) \end{aligned}$$

where $B(t, T)$ is given by equation (1.13). ∎

We now consider a European call option with strike K that matures at time T_c on a zero-coupon bond that matures at time $T_b > T_c$. The price of this option at time t is given by Proposition 6.

The Greeks of the option indicate price sensitivities with respect to some variables. We focus on delta, gamma, and vega. The first two measures indicate sensitivity of the option price with respect to the underlying asset price while vega reflects the effect of changes in the underlying return volatility on the derivative price. The expressions for these Greeks are provided by the following Proposition.

Proposition 12 *The mathematical expressions for the delta, gamma, and vega at time t for a European call option with strike K that matures at time T_c on a zero-coupon bond that matures at time $T_b > T_c$ are given as*

$$\begin{aligned}
\Delta &= \Phi(d_1) \\
\Gamma &= \frac{\phi(d_1)}{P(r_t,t,T_c)F(r_t,t,T_c,T_b)B(T_c,T_b)\sqrt{\widetilde{V}[w_{T_c} \mid r_t]}} \\
\nu &= P(r_t,t,T_c)F(r_t,t,T_c,T_b)\frac{\phi(d_1)}{\sigma}\sqrt{\widetilde{V}[w_{T_c} \mid r_t]}
\end{aligned}$$

where $\Phi(\cdot)$ and $\phi(\cdot)$ denote the standard normal distribution and density functions, respectively, d_1 is given by Proposition 6, $P(r_t,t,T_c)$ and $B(T_c,T_b)$ are given by Proposition 3, $F(r_t,t,T_c,T_b)$ as given by Proposition 5, and $\widetilde{V}[w_{T_c} \mid r_t]$ is given by equation (1.15). ∎

Finally, from a risk management perspective, it is important to analyze the sensitivity of the option price to each of the parameters incorporated into the Fourier component of the long-term level of interest rates. The following proposition describes how a European call option on a zero-coupon bond reacts to changes in the Fourier parameters: the amplitude $A_{n,x}$, the phase $A_{n,y}$, and the temporal frequency ω. These sensitivities are directly obtained using Proposition 6.

Proposition 13 *The sensitivities of the price of a European call option on a zero-coupon bond with respect to the mean reversion parameters are given by:*

$$\begin{aligned}
\frac{\partial c_t(r_t,T_c,T_b,K)}{\partial x} &= P(r_t,t,T_c)F(r_t,t,T_c,T_b)\left(\frac{\partial A(t,T_c)}{\partial x}+\frac{\partial A(T_c,T_b)}{\partial x}-B(T_c,T_b)\frac{\partial \widetilde{E}\left[w_{T_c} \mid r_t\right]}{\partial x}\right)\Phi(d_1) \\
&\quad -KP(r_t,t,T_c)\frac{\partial A(t,T_c)}{\partial x}\Phi(d_2), \quad x = A_{n,x}, A_{n,y}, w
\end{aligned}$$

with $P(r_t,t,T_c)$ and $F(r_t,t,T_c,T_b)$ as given by Propositions 2 and 5, respectively, $B(T_c,T_b)$ as given by (1.13), $\Phi(\cdot)$ denotes the standard normal distribution function, and $\partial A(\cdot,\cdot)/\partial x$ and $\partial \widetilde{E}\left[w_{T_c} \mid r_t\right]/\partial x$ are obtained differentiating (1.12) and (1.14) with respect to the appropriate argument, respectively.

∎

1.5 Empirical Analysis

In this section we analyze the empirical performance of our proposed Fourier model of the term structure, versus two benchmarks, Vasicek (1977) and Nelson and Siegel (1987). Since we have analytical expressions for interest rates, bond prices and derivative prices, we could use realized data on either of these variables to evaluate the model. The reason why we opt for using interest rate data is that a good fit of the term structure and hence, of the discount function for future cash flows, should suggest a potentially good fit of bond and derivative prices. Alternatively, it is unclear that a relatively good fit of bond or derivative prices might necessarily imply a good fit of the term structure. However, we consider analyzing the performance of our model for bond and derivative prices as an interesting issue for further research.

To keep simple the specification of our model, we will just consider the first term in the Fourier series in (3.7), $n = 1$. As mentioned before, the Vasicek specification is a special case of our model, while Nelson and Siegel (1987) suggested to model the yield curve at a point in time by,

$$R(\tau) = \beta_1 + \beta_2 \left(\frac{1 - \exp(-\lambda\tau)}{\lambda\tau} \right) + \beta_3 \left(\frac{1 - \exp(-\lambda\tau)}{\lambda\tau} - \exp(-\lambda\tau) \right) \tag{1.19}$$

where τ is time to maturity, and $\beta_1, \beta_2, \beta_3, \lambda$ are constant parameters. The parameters $\beta_1, \beta_2, \beta_3$ are closely related to the level, slope and curvature of the yield curve, respectively, while λ governs the exponentially decay rate. This is an interesting benchmark since it is one of the most popular models of the yield curve, being used in many central banks in the implementation and evaluation of monetary policy. Besides, Diebold and Li (2006) showed the good forecasting performance of the Nelson-Siegel model in comparison with ten alternative competitors, including Fama and Bliss (1987) and Cochrane and Piazzesi (2005), among others.

1.5.1 Data

The data set used for the empirical study consists of daily US Treasury yield curve rates. In more detail, we take daily observations of the Treasury constant maturity interest rates for 1, 3, and 6 months and for 1, 2, 3, 5, 7, 10, 20, and 30 years, from July 31, 2001 up to September 21, 2012. The 30-year Treasury constant maturity series was discontinued on February 18, 2002, and reintroduced on February 9, 2006. During this period, the US Treasury published an adjustment factor that allowed for estimation of the 30-year nominal rate from the observed daily nominal 20-year interest rate. Figure 1.7 presents a 3-D plot of the yield curve for the whole period and the maturities mentioned.

In the last part of the sample, short rates took very low values, being equal to zero at some point. We will therefore use absolute measures when evaluating forecasts since at those interest rate levels, relative measures of forecast errors might be huge even for small absolute errors.

1.5.2 In-sample model fitting

We start by assessing the in-sample fitting of the three models. For this purpose, we employ the whole sample period, with 2790 daily observations for interest rates at each maturity.

Corollary 6 allows us to formulate the problem of minimizing the sum of squared pricing errors in the form of a regression model. Indeed, the structural parameters of the yield curve for the Fourier model, taking just the first term in (3.7) can be estimated, for each maturity j, from:

$$Y_{j,t} = \delta_1 z_{1j,t} + \delta_2 z_{2j,t} + \delta_3 z_{3j,t} + \delta_4 z_{4j,t} + u_{j,t} \tag{1.20}$$

where:

$$\begin{aligned} Y_{j,t} &= R(r_t, t, T) - \frac{B(t,T)}{T-t} r_t \\ z_{1j,t} &= \frac{B(t,T)}{T-t} - 1 \\ z_{2j,t} &= \frac{1}{2\kappa^2} - \frac{B(t,T)}{(T-t)\kappa^2} + \frac{1-e^{-2\kappa(T-t)}}{4(T-t)\kappa^3} \\ \text{with } B(t,T) &= \frac{1-e^{-\kappa(T-t)}}{\kappa}, \text{and} \\ \delta_1 &= \alpha,\ \delta_2 = \sigma^2,\ \delta_3 = A_x, \delta_4 = A_y. \end{aligned}$$

while the term $Re\left[(A_x + iA_y)\left(\frac{e^{i\omega t}\left(\omega e^{-\kappa(T-t)} + i\kappa - \omega\right) - i\kappa e^{i\omega T}}{\omega(\kappa + i\omega)}\right)\right]$ that appears in the expression for $P(r_t, t, T)$ in Proposition (3) subject to Corollary 6 derives in $\delta_3 z_{3t} + \delta_4 z_{4t}$.[4]

The error term u_t in model (1.20) can be interpreted as the approximation error in the practical implementation of the pricing formula because of taking just one term of the infinite Fourier expansion. The difficulty with this model is that the explanatory variables are functions of the structural parameters κ and ω, so we cannot proceed to estimate as in a simple regression involving observable variables. We estimate the model each day using the cross section of observed interest rates solving a nonlinear optimization problem that searches for the values of $\kappa, \omega, \delta_1, \delta_2, \delta_3$,and δ_4 that minimize the sum of squared residuals in (1.20), $\text{SR}(\hat{\theta}_t) = \sum_{j,t} [Y_{j,t} - (\delta_1 z_{1j,t} + \delta_2 z_{2j,t} + \delta_3 z_{3j,t} + \delta_4 z_{4j,t} + u_{j,t})]^2$.

[4]

$$\begin{aligned} & Re\left[-(A_x + iA_y)\left(\frac{e^{i\omega t}\left(\omega e^{-\kappa(T-t)} + i\kappa - \omega\right) - i\kappa e^{i\omega T}}{\omega(\kappa + i\omega)(T-t)}\right)\right] = \\ & \frac{A_x}{\omega(\kappa^2+\omega^2)(T-t)}\left\{-\kappa\omega\cos(\omega t)e^{-\kappa(T-t)} - \kappa^2(\sin(\omega T) - \sin(\omega t)) - \omega^2\sin(\omega t)\left(e^{-\kappa(T-t)} - 1\right) + \kappa\omega\cos(\omega T)\right\} + \\ & \frac{A_y}{\omega(\kappa^2+\omega^2)(T-t)}\left\{\kappa\omega\sin(\omega t)e^{-\kappa(T-t)} - \kappa^2(\cos(\omega T) - \cos(\omega t)) - \omega^2\cos(\omega t)\left(e^{-\kappa(T-t)} - 1\right) - \kappa\omega\sin(\omega T)\right\} = \\ = \quad & A_x z_{3t} + A_y z_{4t}. \end{aligned}$$

After estimation, we recover the values of the structural parameters $\theta = \left(\alpha, \sigma^2, A_x, A_y, \kappa, \omega\right)$. As a result, we obtain time series for each parameter in θ over the sample period, July 31, 2001 to September 21, 2012.

The Vasicek model obtains when setting $z_{3t} = z_{4t} = 0$ in (1.20). We then estimate the structural parameters $\theta = \left(\alpha, \sigma^2, \kappa\right)$. From the Nelson-Siegel model (1.19), we directly obtain daily estimates for the structural parameters $\theta = (\beta_1, \beta_2, \beta_3, \lambda)$.

Each day we take as initial conditions in estimation the estimates obtained for the previous day. We used the level of the long-term 30-year rate each day as initial condition to estimate δ_1 and β_1. To avoid potential instability in parameter estimates, we imposed an upper bound on daily changes.

Table 1.2 presents the mean and standard deviation of daily estimated parameters over the whole sample. We also show for each model some indication of its ability to fit the observed daily yield curves, through the minimized numerical value of the objective function $\sum_{i,t} \min \mathrm{SR}(\hat{\theta}_t)$, as well as $\sum_{i,t} |\hat{u}_{i,t}|$, the sum of the absolute value of pricing errors, over the whole sample and across all maturities. We can see how the Fourier model provides a significantly better in-sample fitting of the observed yield curve, outperforming both alternative benchmarks. The Fourier model reduces the aggregate sum of squares by 24% relative to the Nelson Siegel model, both of them reducing by 76% and 82% the sum of squares of the Vasicek benchmark.[5] This is an interesting result since we are estimating the Fourier model with $n = 1$. It is encouraging to know that we do not need to go farther away in the Fourier series to achieve a good representation of the term structure.[6] Increasing the number of terms in the Fourier expansion would eventually allow for fitting arbitrarily well the observed yield curve, eventually leading to a no-arbitrage model of the term structure.

Figures 1.8 to 1.10 show the time evolution of estimated parameters for the three models. Parameters for the Fourier model are relatively stable, except for σ^2. However, a cross-section of data is not too adequate to properly identify the value of σ, the size of fluctuations in the spot rate over time. In fact daily estimates of σ turn out to be negligible except for clusters of days distributed over the sample. It is better to examine the ratio σ/κ, since σ enters into the bond valuation formula only through that ratio, as part of the $A(t,T)$ term. in Figure 1.11 we can see how the σ/κ-ratio[7] tends to take higher values during the period when the spot rate, represented by the one-month rate, raises from 1% to 5% to then decrease to the neighborhood of 0%. Over that period, the contribution of the σ/κ-ratio to the first term in $A(t,T)$ is numerically significant. The contribution

[5]The Fourier model reduces the sum of absolute values of fitting errors over the whole sample by 11% relative to the Nelson Siegel model, both of them reducing this statistic by 55% and 60% realtive to the Vasicek benchmark.

[6]Imposing upper bounds on daily parameter changes constitutes a serious disadvantage for Fourier model, which it would deliver an aggregate sum of squares errors of 0.0055 by imposing no restrictions, with an improvement of 74% relative to Nelson-Siegel model.

[7]Figure 1.11 displays the value of $\sqrt{\sigma^2/\kappa^2}$ throughout the sample period. Notice that the square of this ratio enters in the $A(t,T)$ term in the expresion for the price of a bond.

of the σ/κ-ratio is essentially zero anywhere else, except towards the end of the sample, in this case without any correlation with movements in the spot rate.

The speed of reversion of the spot rate to its long-term level oscillates between 0.03 and 0.67, with a mean value $\bar{\kappa} = 0.27$. Estimating a representative value for the σ parameter through the product of the sample average of $|\sigma/\kappa|$ times the sample average of κ leads to $\hat{\sigma} = 0.0080$.

Parameters for Vasicek model display a behaviour similar to the analogous parameters in the Fourier model, although we had to impose an upper bond in the value of κ, the speed of mean reversion, which was reached over the central part of the sample. Estimated parameters for Nelson Siegel behave over time as expected, given the observed time evolution of interest rates. The β_1 parameter follows the fluctuations in interest rates at the longest maturity. The correlation between daily estimates of β_1 and the 30-year interest rate is 0.9390. The sum of β_1 and β_2 closely follows the shortest interest rate. The correlation between the sum of these two parameters and the 1-month interest rate is 0.9986.

1.6 Out-of-sample forecasting

Having compared the in-sample fit of the three models of the yield curve, we now analyze their forecasting performance. Given the good in-sample fit of the Fourier model, we maintain the simplest choice of $n = 1$ when computing out-of-sample forecasts. During the last ten years in the sample the yield curve adopted very different shapes. Hence, we consider three different moments in time to asses the forecasting power of each model. Figure 1.12 shows the observed term structure surface for the three forecast periods chosen, each of them providing a different scenario to stress the strengths and weaknesses of each model. The first forecasting period covers from August 3, 2004 to August 2, 2005, that is 251 daily points. The second forecasting period ranges from August 2, 2006 to July 31, 2007, with 251 daily points. Finally, the third period covers the most recent period, from September 20, 2011 up to September 21, 2012, with 254 daily points. Each period approximately covers one year.

The forecast exercise consists in finding predicted parameters, $\hat{\theta}$, over the forecasting horizon for each model, assuming the parameter vector follows in each case a first-order autoregressive process,

$$\hat{\theta}_t = \hat{c} + \gamma \cdot \hat{\theta}_{t-1} + \varepsilon_t$$

where ε_t represents a vector white noise process. Over a given forecasting period, we take each day the time series for estimated parameter values up to that day, estimate a vector autoregression of order one, and forecast parameter values for the required forecast horizon, $h = 1, 5, 21$ days ahead. Since the Fourier and Vasicek models are both short rate models, we first obtain the forecast $E[r_{t+\Delta t}|r_t]$ where $\Delta t = 1, 5, 21$, for the instantaneous rate, from the Euler discretization: $E[r_{t+\Delta t}|r_t] = r_t +$

$\kappa(\mu - r_t)\Delta t$, where μ is a single parameter in the Vasicek model, and it is a nonlinear function of the structural parameters in our proposed Fourier model. From this forecast, we can readily obtained forecasts for interest rates at other maturities. This computation can be seen in (1.20), where we need to solve for $R(r_{j,t}, t, T)$ given parameter estimates and the forecast $E\left[r_{t+\Delta t}|r_t\right]$ for the spot rate.

1.6.1 From an upward-sloping to a flat yield curve: August 3, 2004 to August 2, 2005

The first forecasting period, from August 3, 2004 to August 2, 2005, is highly interesting because of the significant changes in the term structure over time. At the beginning of the sample the term structure is upward sloping, with yield levels increasing with maturity to a spread between short and long rates of around 3%. However, at the end of the sample the gap among maturities drops to less than 1%. Figure 1.13 presents the observed time-series yield for maturities from 1 month up to 30 years. We see a significant change over time, with short rates displaying a noticeable increment of more than 2 percentage points between 08/03/2004 and 08/02/2005. Medium term yields display a convergence to a common level of around 4% at the end of the period. On the other hand, long rates maintain a roughly constant level over the whole period, except for the 20 and 30-year rates, which decrease somewhat. From 01/12/2005 on, the 20-year rate exceeds the 30-year rate, an interesting particularity corresponding to humped yield curves. This first forecasting period can give us some insights on how each model responds to changes in the shape of the term structure as well as to changes in the levels of interest rates.

Figure 1.14 presents the mean forecast error in basis points for the three models for forecasting horizons of $h = 1, 5, 21$ days. Tables 1.3 to 1.5 summarize the size of forecast errors for each model and maturity. The Fourier model consistently beats its competitors in one-day ahead forecasting. For larger forecasting horizons of 5 or 21-days ahead, the Fourier model still provides better predictions than its competitors although the gap narrows at some maturities.

Figure 1.15 shows 1-day ahead predictions from each model for 1 to 5-year maturities, as well as the corresponding forecasting error, in absolute value. We can see that the three models have a good forecasting performance at the beginning of the sample, when the term structure has a clear upward increasing shape. At the beginning of 2005, as well as in the last part of the sample, the Fourier model predicts clearly better than Vasicek and Nelson-Siegel models, specially at 2- and 5-year maturities.

Over this period, the Fourier model has the lowest sum of squared forecast errors in 23 of the 33 comparisons over maturity and forecasting horizon. The Nelson-Siegel model has the lowest sum of squared errors in 8 comparisons, and the Vasicek model is best in 2 of the comparisons. Using the

sum of absolute square errors turns out very similar results in the three forecasting periods.

1.6.2 Erratic short-tem rates: August 2, 2006 to July 31, 2007

Figure 1.16 presents the observed time-series yield for each maturity ranging from 1 month up to 30 years for the second forecasting period, from August 2, 2006 to July 31, 2007. This period is more erratic with several ups and downs in yield levels, specially at the shorter maturities. Over such changes in levels, the term structure remains relatively flat, with short, medium and long rate maturities remaining close to each other over the whole period.

Figure 1.17 presents the mean forecast error in basis points for the three models, while Tables 1.6 to 1.8 summarize forecasting errors for each model and maturity. Figure 1.17 confirms what intuition has led us to expect, that under such chaotic scenario no model has a nice forecasting performance at all. In particular, the performance of the Vasicek model seriously deteriorates for long rates at each forecasting horizon.

Figure 1.16 shows the 1 month rate presenting several fluctuations in level over the forecasting period. None of the three models seems to anticipate this behaviour when the forecast horizon is 21 days. For the shorter 1 and 5-day forecasting horizons, the Fourier and Vasicek models deliver significant better predictions than the Nelson-Siegel model.

In this forecasting period, the Vasicek model is more competitive, achieving the lowest sum of squared errors in 8 of the 33 comparisons over maturity and forecasting horizon. The Fourier model has the lowest sum of squared errors in 13 of the 33 cases, versus 12 comparisons in which the Nelson-Siegel model has the lowest sum of squared errors.

1.6.3 Stable, low interest rates: September 20, 2011 to September 21, 2012

A glance to realized yields from September 20, 2011 to September 21, 2012, in Figure 1.12, shows that yield levels drastically differ with maturity. In addition, since yield levels at the shortest maturities are extremely low during the whole period, then even a slight deviation from the realized yield produces a huge relative error. Considering the limitations and particularities stated above it is interesting to analyze the forecasting results by maturity.

Figure 1.19 presents the mean forecast error in basis points for the three models. We have intentionally truncated these graphs, because the magnitude of forecasting errors for the Vasicek model at some maturities largely exceeds its model competitors. Tables 1.9 to 1.11 summarize forecast errors for each model and maturity. An interesting fact is that, over this period, the Nelson-Siegel model forecasts for short rates up to 1 year are very poor for every forecasting horizon. On average, the Fourier model again outperforms both competitors, although its forecasting efficiency tends to deteriorate for longer maturities and forecasting horizons.

Figure 1.18 shows the observed time-series yield for each maturity, ranging from 1 month up to 30 years. Roughly speaking, maturities larger than 1 year fluctuate around a mean value during the whole period. Nevertheless, for maturities between 1 and 12 months we can appreciate two different subsamples: a first one, from 09/20/2011 up to 02/14/2012, and a second one, from 02/15/2012 up to 09/21/2012, when there seems to be a change in the mean. We expect that the errors for these yields around 02/15/2012 will tell us something about the performance of each model in the presence of a change in the data structure. In this analysis we have excluded the Vasicek model, focusing our comparison on the Fourier and the Nelson-Siegel models. Figures 1.20 to 1.22 present the time-series of errors in absolute value around the critical date. We can see that for every maturity and forecasting horizon, the Fourier model outperforms the Nelson-Siegel model, producing sharper yield rate predictions in those dates where the data structure changes and suggesting that the Fourier model is more flexible and incorporates this type of anomalies faster that its model competitor.

In this later forecasting period, the Fourier model again has the best forecasting performance, achieving the lowest sum of squared forecast errors in 25 of the 33 comparisons. The Nelson-Siegel model has the lowest sum of squared errors in 7 comparisons, and the Vasicek model in just one of them.

Considering the three forecasting periods together, we can conclude that, on average, the Fourier model outperforms the Vasicek and the Nelson-Siegel models. We have found instances in which the Vasicek and the Nelson-Siegel models produce forecast errors much higher in absolute size than their competitors. That has not been the case for the Fourier model. When the Fourier model is beaten by the Vasicek and Nelson-Siegel models, the difference in forecasting performance is usually quite narrow. This should be an additional important consideration in favor of preferring our proposed Fourier model relative to the Vasicek and Nelson-Siegel alternatives to forecast the term structure.

1.7 Conclusions

We have introduced a new continuous-time model for the term structure of interest rates by assuming that the instantaneous spot rate reverts to a mean level described by a Fourier series. Such specification incorporates a good deal of flexibility, allowing the model to capture a variety of different shapes of the term structure. Our model nests the original one presented in Vasicek (1977), while preserving the analytical tractability of the Vasicek model. Even in its simplest representation, based on a single term of the Fourier expansion, our model is capable of replicating different yield curve shapes: upward sloping, downward sloping, humped, and inverted humped. Moreover, since the yield curve function belongs to a Hilbert space $L^2([t,T])$, any observed yield curve can be perfectly fitted in the mean-quadratic sense by our model by letting an arbitrarily large number of

terms in the Fourier expansion.

Under this framework, we have obtained analytical expressions for the prices of bonds and several fixed income derivatives. Additionally, we have computed risk management measures for bonds, Greeks for European bond options, and performed a sensitivity analysis on the model's parameters.

We have also analysed the empirical performance, both in- and out-of-sample, of the simplest version of the model against two different benchmarks, those proposed in Vasicek (1977) and Nelson and Siegel (1987). Our empirical findings show that the Fourier model provides a better and more reliable in- and out-of-sample estimation of the yield curve, outperforming both benchmark models and providing more accurate forecasts. Furthermore, when it is dominated by its alternatives, the difference in performance is relatively small. These results are very relevant, suggesting that our proposed Fourier model provides a simple and powerful tool for portfolio management, risk management and derivative pricing.

1.8 Appendix of Proofs

Proof of Proposition 4

Define $Y_T = \int_t^T r_s ds$. Since both Y_T and r_T are random normal variables, their joint density function is given by

$$\varphi(r_T; Y_T) = \frac{1}{2\pi\sigma_1\sigma_2} e^{-\frac{1}{2}\frac{\xi}{1-\rho^2}}$$

where

$$\begin{aligned}
\sigma_1 &= \sqrt{\widetilde{V}(r_T|r_t)} \\
\sigma_2 &= \sqrt{\widetilde{V}(Y_T|r_t)(1-\rho^2)} \\
\rho &= \frac{\widetilde{Cov}(r_T; Y_T|r_t)}{\sqrt{\widetilde{V}(r_T|r_t)\widetilde{V}(Y_T|r_t)}} \\
\xi &= \frac{[r_T - \widetilde{E}(r_T|r_t)]^2}{\widetilde{V}(r_T|r_t)} + \frac{[Y_T - \widetilde{E}(Y_T|r_t)]^2}{\widetilde{V}(Y_T|r_t)} - \frac{2\rho[r_T - \widetilde{E}(r_T|r_t)][Y_T - \widetilde{E}(Y_T|r_t)]}{\sqrt{\widetilde{V}(r_T|r_t)\widetilde{V}(Y_T|r_t)}}
\end{aligned}$$

We have previously computed the conditional expectation and variance for both r_T and Y_T (see equations (1.6)-(1.7) and (1.10)-(1.11)). We now compute the covariance between both variables:

$$\begin{aligned}
\widetilde{Cov}[r_T; Y_T \mid r_t] &= \widetilde{E}\left[\left(\sigma\int_t^T e^{-\kappa(T-u)}d\widetilde{W}_u\right)\left(\sigma\int_t^T\int_t^s e^{-\kappa(s-u)}d\widetilde{W}_u ds\right) \mid r_t\right] \\
&= \sigma^2\int_t^T ds\int_t^s e^{-\kappa(T+s-2u)}du = \frac{\sigma^2}{2\kappa^2}\left(1-e^{-\kappa(T-t)}\right)^2
\end{aligned}$$

The price at time t of the derivative, $U_t(r_t, t, T)$, is equal to the discounted expected pay-off under the risk-neutral measure, that is,

$$U_t(r_t, t, T) = \widetilde{E}\left[e^{-Y_T}U_T(r_T) \mid r_t\right] = \int_{-\infty}^{\infty}\int_{-\infty}^{\infty} e^{-Y_T}U_T(r_T)\varphi(r_T; Y_T)dY_T dr_T$$

Completing the square for Y_T and r_T in $\varphi(r_T; Y_T)e^{-Y_T}$ and setting

$$\begin{aligned}
\mu_1 &= \widetilde{E}(r_T|r_t) - \widetilde{Cov}(r_T; Y_T|r_t) \\
\mu_2 &= \widetilde{E}(Y_T|r_t) - \widetilde{V}(Y_T|r_t)(1-\rho^2) + \frac{\sqrt{\widetilde{V}(Y_T|r_t)}\rho[r_T - \widetilde{E}(r_T|r_t)]}{\sqrt{\widetilde{V}(r_T|r_t)}}
\end{aligned}$$

we get

$$\begin{aligned}
\varphi(r_T; Y_T)e^{-Y_T} &= \frac{1}{2\pi\sigma_1\sigma_2}\exp\left\{-\frac{1}{2}\left(\frac{Y_T-\mu_2}{\sigma_2}\right)^2 - \frac{1}{2}\left(\frac{r_T-\mu_1}{\sigma_1}\right)^2 - \widetilde{E}(Y_T|r_t) + \frac{1}{2}\widetilde{V}(Y_T|r_t)\right\} \\
&= P(r_t, t, T)\varphi(\mu_1; \sigma_1)\varphi(\mu_2; \sigma_2)
\end{aligned}$$

Therefore

$$\begin{aligned} U_t(r_t,t,T) &= P(r_t,t,T)\int_{-\infty}^{\infty} U_T(r_T)\varphi(\mu_1;\sigma_1)dr_T \int_{-\infty}^{\infty}\varphi(\mu_2;\sigma_2)dY_T \\ &= P(r_t,t,T)\int_{-\infty}^{\infty} U_T(r_T)\varphi(\mu_1;\sigma_1)dr_T \end{aligned}$$

or, equivalently,

$$U_t(r_t,t,T) = P(r_t,t,T)\widetilde{E}\left[U_T(w_T)\mid r_t\right],\ w_T \sim N(\mu_1,\sigma_1^2)$$

■

1.9 Appendix of Tables

Table 1.1: Term Structure Models.

Author(s)	Model Specification	
Merton (1973)	$dr = \theta dt + \sigma dw$	$\theta,\ \sigma$ are constant
Vasicek (1977)	$dr = \kappa(\theta - r)dt + \sigma dw$	$\kappa,\ \theta,\ \sigma$ are constant
Cox *et al.* (1985)	$dr = \kappa(\theta - r)dt + \sigma\sqrt{r}dw$	$\kappa,\ \theta,\ \sigma$ are constant
Chan *et al.* (1992)	$dr = \kappa(\theta - r)dt + \sigma r^{\gamma}dw$	$\kappa,\ \theta,\ \sigma,\ \gamma$ are constant
Ho and Lee (1986)	$dr = \theta_t dt + \sigma dw$	θ_t is time-varying and σ is constant
Black *et al.* (1990)	$d\ln(r) = \left[\theta_t - \frac{\sigma_t'}{\sigma_t}\ln(r)\right]dt + \sigma_t dw$	$\theta_t,\ \sigma_t$ are time-varying
Hull and White (1990, 1993)	$dr = \kappa(\theta_t - r)dt + \sigma_t r^{\gamma}dw$	$\theta_t,\ \sigma_t$ are time-varying, $\gamma = 0, 1/2$
Black and Karasinski (1991)	$d\ln(r) = \phi_t\left[\ln(\mu_t) - \ln(r)\right]dt + \sigma_t dw$	$\phi_t,\ \mu_t$ are time-varying
Heath *et al.* (1992)	$df = \alpha_t dt + \sigma_t dw$	f is the forward rate
Mercurio and Moraleda (2000)	$dr = r\left[\eta_t - \left(\lambda - \frac{\gamma}{1+\gamma t}\right)\ln(r)\right]dt + \sigma r dw$	η_t is time-varying and $\lambda,\ \gamma,\ \sigma$ are constant
Brennan and Schwartz (1979)	$dr = \theta_r dt + \sigma_{r1}dw_1 + \sigma_{r2}dw_2$	$\theta_i,\ \sigma_{ij},\ i = r, l,\ j = 1, 2$
	$dl = \theta_l dt + \sigma_{l1}dw_1 + \sigma_{l2}dw_2$	are constant
Schaefer and Schwartz (1984)	$ds = m(\mu - s)dt + \eta dw_1$	$m,\ \mu,\ \eta,\ \sigma$
	$dl = (\sigma^2 - ls)dt + \sigma\sqrt{l}dw_2$	are constant
Longstaff and Schwartz (1992)	$dx = (\gamma - \delta x)dt + \sqrt{x}dw_1$	$\gamma,\ \delta,\ \eta,\ \nu$ are constant
	$dy = (\eta - \nu y)dt + \sqrt{y}dw_2$	
Duffie and Kan (1996)	$dX_1 = (b_1 + \sum_{i=1}^{2} a_{1i}X_i)dt + \sigma_{11}\sqrt{\alpha_1 + \sum_{i=1}^{2}\beta_{1i}X_i}dw_1$	$X_i,\ i = 1, 2$ are the yields
	$dX_2 = (b_2 + \sum_{i=1}^{2} a_{2i}X_i)dt + \sigma_{22}\sqrt{\alpha_2 + \sum_{i=1}^{2}\beta_{2i}X_i}dw_2$	of two zero-coupon bonds
Chen (1996)	$dr = \kappa(\theta - r)dt + \sqrt{\sigma}\sqrt{r}dw_1$	$\kappa,\ \nu,\ \hat{\theta},\ \zeta,\ \mu,\ \hat{\sigma},\ \eta$
	$d\theta = \nu(\hat{\theta} - \theta)dt + \zeta\sqrt{\theta}dw_2$	are constant
	$d\sigma = \mu(\hat{\sigma} - \sigma)dt + \eta\sqrt{\sigma}dw_3$	
Fourier Model	$dr = \kappa(f(t) - r)dt + \sigma dw$	$f(t) = \sum_{n=0}^{\infty} Re\left[A_n e^{in\omega t}\right]$

Table 1.2: Parameters estimates. In-Sample Estimation

Parameter	Fourier	Vasicek	Nelson-Siegel
$\hat{\delta_1} * 100$	5.248(0.003)	5.338(0.035)	-
$\hat{\beta_1} * 100$	-	-	4.973(0.002)
$\hat{\delta_2} * 100$	0.040(0.000)	0.210(0.020)	-
$\hat{\beta_2} * 100$	-	-	-3.248(0.002)
$\hat{\delta}_3 * 100$	0.269(0.004)	-	-
$\hat{\beta}_3 * 100$	-	-	-2.793(0.003)
$\hat{\delta}_4 * 100$	0.100(0.005)	-	-
$\hat{\kappa}$	0.2747(0.0002)	0.3998(0.0024)	-
$\hat{\lambda}$	-	-	0.6091(0.0006)
$\hat{\omega}$	1.2409(0.0001)	-	-
$\sum_{i,t} \min \mathrm{SR}(\hat{\theta}_{i,t})$	0.0160	0.0881	0.0210
$\sum_{i,t} \lvert\hat{u}_{i,t}\rvert$	16.2672	40.0327	18.2915

Note: This table presents the mean and standard deviation of the daily estimated parameters over the whole sample. $\sum_{i,t} \min \mathrm{SR}(\hat{\theta}_{i,t})$ represents the least squares pricing error, $\sum_{i,t} \lvert\hat{u}_{i,t}\rvert$ shows the pricing errors in absolute value, both of them for the whole period and every maturity.

Table 1.3: Out-of-Sample 1-day-Ahead Forecasting errors. Period 1

	Fourier		Vasicek		Nelson-Siegel	
Maturity	$\sum_t \hat{u}_t^2$	$\sum_t \lvert\hat{u}_t\rvert$	$\sum_t \hat{u}_t^2$	$\sum_t \lvert\hat{u}_t\rvert$	$\sum_t \hat{u}_t^2$	$\sum_t \lvert\hat{u}_t\rvert$
1 month	0.0465	77	0.0469	77	0.6021	343
3 months	0.0723	106	0.1825	167	0.0407	82
6 months	0.2388	222	0.8116	402	0.4095	299
1 year	0.0566	97	0.3215	239	0.2326	217
2 years	0.0817	110	0.1953	189	0.2932	239
3 years	0.1288	145	0.0825	113	0.0615	94
5 years	0.0916	119	0.3410	251	0.2222	198
7 years	0.1631	164	0.3497	250	0.2890	221
10 years	0.1226	146	0.2061	196	0.1956	190
20 years	0.2777	238	0.5914	356	0.4668	317
30 years	0.1205	143	0.1290	148	0.0878	122
$\sum_{i,t} \hat{u}_{i,t}^2$	1.4002		3.2575		2.9007	
$\sum_{i,t} \lvert\hat{u}_{i,t}\rvert$		1568		2389		2323

Note: This table presents the size of forecast errors for each model and maturity obtained for the period 1 and the forecast horizon $h = 1$. Every value must be multiplied by a factor 10^{-3}

Table 1.4: Out-of-Sample 5-day-Ahead Forecasting errors. Period 1

	Fourier		Vasicek		Nelson-Siegel	
Maturity	$\sum_t \hat{u}_t^2$	$\sum_t \lvert\hat{u}_t\rvert$	$\sum_t \hat{u}_t^2$	$\sum_t \lvert\hat{u}_t\rvert$	$\sum_t \hat{u}_t^2$	$\sum_t \lvert\hat{u}_t\rvert$
1 month	0.1547	152	0.1608	155	0.4453	262
3 months	0.1210	138	0.2680	206	0.0763	112
6 months	0.2945	244	0.9370	431	0.6689	385
1 year	0.1111	131	0.4454	284	0.4489	301
2 years	0.2358	190	0.3733	264	0.5669	333
3 years	0.3835	264	0.2467	197	0.2607	211
5 years	0.3199	234	0.5285	295	0.4049	254
7 years	0.4056	258	0.5742	306	0.5050	285
10 years	0.3755	256	0.4490	276	0.4178	263
20 years	0.4394	265	0.7307	351	0.6173	322
30 years	0.3546	245	0.3347	241	0.2897	224
$\sum_{i,t} \hat{u}_{i,t}^2$	3.1956		5.0484		4.7019	
$\sum_{i,t} \lvert\hat{u}_{i,t}\rvert$		2377		3006		2951

Note: This table presents the size of forecast errors for each model and maturity obtained for the period 1 and the forecast horizon $h = 5$. Every value must be multiplied by a factor 10^{-3}

Table 1.5: Out-of-Sample 21-day-Ahead Forecasting errors. Period 1

	Fourier		Vasicek		Nelson-Siegel	
Maturity	$\sum_t \hat{u}_t^2$	$\sum_t \lvert\hat{u}_t\rvert$	$\sum_t \hat{u}_t^2$	$\sum_t \lvert\hat{u}_t\rvert$	$\sum_t \hat{u}_t^2$	$\sum_t \lvert\hat{u}_t\rvert$
1 month	0.5380	309	0.6287	334	0.5773	321
3 months	0.3794	254	0.7038	339	0.9795	426
6 months	0.6593	338	1.5803	534	2.5067	745
1 year	0.4945	286	1.0894	437	1.9873	625
2 years	0.9128	378	1.1499	439	2.0756	618
3 years	1.4250	486	0.9973	404	1.3280	466
5 years	1.2154	445	1.3308	480	1.1973	434
7 years	1.2893	468	1.4385	497	1.2859	458
10 years	1.2473	470	1.3112	483	1.1345	446
20 years	0.8849	368	1.0867	389	1.0305	386
30 years	1.0320	426	0.9009	396	0.8422	378
$\sum_{i,t} \hat{u}_{i,t}^2$	10.0778		12.2175		14.9450	
$\sum_{i,t} \lvert\hat{u}_{i,t}\rvert$		4227		4732		5303

Note: This table presents the size of forecast errors for each model and maturity obtained for the period 1 and the forecast horizon $h = 21$. Every value must be multiplied by a factor 10^{-3}

Table 1.6: Out-of-Sample 1-day-Ahead Forecasting errors. Period 2

	Fourier		Vasicek		Nelson-Siegel	
Maturity	$\sum_t \hat{u}_t^2$	$\sum_t \lvert\hat{u}_t\rvert$	$\sum_t \hat{u}_t^2$	$\sum_t \lvert\hat{u}_t\rvert$	$\sum_t \hat{u}_t^2$	$\sum_t \lvert\hat{u}_t\rvert$
1 month	0.0900	95	0.0899	95	0.5260	292
3 months	0.2625	209	0.3036	219	0.1073	133
6 months	0.2182	187	0.6223	334	0.4225	295
1 year	0.0567	97	0.1565	160	0.2820	248
2 years	0.1638	151	0.4237	276	0.0813	106
3 years	0.2924	236	0.5613	344	0.1250	141
5 years	0.1591	160	0.4174	300	0.1695	171
7 years	0.1628	169	0.2475	223	0.1663	170
10 years	0.1254	148	0.0814	113	0.1054	135
20 years	0.2497	226	1.0717	494	0.3772	285
30 years	0.0808	110	0.4528	299	0.0952	127
$\sum_{i,t} \hat{u}_{i,t}^2$	1.8613		4.4281		2.4579	
$\sum_{i,t} \lvert\hat{u}_{i,t}\rvert$		1788		2856		2104

Note: This table presents the size of forecast errors for each model and maturity obtained for the period 2 and the forecast horizon $h = 1$. Every value must be multiplied by a factor 10^{-3}

Table 1.7: Out-of-Sample 5-day-Ahead Forecasting errors. Period 2

	Fourier		Vasicek		Nelson-Siegel	
Maturity	$\sum_t \hat{u}_t^2$	$\sum_t \lvert\hat{u}_t\rvert$	$\sum_t \hat{u}_t^2$	$\sum_t \lvert\hat{u}_t\rvert$	$\sum_t \hat{u}_t^2$	$\sum_t \lvert\hat{u}_t\rvert$
1 month	0.4339	234	0.4276	233	0.7148	326
3 months	0.3900	251	0.4122	251	0.2316	196
6 months	0.2315	187	0.6228	331	0.4277	279
1 year	0.1245	139	0.1949	175	0.2975	235
2 years	0.3243	218	0.5669	305	0.2599	199
3 years	0.4925	297	0.7298	363	0.3440	231
5 years	0.3966	251	0.5892	325	0.3882	252
7 years	0.3707	242	0.4139	260	0.3647	244
10 years	0.3143	224	0.2365	197	0.2703	209
20 years	0.3978	263	1.2303	496	0.5243	309
30 years	0.2319	192	0.6232	328	0.2269	188
$\sum_{i,t} \hat{u}_{i,t}^2$	3.7082		6.0471		4.0497	
$\sum_{i,t} \lvert\hat{u}_{i,t}\rvert$		2499		3264		2668

Note: This table presents the size of forecast errors for each model and maturity obtained for the period 2 and the forecast horizon $h = 5$. Every value must be multiplied by a factor 10^{-3}

Table 1.8: Out-of-Sample 21-day-Ahead Forecasting errors. Period 2

	Fourier		Vasicek		Nelson-Siegel	
Maturity	$\sum_t \hat{u}_t^2$	$\sum_t \lvert\hat{u}_t\rvert$	$\sum_t \hat{u}_t^2$	$\sum_t \lvert\hat{u}_t\rvert$	$\sum_t \hat{u}_t^2$	$\sum_t \lvert\hat{u}_t\rvert$
1 month	2.0097	577	1.8642	559	2.0527	555
3 months	0.7033	372	0.6293	324	0.6968	369
6 months	0.2864	211	0.6328	304	0.4709	249
1 year	0.3490	229	0.3682	238	0.3788	245
2 years	1.0549	420	1.1371	444	0.8728	389
3 years	1.4563	487	1.4281	502	1.1828	459
5 years	1.2583	476	1.3734	492	1.3598	498
7 years	1.2391	478	1.2213	469	1.3082	489
10 years	1.1313	456	1.0437	439	1.0820	445
20 years	1.1132	418	2.0837	573	1.1412	419
30 years	0.8541	392	1.4589	485	0.6937	353
$\sum_{i,t} \hat{u}_{i,t}^2$	11.4556		13.2408		11.2398	
$\sum_{i,t} \lvert\hat{u}_{i,t}\rvert$		4515		4828		4470

Note: This table presents the size of forecast errors for each model and maturity obtained for the period 2 and the forecast horizon $h = 21$. Every value must be multiplied by a factor 10^{-3}

Table 1.9: Out-of-Sample 1-day-Ahead Forecasting errors. Period 3

	Fourier		Vasicek		Nelson-Siegel	
Maturity	$\sum_t \hat{u}_t^2$	$\sum_t \lvert\hat{u}_t\rvert$	$\sum_t \hat{u}_t^2$	$\sum_t \lvert\hat{u}_t\rvert$	$\sum_t \hat{u}_t^2$	$\sum_t \lvert\hat{u}_t\rvert$
1 month	0.0037	21	0.0038	22	0.0482	103
3 months	0.0082	39	0.0606	112	0.0087	41
6 months	0.0081	37	0.1176	153	0.0283	79
1 year	0.0038	25	0.4247	312	0.0807	139
2 years	0.0103	41	1.2825	558	0.0384	89
3 years	0.0212	59	2.2555	745	0.0691	115
5 years	0.0547	93	1.1933	528	0.1460	169
7 years	0.0823	116	0.1713	171	0.0762	107
10 years	0.0905	121	0.8881	447	0.2359	212
20 years	0.1137	135	0.3338	251	0.1273	147
30 years	0.1165	135	0.1504	153	0.1090	128
$\sum_{i,t} \hat{u}_{i,t}^2$	0.5131		6.8816		0.9677	
$\sum_{i,t} \lvert\hat{u}_{i,t}\rvert$		820		3450		1329

Note: This table presents the size of forecast errors for each model and maturity obtained for the period 3 and the forecast horizon $h = 1$. Every value must be multiplied by a factor 10^{-3}

Table 1.10: Out-of-Sample 5-day-Ahead Forecasting errors. Period 3

	Fourier		Vasicek		Nelson-Siegel	
Maturity	$\sum_t \hat{u}_t^2$	$\sum_t \lvert\hat{u}_t\rvert$	$\sum_t \hat{u}_t^2$	$\sum_t \lvert\hat{u}_t\rvert$	$\sum_t \hat{u}_t^2$	$\sum_t \lvert\hat{u}_t\rvert$
1 month	0.0090	36	0.0106	39	0.0400	88
3 months	0.0116	47	0.0786	128	0.0081	37
6 months	0.0090	38	0.1401	168	0.0427	96
1 year	0.0060	32	0.4669	327	0.1037	156
2 years	0.0291	71	1.3660	572	0.0685	111
3 years	0.0747	113	2.3855	758	0.1081	132
5 years	0.2283	185	1.3788	551	0.2866	218
7 years	0.3744	238	0.3977	250	0.3248	217
10 years	0.4289	256	1.1401	456	0.5557	294
20 years	0.5326	285	0.7249	332	0.5404	294
30 years	0.5533	288	0.5667	296	0.5365	286
$\sum_{i,t} \hat{u}_{i,t}^2$	2.2567		8.6558		2.6151	
$\sum_{i,t} \lvert\hat{u}_{i,t}\rvert$		1590		3877		1930

Note: This table presents the size of forecast errors for each model and maturity obtained for the period 3 and the forecast horizon $h = 5$. Every value must be multiplied by a factor 10^{-3}

Table 1.11: Out-of-Sample 21-day-Ahead Forecasting errors. Period 3

	Fourier		Vasicek		Nelson-Siegel	
Maturity	$\sum_t \hat{u}_t^2$	$\sum_t \lvert\hat{u}_t\rvert$	$\sum_t \hat{u}_t^2$	$\sum_t \lvert\hat{u}_t\rvert$	$\sum_t \hat{u}_t^2$	$\sum_t \lvert\hat{u}_t\rvert$
1 month	0.0177	54	0.0434	90	0.0182	55
3 months	0.0232	67	0.1645	188	0.0227	56
6 months	0.0134	46	0.2458	227	0.1198	165
1 year	0.0153	50	0.6508	387	0.2174	224
2 years	0.0733	108	1.6900	632	0.1855	185
3 years	0.1952	180	2.8375	818	0.1968	180
5 years	0.5150	288	1.8503	613	0.5543	310
7 years	0.8568	375	0.8079	375	0.7953	356
10 years	1.0476	420	1.4420	481	1.1051	423
20 years	1.3240	472	1.3640	484	1.3315	469
30 years	1.4326	483	1.3441	472	1.3651	472
$\sum_{i,t} \hat{u}_{i,t}^2$	5.5139		12.4404		5.9116	
$\sum_{i,t} \lvert\hat{u}_{i,t}\rvert$		2544		4769		2896

Note: This table presents the size of forecast errors for each model and maturity obtained for the period 3 and the forecast horizon $h = 21$. Every value must be multiplied by a factor 10^{-3}

1.10 Appendix of Figures

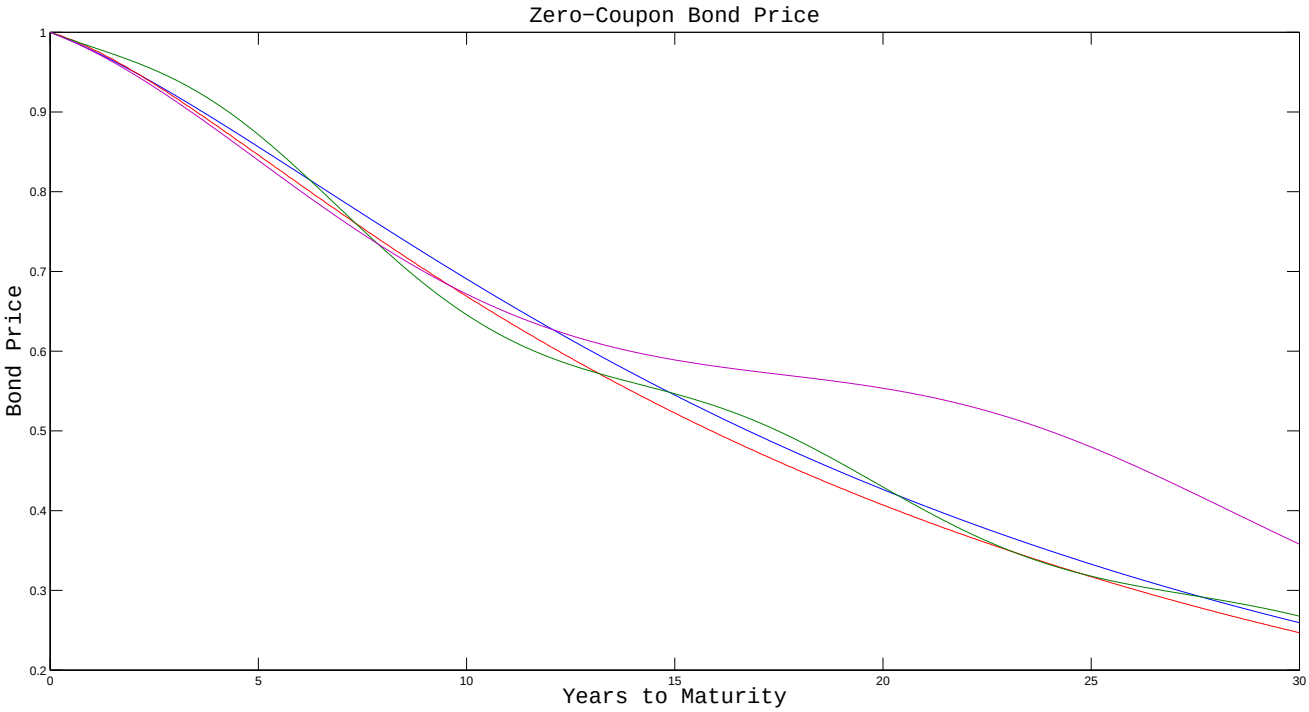

Figure 1.1: Simulation of the Zero-coupon bond price term structure for an arbitrary set of parameters.
Parameter Values Vasicek Model:
Blue line: $r_0 = 0.02,\ \alpha = 0.05,\ \sigma = 0.002,\ \kappa = 0.2.$
Parameter Values Fourier Model :
Red line: $r_0 = 0.02,\ \alpha = 0.05,\ \sigma = 0.0011,\ \kappa = 0.3397, \omega = 20, n = 5,\ A_{1,x} = 0.1758,\ A_{1,y} = 0.0402,\ A_{2,x} = -0.3011,\ A_{2,y} = 0.0172,\ A_{3,x} = 0.0498, A_{3,y} = -0.1215,\ A_{4,x} = 0.0798,\ A_{4,y} = 0.1618,\ A_{5,x} = 0.0894,\ A_{5,y} = 0.0655.$
Green line: $r_0 = 0.02,\ \alpha = 0.07,\ \sigma = 0.0005,\ \kappa = 0.018, \omega = 0.48, n = 2,\ A_{1,x} = -1.8,\ A_{1,y} = 1,\ A_{2,x} = 1.5,\ A_{2,y} = -1.5.$
Violet line: $r_0 = 0.02,\ \alpha = 0.08,\ \sigma = 0.0002,\ \kappa = 0.02, \omega = 0.25, n = 1,\ A_{1,x} = 0.3,\ A_{1,y} = 0.03$

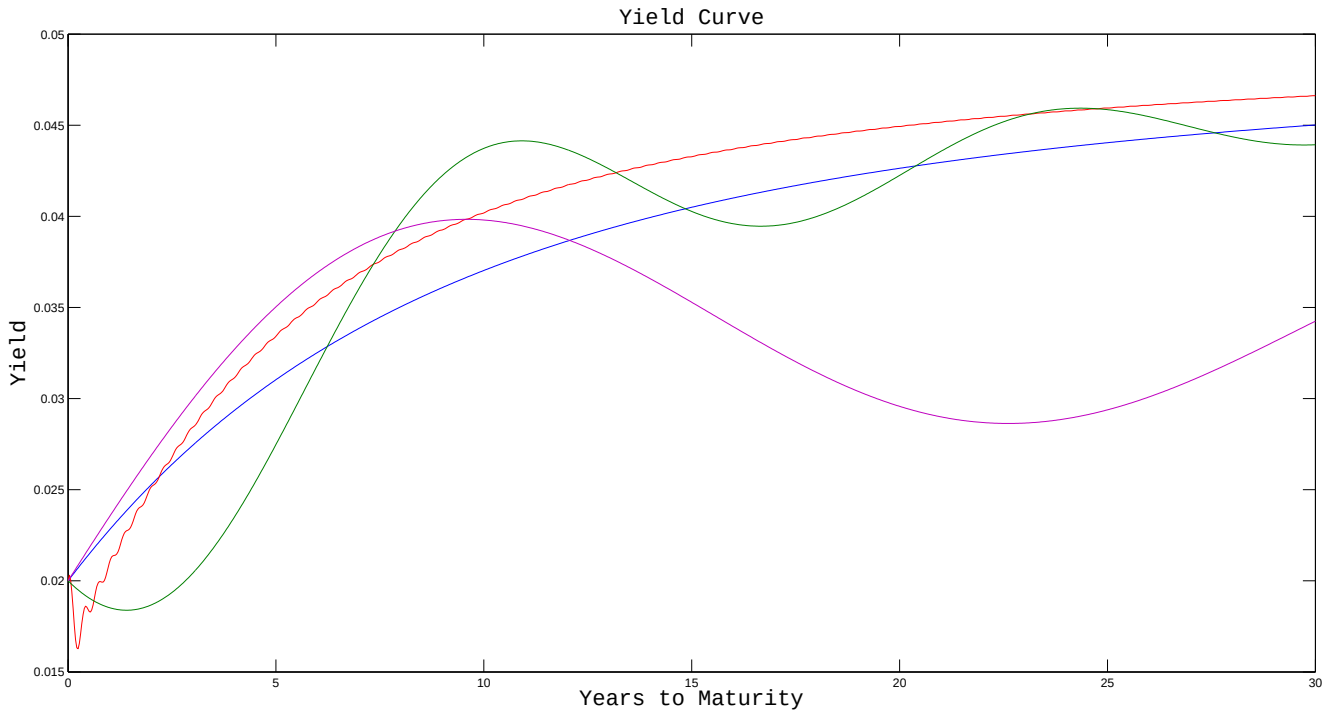

Figure 1.2: Term Structure of Interest Rates for an arbitrary set of parameters.

Parameter Values Vasicek Model:

Blue line: $r_0 = 0.02,\ \alpha = 0.05,\ \sigma = 0.002,\ \kappa = 0.2.$

Parameter Values Fourier Model:

Red line: $r_0 = 0.02,\ \alpha = 0.05,\ \sigma = 0.0011,\ \kappa = 0.3397, \omega = 20, n = 5,\ A_{1,x} = 0.1758,\ A_{1,y} = 0.0402,\ A_{2,x} = -0.3011,\ A_{2,y} = 0.0172,\ A_{3,x} = 0.0498, A_{3,y} = -0.1215,\ A_{4,x} = 0.0798,\ A_{4,y} = 0.1618,\ A_{5,x} = 0.0894,\ A_{5,y} = 0.0655.$

Green line: $r_0 = 0.02,\ \alpha = 0.07,\ \sigma = 0.0005,\ \kappa = 0.018, \omega = 0.48, n = 2,\ A_{1,x} = -1.8,\ A_{1,y} = 1,\ A_{2,x} = 1.5,\ A_{2,y} = -1.5.$

Violet line: $r_0 = 0.02,\ \alpha = 0.08,\ \sigma = 0.0002,\ \kappa = 0.02, \omega = 0.25, n = 1,\ A_{1,x} = 0.3,\ A_{1,y} = 0.03$

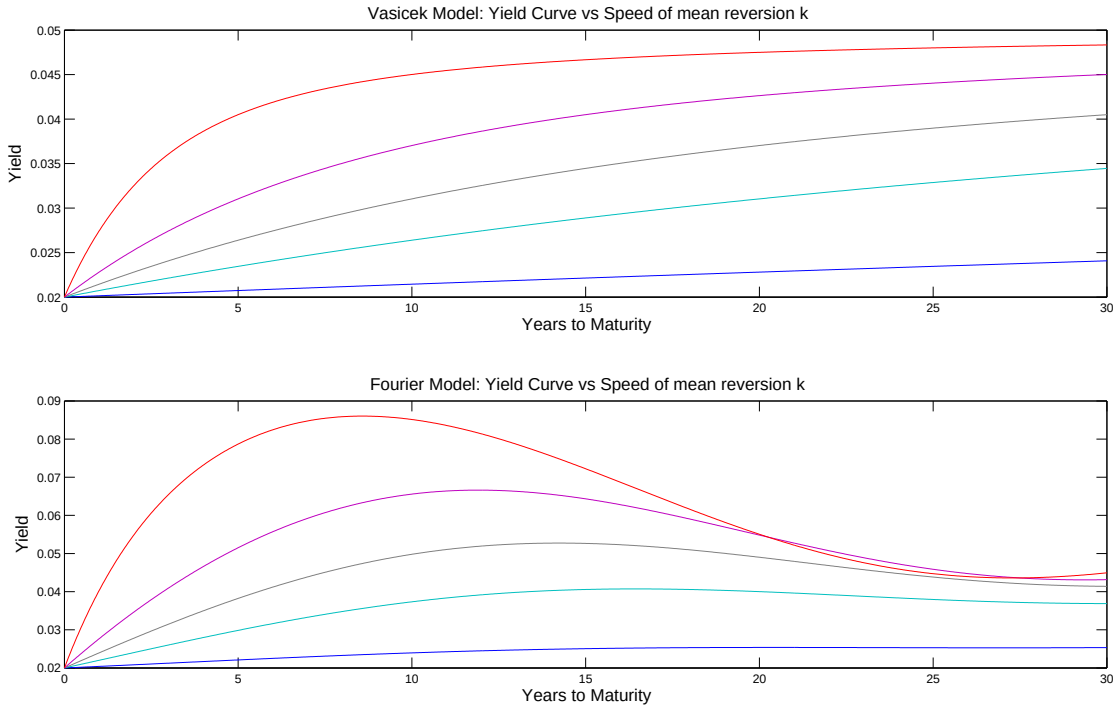

Figure 1.3: Term structure of interest rates for different values of the speed of mean reversion κ. In both models, the values of κ corresponding to the curves from the top down are $0.6, 0.2, 0.1, 0.05$, and 0.01, respectively.

Parameter Values Vasicek Model: $r_0 = 0.02,\ \alpha = 0.05,\ \sigma = 0.0002$.

Parameter Values Fourier Model: $r_0 = 0.02,\ \alpha = 0.05,\ \sigma = 0.0002, \omega = 0.20, n = 1,\ A_{1,x} = 0.05,\ A_{1,y} = -0.03$.

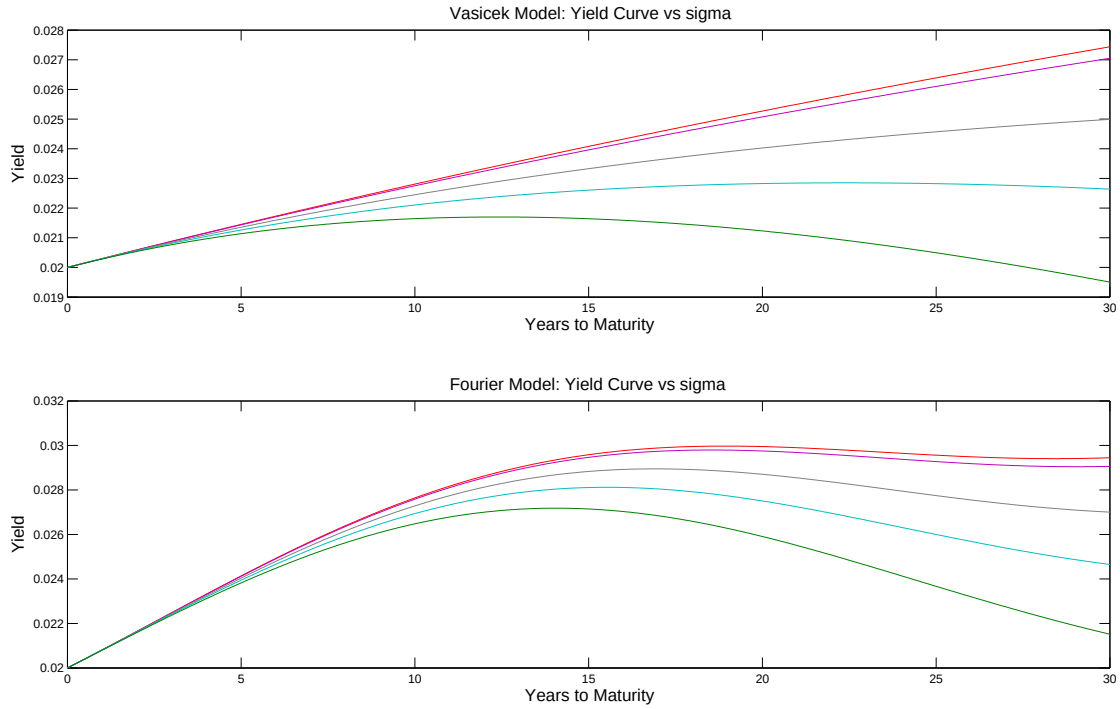

Figure 1.4: Term structure of interest rates for different values of σ. In both models, the values of σ corresponding to the curves from the top down are $0.0002, 0.002, 0.005, 0.007$, and 0.009, respectively.
Parameter Values Vasicek Model: $r_0 = 0.02,\ \alpha = 0.05,\ \kappa = 0.02$.
Parameter Values Fourier Model: $r_0 = 0.02,\ \alpha = 0.05,\ \kappa = 0.02, \omega = 0.20, n = 1,\ A_{1,x} = 0.05,\ A_{1,y} = -0.03$.

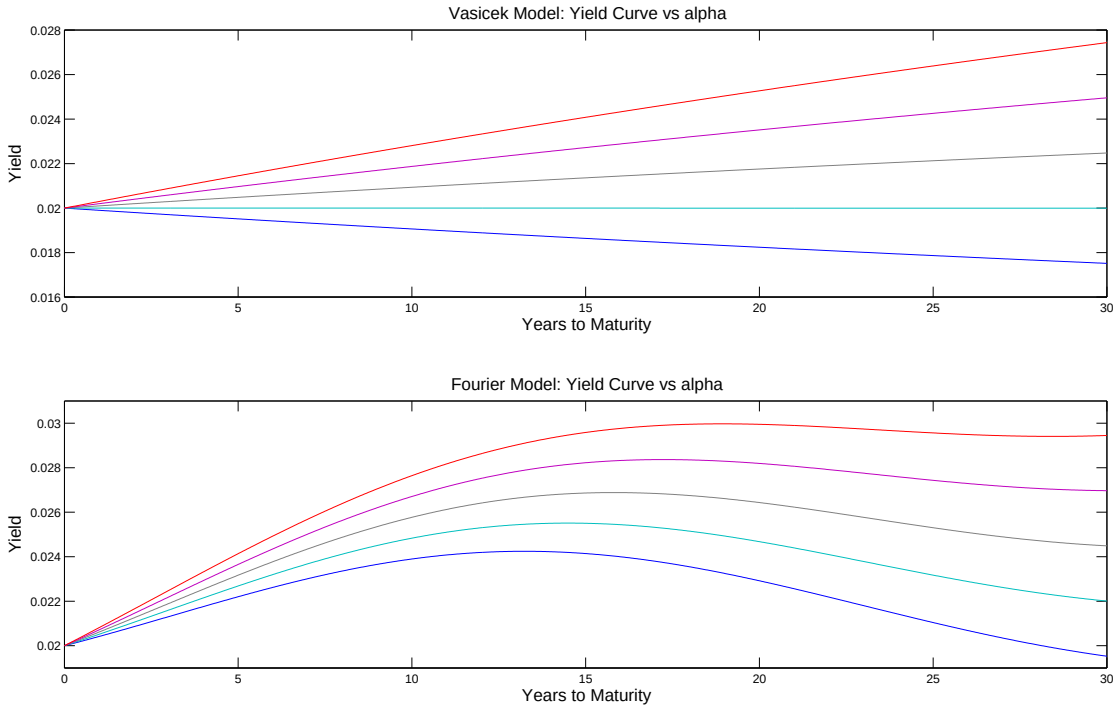

Figure 1.5: Term structure of interest rates for different values of the mean reversion level α. In both models, the values of α corresponding to the curves from the top down are $0.05, 0.04, 0.03, 0.02$, and 0.01, respectively.
Parameter Values Vasicek Model: $r_0 = 0.02,\ \sigma = 0.0002,\ \kappa = 0.02$.
Parameter Values Fourier Model: $r_0 = 0.02,\ \sigma = 0.0002,\ \kappa = 0.02, \omega = 0.20, n = 1,\ A_{1,x} = 0.05,\ A_{1,y} = -0.03$.

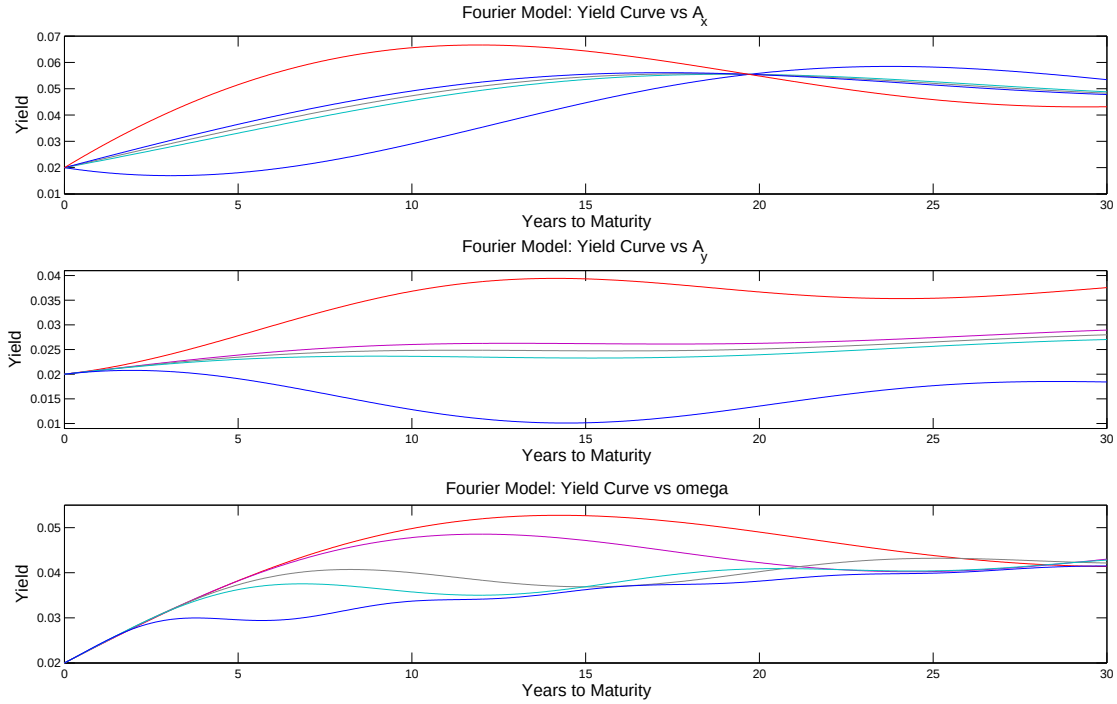

Figure 1.6: Term structure of interest rates for different values of the Fourier parameters.
First Graph: $r_0 = 0.02,\ \alpha = 0.05,\ \sigma = 0.0002,\ \kappa = 0.2, \omega = 0.20, n = 1,\ A_{1,y} = -0.03.$ and $A_{1,x} = -0.05; -0.005; 0; 0.005; 0.05.$
Second Graph: $r_0 = 0.02,\ \alpha = 0.05,\ \sigma = 0.0002,\ \kappa = 0.02, \omega = 0.30, n = 1,\ A_{1,x} = 0.05.$ and $A_{1,y} = -0.2; -0.02; 0; 0.02; 0.2.$
Third Graph: $r_0 = 0.02,\ \alpha = 0.05,\ \sigma = 0.0002,\ \kappa = 0.1, n = 1,\ A_{1,x} = 0.05,\ A_{1,y} = -0.03$ and $\omega = 0.2; 0.25; 0.4; 0.5; 1.$

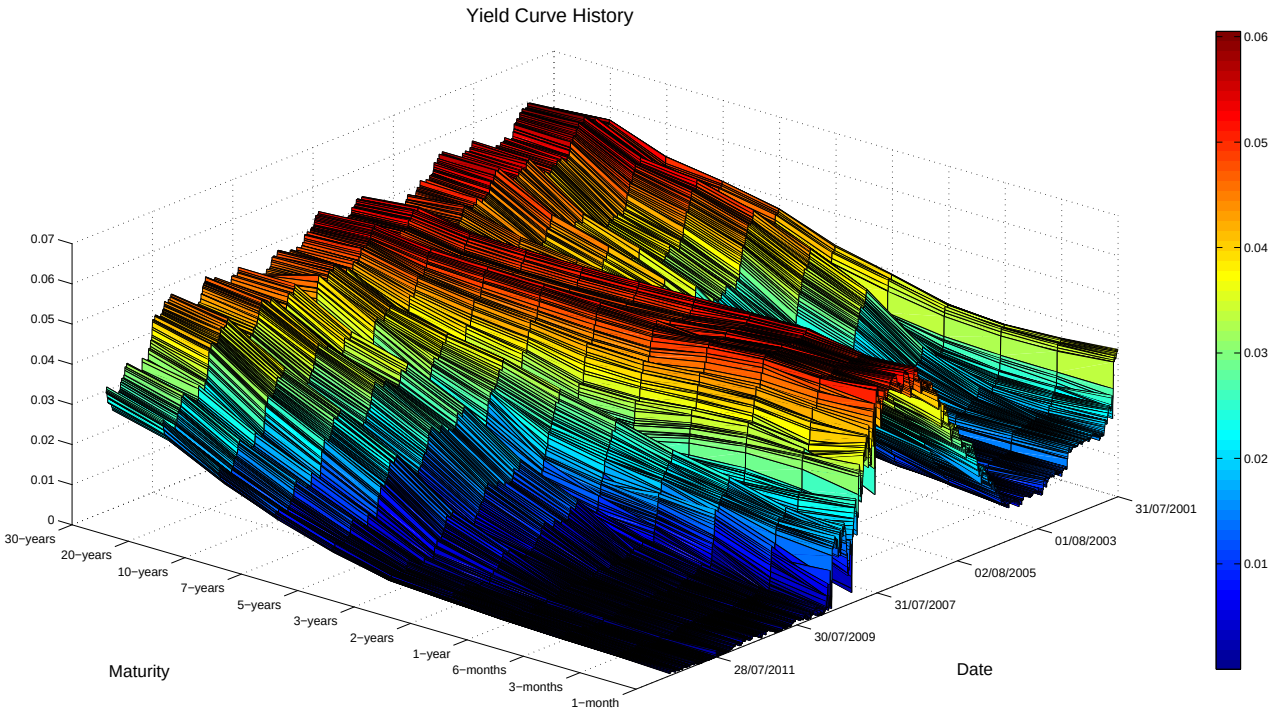

Figure 1.7: Historical evolution of the Yield Curve from July 31, 2001 up to September 21, 2012.

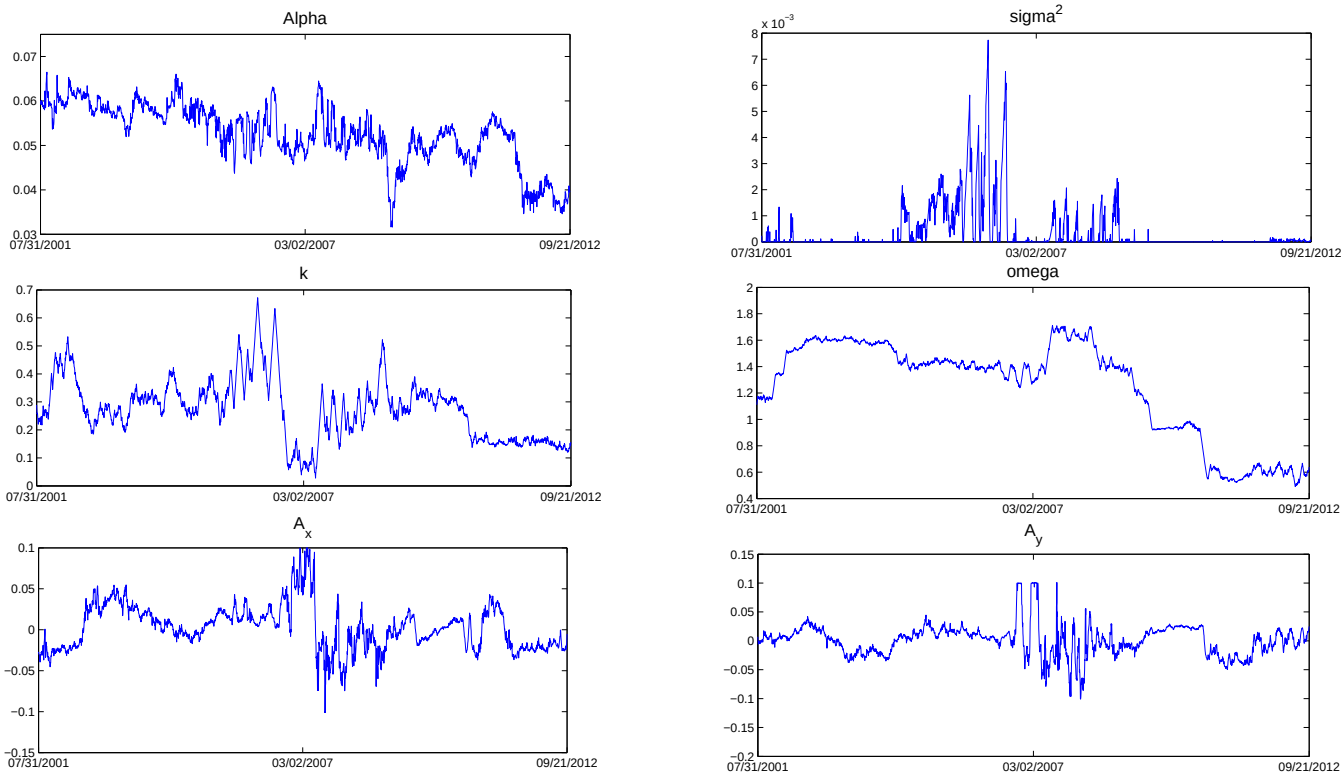

Figure 1.8: Estimated parameters from Fourier Model

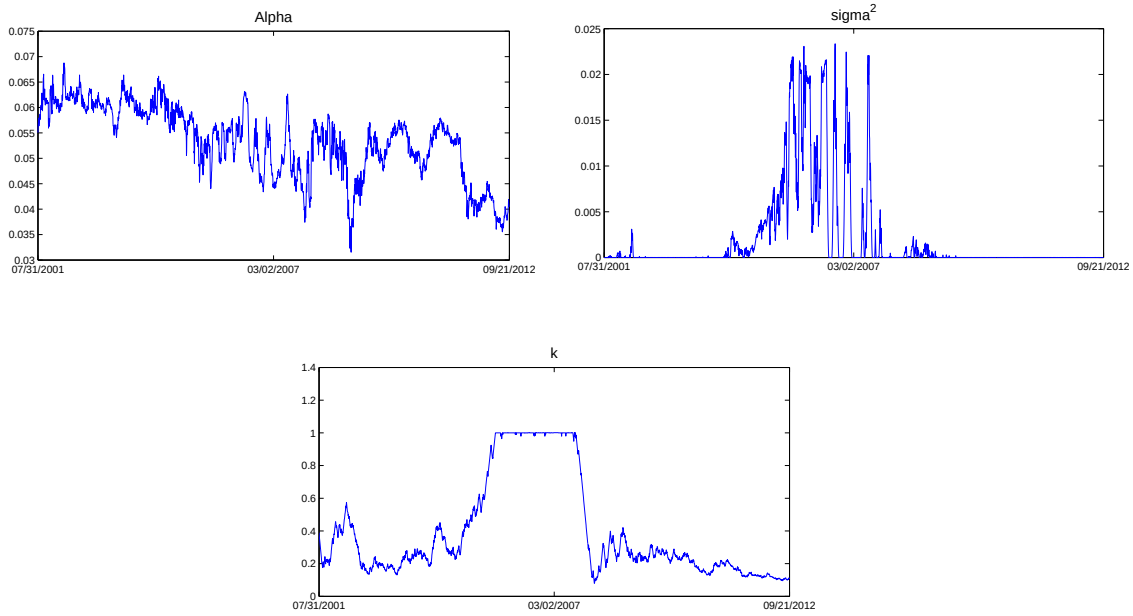

Figure 1.9: Estimated parameters from Vasicek Model

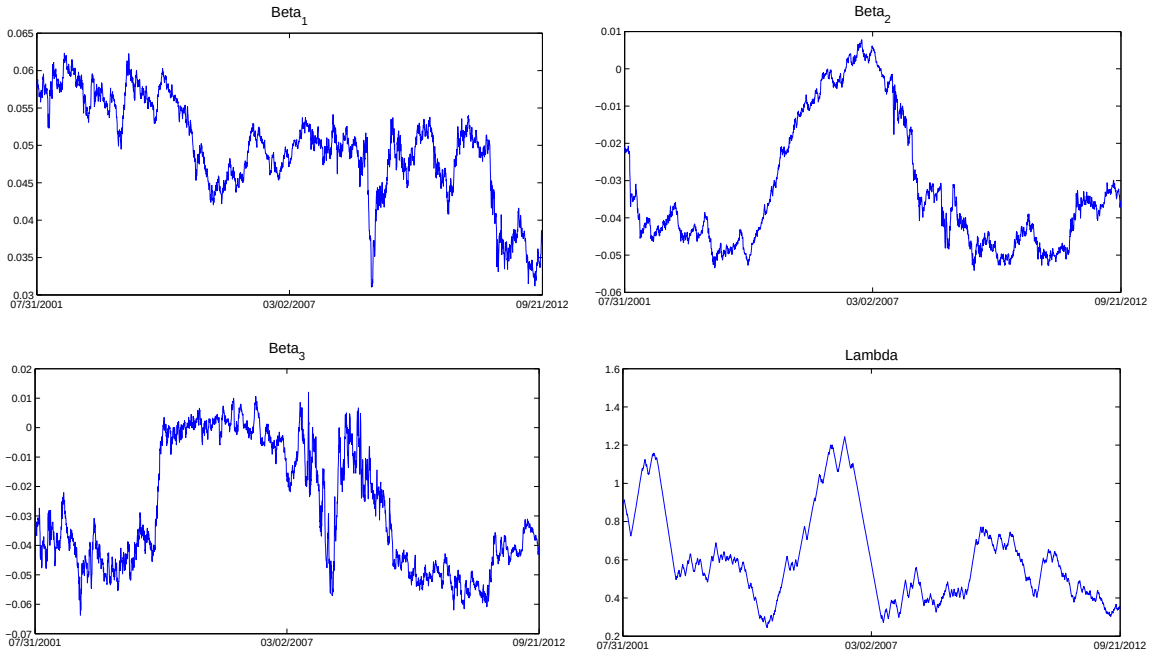

Figure 1.10: Estimated parameters from Nelson-Siegel Model

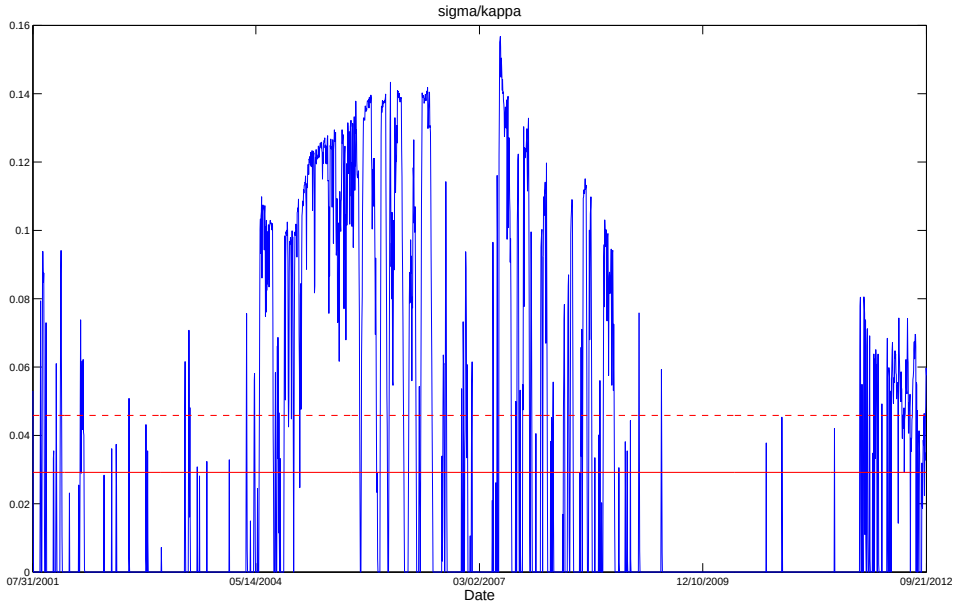

Figure 1.11: $\frac{\sigma}{\kappa}$ evolution. The red line corresponds to the sample mean of the ratio, while the dashed line represents its standard deviation.

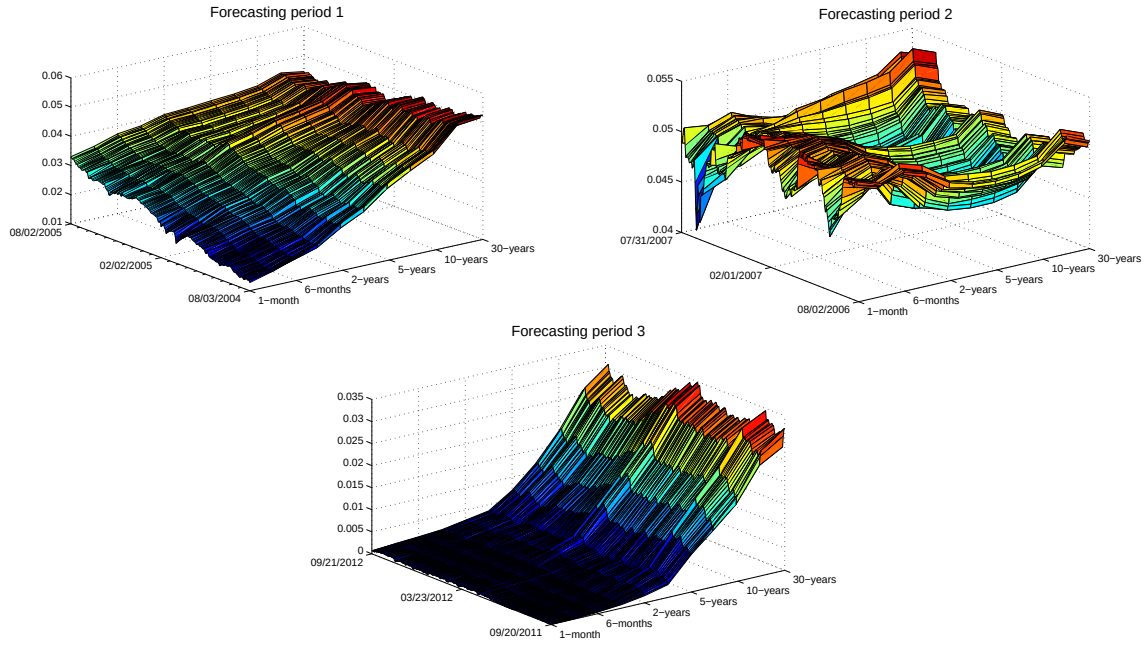

Figure 1.12: Observed term structure of interest rates for the three forecasting periods

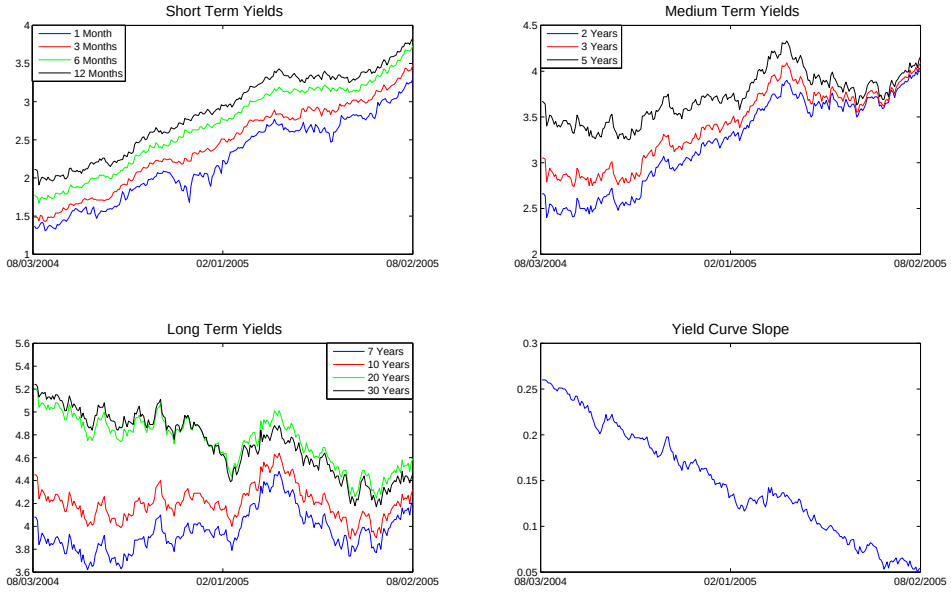

Figure 1.13: Time-series yields from 08/03/2004 to 08/02/2005 and the evolution of the term structure slope.

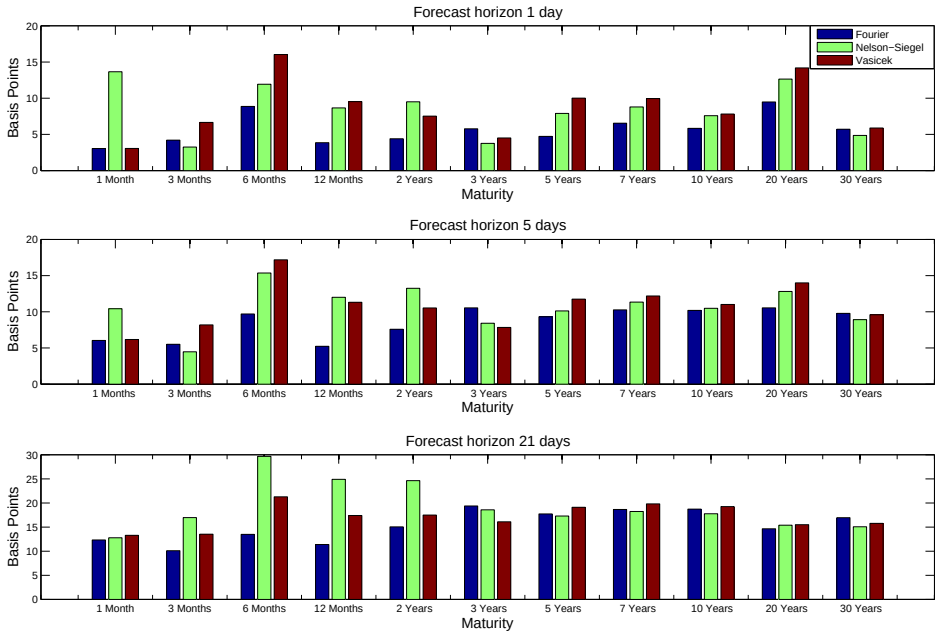

Figure 1.14: Mean absolute forecast error across maturities, in basis points, for forecasting period 1.

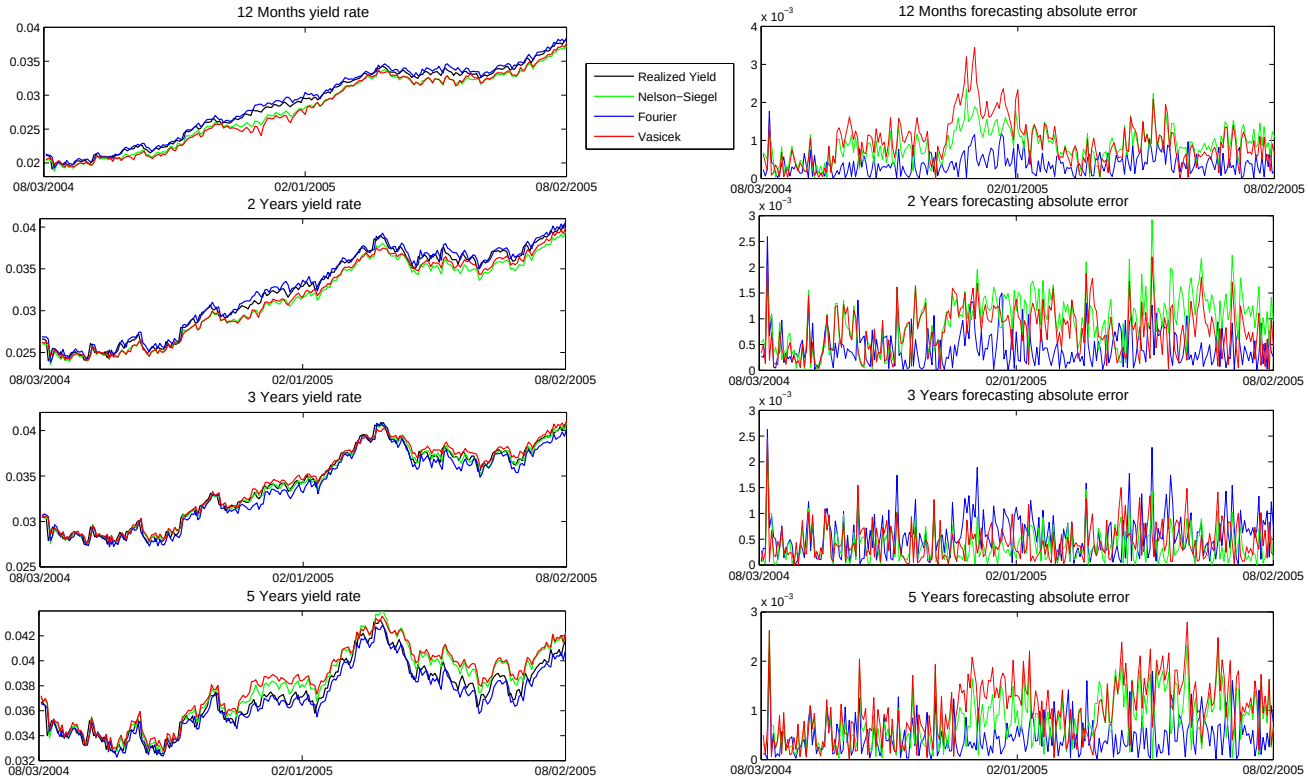

Figure 1.15: One day ahead prediction from each model for 1- to 5-year maturities, and the associated forecasting error, in absolute value

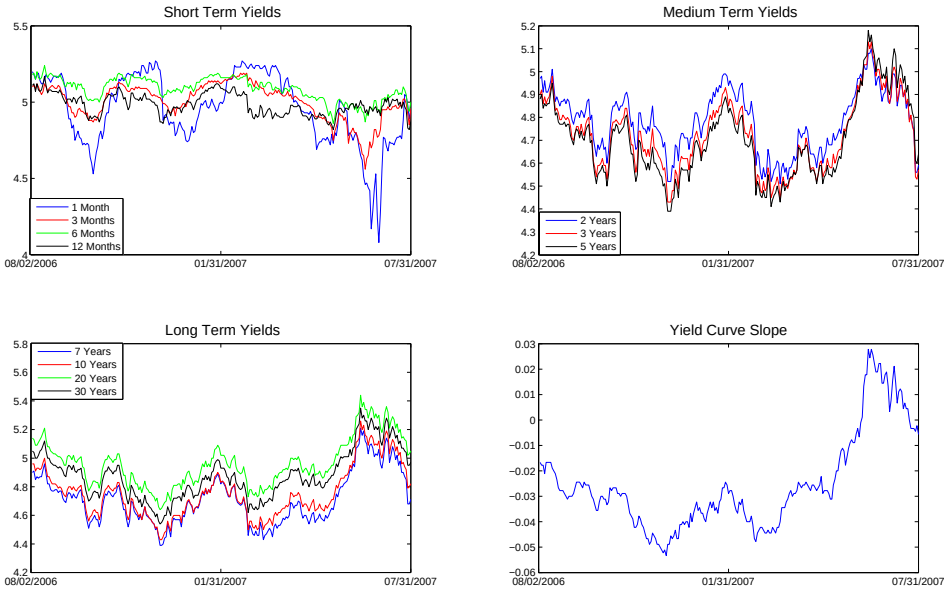

Figure 1.16: Time-series yields from 08/02/2006 to 07/31/2007 and the evolution of the term structure slope.

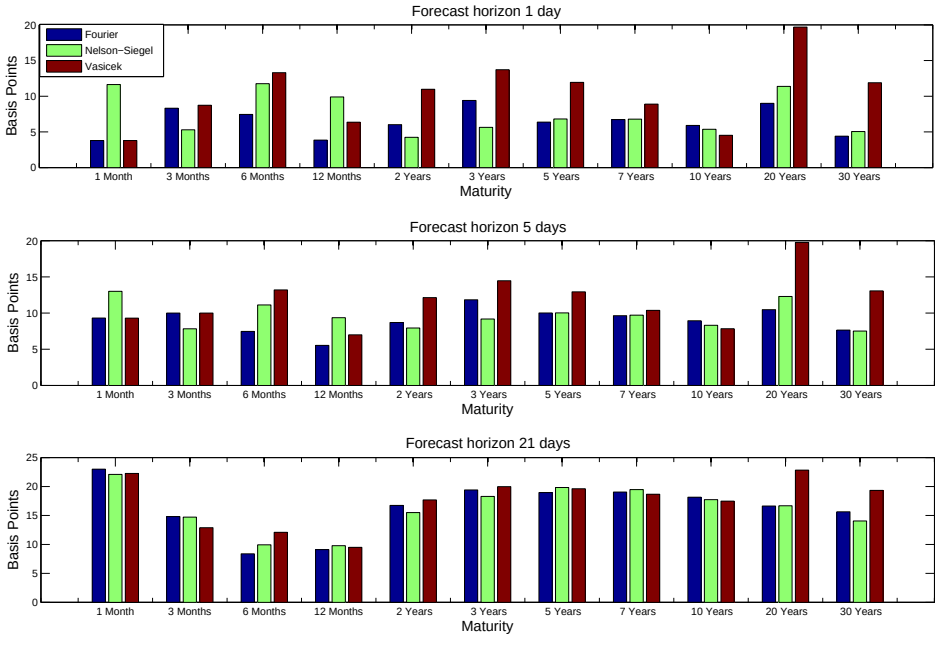

Figure 1.17: Mean absolute forecast error across maturities, in basis points, for forecasting period 2.

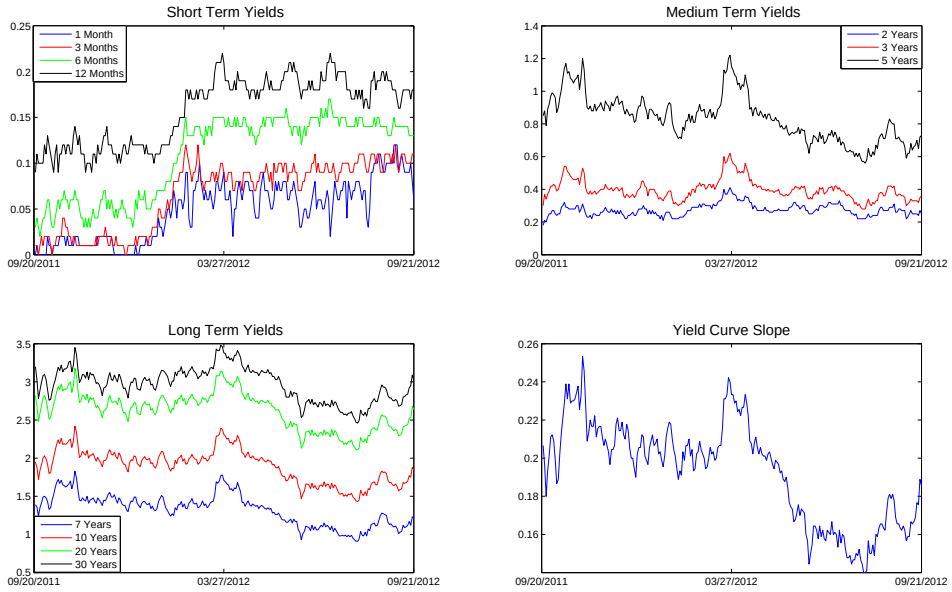

Figure 1.18: Time-series yields from 09/20/2011 to 09/21/2012 and the evolution of the term structure slope.

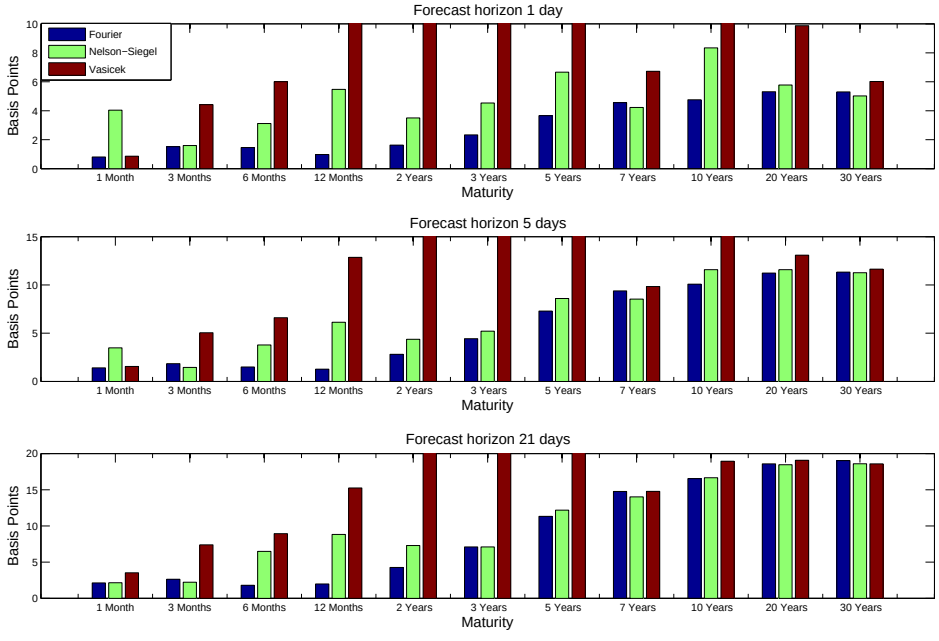

Figure 1.19: Mean absolute forecast error across maturities, in basis points, for forecasting period 3.

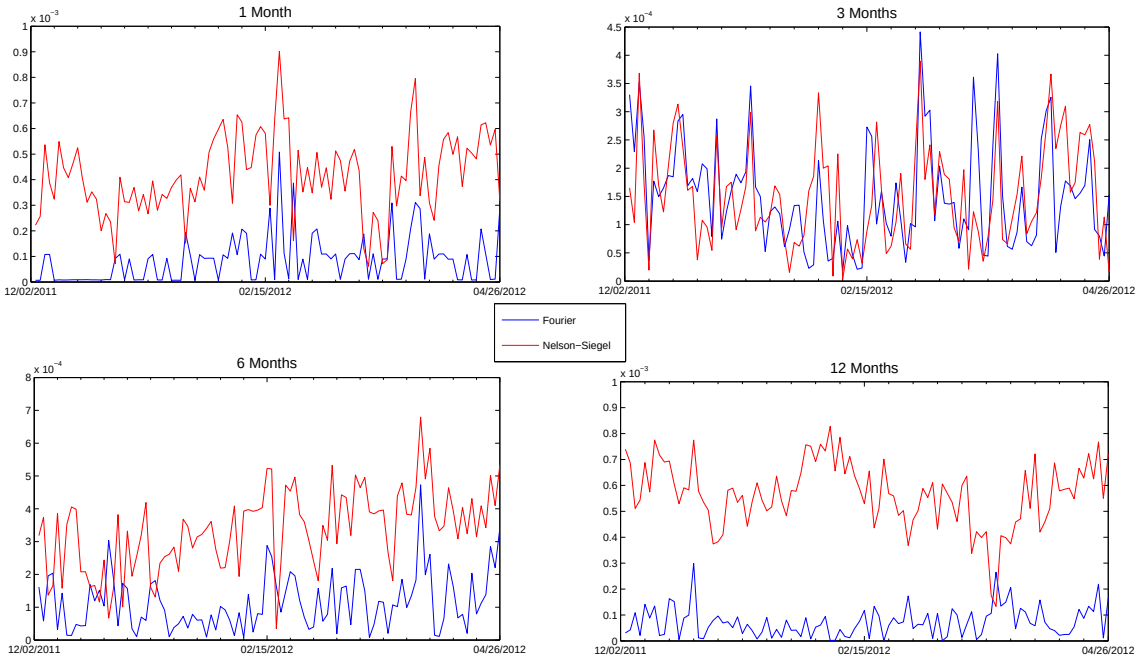

Figure 1.20: Time series of 1-day ahead forecasting errors, in absolute value, around 02/15/2012

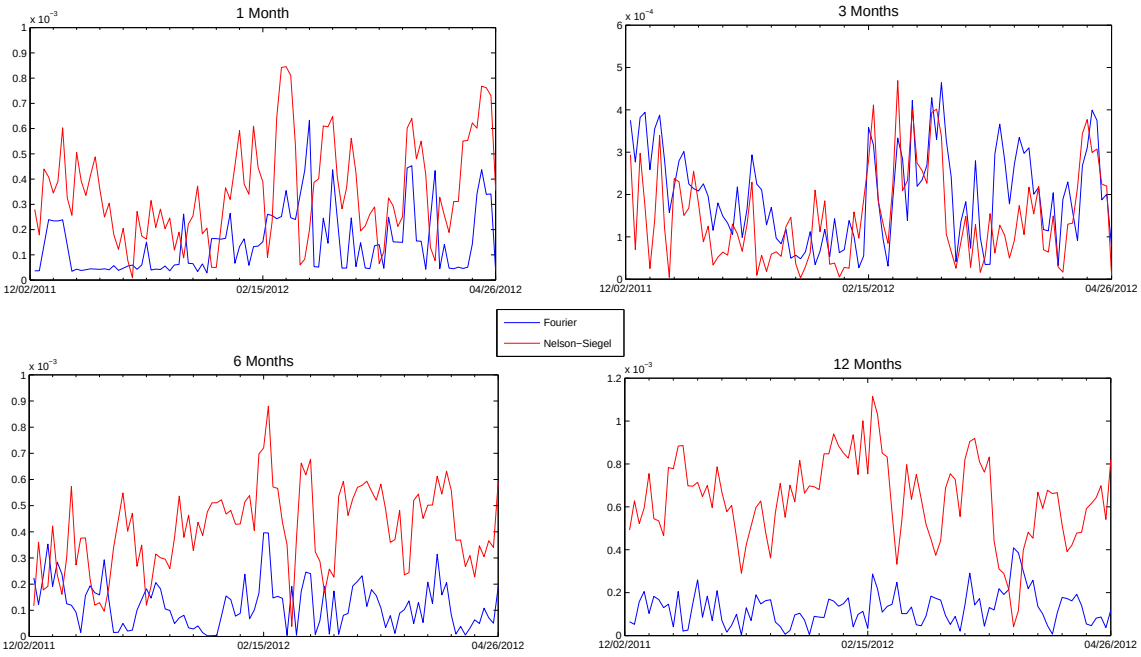

Figure 1.21: Time series of 5-days ahead forecasting errors, in absolute value, around 02/15/2012

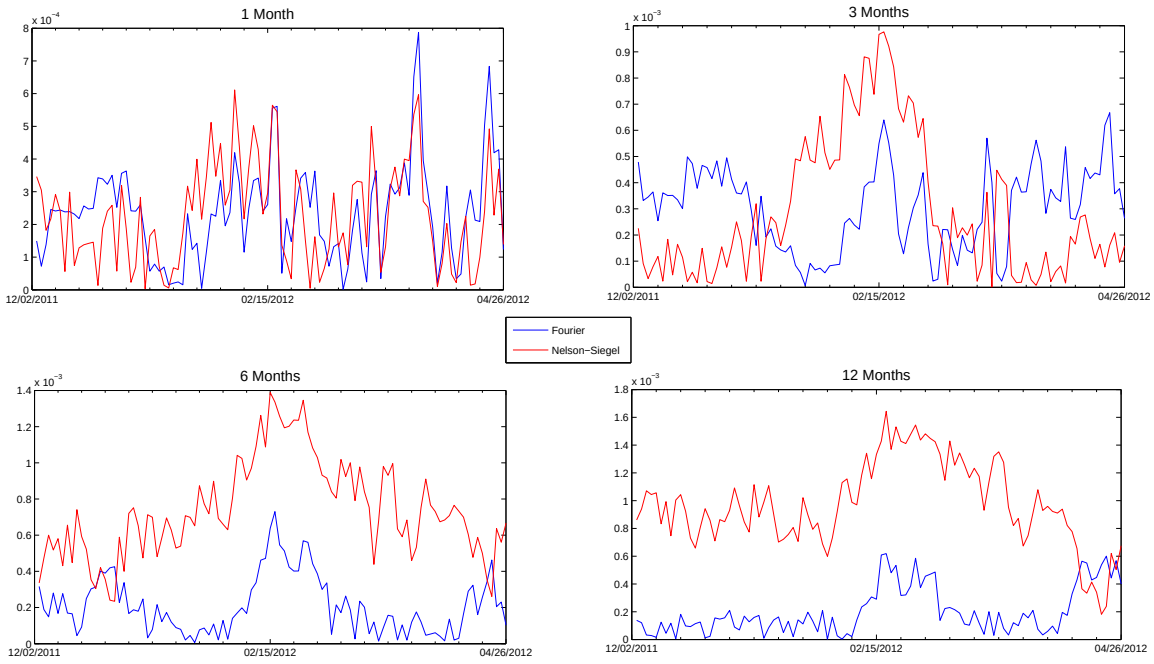

Figure 1.22: Time series of 21-days ahead forecasting errors, in absolute value, around 02/15/2012

Bibliography

[1] Black, F., E. Dermand and W. Toy (1990). A One-Factor Model of Interest Rates and its Application to Treasury Bond Options. *Financial Analysts Journal*, 46, 33–39.

[2] Black, F. and P. Karasinski (1991). Bond and Option Pricing when Short Rates are Lognormal. *Financial Analysts Journal*, 47, 52-59.

[3] Brennan, M.J. and E.S. Schwartz (1979). A Continuous Time Approach to the Pricing of Bonds. *Journal of Banking and Finance*, 3, 133-155.

[4] Brennan, M.J. and E.S. Schwartz (1980). Analyzing Convertible Secirities. *Journal of Financial and Quantitative Analysis*, 15, 4, 907-929.

[5] Brigo, D. and F. Mercurio (2006). *Interest Rate Models – Theory and Practice*, Springer-Verlag Berlin Heidelberg.

[6] Chan, K.C., G.A. Karolyi, F.A. Longstaff, and A.B. Sanders (1992). An Empirical Comparison of Alternative Models of the Short-Term Interest Rate. *Journal of Finance*, 47, 3, 1209-1227.

[7] Chen, L. (1996). *Interest Rate Dynamics, Derivatives Pricing, and Risk Management*. Springer-Verlag, Berlin.

[8] Cochrane, J.H. and M. Piazzesi (2005). Bond Risk Premia. *American Economic Review*, 95, 1, 138-160.

[9] Cox, J.C., J.E. Ingersoll, and S.A. Ross (1985). A Theory of the Term Structure of Interest Rates. *Econometrica*, 53, 2, 385-408.

[10] Diebold, F.X. and C. Li (2006). Forecasting the Term Structure of Government Bond Yields. *Journal of Econometrics*, 130, 337-364.

[11] Duffie, D. and R. Kan (1996). A Yield-Factor Model of Interest Rates. *Mathematical Finance*, 6, 4, 379-406.

[12] Fama, E. and R. Bliss (1987). The Information in Long-Maturity Forward Rates. *American Economic Review*, 77, 680-692.

[13] Filipović, D. (2009). *Term Structure Models – A Graduate Course*, Springer-Verlag Berlin Heidelberg.

[14] Heath, D., R. Jarrow, and A. Morton (1992). Bond Pricing and the Term Structure of Interest Rates: A New Methodology for Contingent Claims Valuation. *Econometrica*, 60, 77-105.

[15] Ho, T.S.Y. and S. Lee (1986). Term Structure Movements and Pricing Interest Rate Contingent Claims. *Journal of Finance*, 41, 5, 1011-1029.

[16] Hull, J. and A. White (1990). Pricing Interest-Rate-Derivative Securities. *Review of Financial Studies*, 3, 4, 573–592.

[17] Hull, J. and A. White (1993). One-Factor Interest-Rate Models and the Valuation of Interest-Rate Derivative Securities, *Journal of Financial and Quantitative Analysis*, 28, 2, 235-254.

[18] Jamshidian, F. (1989). An Exact Bond Option Formula. *Journal of Finance*, 44, 1, 205-209.

[19] Longstaff, F.A. and E.S. Schwartz (1992). Interest Rate Volatility and the Term Structure: A Two-Factor General Equilibrium Model. *Journal of Finance*, 47, 4, 1259-1282.

[20] Mercurio, F. and J.M. Moraleda (2000). An Analytically Tractable Interest Rate Model with Humped Volatility. *European Journal of Operational Research*, 120, 205-214.

[21] Merton, R.C. (1973). Theory of Rational Option Pricing. *Bell Journal of Economics and Management Science*, 4, 1, 141-183.

[22] Nelson, C.R. and A.F. Siegel (1987). Parsimonious Modeling of Yield Curves. *Journal of Business*, 60, 4, 473-489.

[23] Schaefer, S.M. and E.S. Schwartz (1984). A Two-Factor Model of the Term Structure: An Approximate Analytical Solution. *Journal of Financial and Quantitative Analysis*, 19, 4, 413-424.

[24] Vasicek, O. (1977). An Equilibrium Characterization of the Term Structure. *Journal of Financial Economics*, 5, 2, 177-188.

[25] Webber, N. and J. James (2001). *Interest Rate Modelling: Financial Engineering*, John Wiley & Sons, Ltd, England.

Chapter 2

Derivatives Pricing under a New Macro-financial Square-root Process for the Term Structure of Interest Rates

2.1 Introduction

Through the time, modelling the term structure of interest rates has been the object of many studies and the aim of attention for economists and financial institutions. This chapter proposes a new square-root model where the instantaneous interest rate is pulled back to a certain time-dependent long term level characterized by an harmonic oscillator. Cox et al. (1985) has shown that square-root processes of this type follow a rescaled non-central chi-square distribution. Therefore, assuming a time-dependent mean reversion level will derive in a time-dependent spot rate volatility. As the empirical evidence (see, for instance, Chan *et al.* (1992)) has illustrated that interest rate volatility depends on the interest rates level, it seems natural to model the interest rate volatility using a similar functional form as that in the mean reversion level.

Continuous-time models proposed in the academic literature for the analysis of the term structure of interest rates can be classified in endogenous and exogenous. Endogenous models make certain assumptions on the factors that drive the term structure and on the stochastic processes followed by these factors. As a consequence, the term structure is fully characterized by the underlying factors meaning that the current term structure of rates is an output (and not an input) of the model. Examples of one-factor endogenous models are Vasicek (1977), Brennan and Schwartz (1980), or Cox *et al.* (1985) (CIR from now on). The main drawback of these models is the lack of empirical realism as they imply perfect correlation between returns of bonds that differ in their maturity, in contrast to empirical evidence. Consequently, these models do not fit accurately the current term structure and, then, they do not price correctly the associated interest rate derivatives. In order to cope with this problem, several two-factor endogenous models have been proposed in, for instance, Schaefer and Schwartz (1984), Longstaff and Schwartz (1992), or Duffie and Kan (1996). In addition, Chen (1996) introduced a three-factor model.

On the other hand, exogenous models take the current term structure as given and derive future changes in interest rates avoiding intertemporal arbitrage opportunities. One of the first contributions in this type of modelling was proposed in Ho and Lee (1986) who built a model consistent with the initial term structure of interest rates. Because of the limitations of this model, some other exogenous models have bee proposed by a number of authors such as Black *et al.* (1990), Hull and White (1990, 1993), Black and Karasinski (1991), Heath *et al.* (1992), and Mercurio and Moraleda (2000). We can mention the models introduced in Hull and White (1990, 1993) that extend those presented in Vasicek (1977) and Cox *et al.* (1985) by introducing some time-dependent parameters and adding more flexibility to fit the initial term structure of interest rates. For a thoroughly literature review on term structure models see, for instance, Webber and James (2001), Brigo and Mercurio (2006), or Filipović (2009).

Our model assumes that the mean reversion level at which interest rates are converging and the

spot rate volatility follow a cyclic process characterized by an harmonic oscillator. Then, the whole term structure of interest rates is fully determined by the instantaneous spot rate. Under these assumptions, we obtain closed-form expressions for prices of bonds and different derivatives such as bond forward agreements, European options on zero-coupon and coupon-bearing bonds, European bond forward options, swaps, swaptions, caps, floors, collars, and provide some risk management measures.

This chapter is organized as follows. Section 2.2 introduces the new square-root model and its practical implications. Section 2.3 presents the general pricing partial differential equation and derives closed-form expressions for different derivatives. Finally, Section 2.4 summarizes the main findings and conclusions. Mathematical proofs are deferred to the Appendix.

2.2 A New Square-root Model for the Term Structure

In this section, we propose our model, the specific functional form for each time-dependent parameter, and describe all the practical implications arising from this model.

Unlike many other one-factor models that allow the spot rate process for time-dependent parameters (see, for instance, Hull and White (1990, 1993)), we now assume that the mean reversion level depends on the business cycle. We also consider that the interest rate volatility depends on the interest rate level. In order to model the behaviour of both variables, we assume a harmonic oscillator given as

$$f(t) = A\sin(\varphi - \omega t)$$

where A denotes the amplitude of the wave, φ the offset phase, and w the temporal frequency.

We now define the mean reversion level, θ_t, and the volatility, σ_t^2, as

$$\theta_t = A_\theta \sin^2(\varphi - \omega t) \tag{2.1}$$

$$\sigma_t^2 = A_\sigma \sin^2(\varphi - \omega t) \tag{2.2}$$

Hence, the positiveness of the mean reversion level and the interest rate volatility is guaranteed.

Let r_t denote the instantaneous interest rate available at time t whose dynamic is

$$dr_t = \mu_r dt + \sigma_r dW_t \tag{2.3}$$

where W_t is a standard Wiener process and

$$\mu_r = \kappa(\theta_t - r_t) \tag{2.4}$$

$$\sigma_r = \sigma_t\sqrt{r_t} \tag{2.5}$$

where $\kappa \in \mathbb{R}^+$. Looking at these expressions, it is clear that our model nests that presented in Cox *et al.* (1985) taking $\omega = 0$ in equations (2.1)-(2.2).

For square-root processes of this type, Cox *et al.* (1985) shows that the distribution function of interest rates is a rescaled non-central chi-square with δ degrees of freedom. Note that, whenever δ is not a positive integer, the distribution of r_t is unknown.

Besides, the dimension of the process r_t is given by $\delta = \frac{4\theta_t\kappa}{\sigma_t^2}$. As both waves are in phase, the model's dimension can be represented as $\delta = \frac{4A_\theta\kappa}{A_\sigma} > 0$. [1]

Our model guarantees the positiveness of interest rates. On this respect, Feller (1951) studied the Fokker-Plank-Kolmogorov equation for the transition density and showed that $r_t > 0$ if $\delta \geq 2$, however it can become null if $\delta < 2$ but will never become negative.

2.3 Pricing

This section presents closed-form expressions for the price of zero-coupon bonds and, later, we analytically compute closed-form formulas for the prices of different securities.

Let $P(r_t, t, T)$ denote the price at time t of a zero-coupon bond that pays \$1 at maturity T. Then, the bond price dynamics is given by the process

$$dP = \mu_P(r_t, t, T)P(r_t, t, T)dt + \sigma_P(r_t, t, T)P(r_t, t, T)dW_t \tag{2.6}$$

Applying Itô's Lemma and using (2.3), it can be shown that

$$\mu_P = \frac{1}{P}\left(P_t + \mu_r P_r + \frac{1}{2}\sigma_r^2 P_{rr}\right) \tag{2.7}$$

$$\sigma_P = \sigma_r \frac{P_r}{P} \tag{2.8}$$

where arguments have been omitted and subscripts in P indicate the corresponding partial derivative. Applying standard no-arbitrage arguments, there exists a factor $\Lambda(r_t, t)$, called market price of risk, such that

$$\mu_P(r_t, t, T) - r_t = \Lambda(r_t, t)\sigma_P(r_t, t, T) \tag{2.9}$$

Finally, some trivial algebra leads to the following partial differential equation (PDE)

$$P_t(r_t, t, T) + (\mu_r - \Lambda(r_t, t)\sigma_r)P_r(r_t, t, T) + \frac{1}{2}\sigma_r^2 P_{rr}(r_t, t, T) - r_t P(r_t, t, T) = 0 \tag{2.10}$$

that must be verified by the price of any derivative.

[1] Note that, if $\sin(\varphi - \omega t)$ is equal to zero, then δ becomes indeterminate. As this case would only occur for a infinitesimal period of time, we do not consider this possibility.

2.3.1 Bond Pricing

We consider a market price of risk such as

$$\Lambda(r_t, t) = \frac{\lambda_t \sqrt{r_t}}{\sigma_t} \tag{2.11}$$

Using expressions (2.5)-(2.11), the PDE (2.10) becomes

$$P_t(r_t, t, T) + (\kappa(\theta_t - r_t) - \lambda_t r_t) P_r(r_t, t, T) + \frac{1}{2}\sigma_t^2 r_t P_{rr}(r_t, t, T) - r_t P(r_t, t, T) = 0 \tag{2.12}$$

The solution of this PDE, subject to the boundary condition $P(r_T, T, T) = 1, \ \forall r_T$, is given by the following Proposition.

Proposition 14 *The price at time t of a zero-coupon bond with maturity T and \$1 face value is given by*

$$P(r_t, \tau) = A(\tau) e^{-B(\tau) r_t}$$

where

$$\begin{aligned}
A(\tau) &= \exp\left\{ -\int_t^T \kappa \theta_t B(\tau) dt \right\} \\
B(\tau) &= \frac{c_1 MC(a,q,x) + MS(a,q,x)}{\frac{1}{2}(\lambda + \kappa)\left(c_1 MC(a,q,x) + MS(a,q,x)\right) + \omega\left(c_1 MCP(a,q,x) + MSP(a,q,x)\right)} \\
a &= -\frac{A_\sigma + (\lambda + \kappa)^2}{4\omega^2} \\
q &= -\frac{A_\sigma}{8\omega^2} \\
x &= \varphi - \omega t \\
c_1 &= -\frac{MS(a,q,\varphi - \omega T)}{MC(a,q,\varphi - \omega T)} \\
\tau &= T - t
\end{aligned}$$

where θ_t is given by (2.1), MC and MS represent the Mathieu cosine and sine function, respectively, and MCP and MSP represent the derivative with respect to x of the Mathieu cosine and sine function, respectively. ■

Proof. See the Appendix ■

Remark 2 *An interesting approximation arises for $q \approx 0$, that is, periods of low volatility where the underlying frequency in the Mathieu function is relatively high. Satisfying this requirement will derive in*

$$MC(a,q,x) \approx \cos(\sqrt{a} \cdot x), \quad MS(a,q,x) \approx \frac{\sin(\sqrt{a} \cdot x)}{\sqrt{a}}$$

■

Figure 2.1 compares the bond price in the CIR model against three alternatives in our model. We check that, in our model, the bond price does not decrease monotonically with time to maturity. Additionally, we provide much more flexibility than the CIR model with the same analytical tractability. We can also visualize the presence of humps, which is a very desirable effect not only here but also in any interest rate derivative.

The following Corollary immediately arises.

Corollary 4 *As a coupon bond can be interpreted as a portfolio of zero-coupon bonds, pricing of coupon bonds is straightforward applying Proposition 14.* ∎

Replacing the bond price expression obtained in Proposition 14 into (2.7)-(2.8) and using (2.5)-(2.11), we get the next Corollary.

Corollary 5 *The bond price dynamics under the no-arbitrage condition is given as*

$$dP(r_t,t,T) = \mu_P(r_t,t,T)P(r_t,t,T)dt + \sigma_P(r_t,t,T)P(r_t,t,T)dW_t$$

where

$$\mu_P(r_t,t,T) = r_t(1-\lambda_t B), \quad \sigma_P(r_t,t,T) = -B\sigma_t\sqrt{r_t}$$

∎

Note that, in a risk-neutral world, where $\lambda_t = 0$, the bond price process is a martingale. Under this framework, the term structure is fully characterized considering the zero-coupon bond price $P(r_t,t,T)$ given by Proposition 14, as stated in the following Corollary.

Corollary 6 *The yield to maturity, $R(r_t,t,T)$, is given by*

$$R(r_t,t,T) = -\frac{1}{\tau}\ln P(r_t,t,T),\ \tau = T-t$$

The short-term interest rate is defined as the instantaneous interest rate at time t, that is,

$$r_t = \lim_{\tau\to 0} R(r_t,t,T) = R(r_t,t,t)$$

The instantaneous forward rate is given as

$$f(r_t,t,T) = -\frac{\partial \ln(P(r_t,t,T))}{\partial T}$$

∎

Figure 2.2 shows the term structure of interest rates in the CIR model and three alternatives in our model. We can see how our model adds flexibility as we can reflect different behaviours for the term structure.

For illustrative purposes, Figures 2.3 and 2.4 show how the term structure of interest rates responds to changes in the mean reversion speed and volatility in both models. In the CIR model, the higher the speed of mean reversion, the higher the interest rate while, in our model, the lower the mean reversion speed, the flatter the term structure. Besides, in our model, there is a twist in the pattern due to the cyclic behaviour. In Figure 2.4, for both models, the higher the volatility, the lower the term structure.

Figures 2.5 and 2.6 reflect the response of the term structure of interest rates to different values of the mean reversion level in both models. In the CIR model, the higher the mean reversion level, the higher the yield. In our model, it is harder to analyse this response as it depends on three parameters. Anyway, we observe that the lower the amplitude, the flatter and the lower the term structure. When changing the temporal frequency, it seems clear that the higher the temporal frequency, the more humped the term structure. Finally, for different offset phases, the curves occasionally crossover each other.

On the risk management side, we get the following corollary.

Corollary 7 *The two major bond risk measures, duration and convexity, are given as*

- *Duration measures the bond price sensitivity for a change in interest rates:*

$$Duration = -\frac{1}{P(t,T)}\frac{\partial P(t,T)}{\partial r_t} = B(t,T)$$

- *Convexity measures how duration changes with interest rates:*

$$Convexity = \frac{1}{P(t,T)}\frac{\partial^2 P(t,T)}{\partial r_t^2} = B^2(t,T)$$

with $B(t,T)$ as given by Proposition 14. ∎

2.3.2 Pricing of Bond Derivatives

The PDE (2.12) subject to the appropriate boundary condition will lead us to value any interest rate derivative. Consider a derivative whose pay-off at time s is given by $U_s(r_s)$.[2] Applying the fundamental results of Heath *et al.* (1992), there exists an unique equivalent risk-neutral measure $\widetilde{P}$ such that the value at time t of this derivative U_t can be represented as

$$U_t(r_t,t,s) = \widetilde{E}\left[e^{-\int_t^s r_u du}U_s(r_s)|r_t\right]$$

[2]Clearly, if $U_s(r_s) = 1$, the previous bond price expression is obtained.

where $\widetilde{E}$ denotes expectation with respect to the risk-neutral measure $\widetilde{P}$.

Let

$$\widetilde{W}_t = W_t + \int_0^t \Lambda_u du \tag{2.13}$$

denote the Wiener process under $\widetilde{P}$. Under this measure, applying (2.6), (2.9), and (2.13), the risk-neutral dynamics of the bond price is given as

$$dP(r_t, t, s) = r_t P(r_t, t, s)dt + \sigma_P P(r_t, t, s)d\widetilde{W}_t$$

Hence, the discount bond price process is a martingale.

Define $g(P(r_t, t, s)) = \ln P(r_t, t, s)$. Then, applying Itô's Lemma, we get

$$dg_t = \frac{\partial g(P)}{\partial P}dP - \frac{1}{2}\frac{\partial^2 g(P)}{\partial P^2}(dP)^2 = \frac{1}{P}\left(r_t P dt + \sigma_P P d\widetilde{W}_t\right) - \frac{1}{2}\frac{1}{P^2}\sigma_P^2 P^2 dt$$

where the corresponding arguments have been omitted. Integrating from 0 to t, we get

$$P(r_t, t, s) = P(r_0, 0, s)\exp\left(\int_0^t r_u du + \int_0^t \sigma_P(u, s)d\widetilde{W}_u - \frac{1}{2}\int_0^t \sigma_P^2(u, s)du\right)$$

Hence, for each $s \in [t, T]$, the process Z_t^s defined as

$$Z_t^s = \frac{P(r_t, t, s)}{P(r_0, 0, s)}e^{-\int_0^t r_u du} = \exp\left(\int_0^t \sigma_P(u, s)d\widetilde{W}_u - \frac{1}{2}\int_0^t \sigma_P^2(u, s)du\right)$$

is a martingale. Moreover, in line with Karatzas and Shreve (1988), we get

$$Z_t^s = 1 + \int_0^t \sigma_P(u, s)\exp\left(\int_0^t \sigma_P(x, s)d\widetilde{W}_x - \frac{1}{2}\int_0^t \sigma_P^2(x, s)dx\right)d\widetilde{W}_u$$

Thus, by the Girsanov's theorem, for each $s \in [t, T]$, there exists an equivalent s-forward measure P^s such that

$$W_t^s = \widetilde{W}_t + \int_0^t \sigma_P(u, s)du \tag{2.14}$$

where W_t^s represent a standard Wiener process under P^s.

Karatzas and Shreve (1988) shows that, for a random variable Y

$$E^s[Y|F_t] = \frac{1}{Z_t^t}E[Z_t^s Y|F_t]$$

Then, the following Proposition presents the equivalent change of measure.

Proposition 15 *Under $\widetilde{P}$, the value at time t of any derivative $U_t(r_t, t, s)$ given by*

$$U_t(r_t, t, s) = \widetilde{E}\left[e^{-\int_t^s r_u du}U_s(r_s)|r_t\right]$$

has an equivalent s-forward measure, P^s, such that

$$U_t(r_t,t,s) = P(r_t,t,s)\widetilde{E}\left[\frac{Z_t^s}{Z_t^t}U_s(r_s)|r_t\right] = P(r_t,t,s)E^s\left[U_s(r_s)|r_t\right]$$

where E^s represents expectation under P^s and

$$\frac{Z_t^s}{Z_t^t} = \frac{e^{-\int_t^s r_u du}}{P(r_t,t,s)}$$

■

Moreover, the instantaneous forward rate is given as

$$f(r_t,t,T) = D(t,T) + B_T(t,T)r_t \tag{2.15}$$

with

$$D(t,T) = -\frac{A_T(t,T)}{A(t,T)} = \frac{\delta}{4}\int_t^T B_T(u,T)\sigma_u^2 du \tag{2.16}$$

Applying Itô's Lemma and using the spot rate dynamics (2.3), we get

$$df(r_t,t,T) = \mu_f dt + \sigma_f dW_t \tag{2.17}$$

where

$$\mu_f = \left(B_{Tt}(t,T) - \kappa B_T(t,T)\right)r_t, \quad \sigma_f = B_T(t,T)\sigma_t\sqrt{r_t}$$

Similarly to Heath *et al.* (1992), the following restriction on the forward rate drift is verified

$$\mu_f(\omega,t,T) = \sigma_f(\omega,t,T)\left[\int_t^T \sigma_f(\omega,t,x)dx + \Lambda_t\right]$$

Now, replacing (2.14) into the forward rate process (2.17), we get

$$df(r_t,t,s) = \sigma_f\left[\int_t^s \sigma_f(t,v)dv + \Lambda_t\right]dt + \sigma_f\left(dW_t^s - \Lambda_t dt - \sigma_P dt\right)$$

Hence, using $\int_t^s \sigma_f(r_t,t,v)dv = \sigma_P(r_t,t,s)$ leads to

$$df(r_t,t,s) = \sigma_f(r_t,t,s)dW_t^s = B_s(t,s)\sigma_t\sqrt{r_t}dW_t^s \tag{2.18}$$

Then, comparing equations (2.17) and (2.18), we get

$$dr_t = \kappa^s\left(\theta_t^s - r_t\right)dt + \sigma_t\sqrt{r_t}dW_t^s$$

where

$$\begin{aligned}\kappa^s &= \frac{B_{st}(t,s)}{B_s(t,s)}\\ \theta_t^s &= \frac{\kappa}{\kappa^s}\theta_t\end{aligned}$$

Hence, under the s-forward measure, the instantaneous interest rate follows a CIR-type process with speed and level of mean reversion given by κ^s and θ_t^s, respectively. Then, standard methods applied in Cox *et al.* (1985) can be used.

Define the state variable $X^s(t) = (x_1^s(t), ..., x_d^s(t))$ as the process generating $r_s = \| X^s \|^2$. The state variable dynamics for $x_i^s(t)$ is given by

$$dx_i^s(t) = \frac{1}{2}\sigma_t \sqrt{B_s(t,s)} dW_i^s(t)$$

Hence,

$$\begin{aligned} r_s &= \sum_{i=1}^{d} \left[\frac{1}{2} \int_t^s \sigma_u \sqrt{B_s(u,s)} dW_i^s(u) + x_i^s(u) \right]^2 \\ &= \frac{d}{4} \int_t^s \sigma_u^2 B_s(u,s) du + \| X^s(t) \| \int_t^s \sigma_u \sqrt{B_s(u,s)} dW^s(u) + \| X^s(t) \|^2 \end{aligned} \tag{2.19}$$

where $W^s(t) = (W_1^s(t), ..., W_d^s(t))$ is a d-dimensional Wiener process under P^s.

Note that, under P^s, the instantaneous forward rate can be represented as

$$f(t,s) = \| X^s(t) \|^2 + D(t,s) \tag{2.20}$$

Taking conditional expectations under P^s in (2.19) and using (2.15)-(2.16) and (2.20), we get

$$E^s [r_s | r_t] = D(t,s) + B_s(t,s) r_t$$

Defining $d = \delta = \frac{4\theta_t \kappa}{\sigma_t^2}$ and $\varpi = \frac{\delta}{D(t,s)} r_s$, we obtain

$$E^s [\varpi | r_t] = \delta + \frac{\delta B_s(t,s)}{D(t,s)} r_t$$

Hence, ϖ follows a non-central chi-square distribution with δ degrees of freedom and non-centrality parameter $(\delta B_s(t,s)/D(t,s))\, r_t$.

The value at time t of a derivative whose pay-off at time s is given by $U_s(r_s)$ will read as

$$U_t(r_t, t, s) = \widetilde{E} \left[e^{-\int_t^s r_u du} U_s(r_s) | r_t \right]$$

Applying Proposition 15, the next Proposition arises.

Proposition 16 *The value at time t of any interest rate derivative with terminal pay-off $U_s(r_s)$ is given by*

$$U_t(r_t, t, s) = P(r_t, t, s) E^s [U_s(\varpi) | r_t]$$

where $P(r_t, t, s)$ is given by Proposition 14, E^s represents expectation under P^s, and

$$\varpi = \frac{\delta}{D(t,s)} r_s \sim \chi^2 \left(\delta, \frac{\delta B_s(t,s)}{D(t,s)} r_t \right) \tag{2.21}$$

with $B(s,T)$ as given by Proposition 14 and $D(t,s)$ as given by (2.16). ∎

After obtaining this general closed-form expression, we analyse several particular cases:

1. **Forward on zero-coupon bond**

   Consider a forward contract expiring at time s written on a zero-coupon bond maturing at time $T > s$ and \$1 face value. Then, under the s-forward measure P^s, the delivery price established at time t for this forward contract is given as

   $$F(r_t, t, s, T) = E^s \left[P(r_s, s, T) | r_t \right]$$

   Then, using Proposition 16, the value of this bond forward is given as follows.

   Proposition 17 *The value at time t of a bond forward maturing at time s, written on a zero-coupon bond expiring at time T and \$1 face value is given by*

   $$\begin{aligned} F(r_t, t, s, T) &= E^s \left[P(r_s, s, T) | r_t \right] \\ &= \frac{A(s,T) e^{-\frac{1}{2}(\xi_1 - \xi_2)}}{\left(\frac{2}{\delta} B(s,T) D(t,s) + 1 \right)^{\frac{\delta}{2}}} \end{aligned}$$

   where $A(s,T)$ and $B(s,T)$ are given by Proposition 14, $D(t,s)$ as given by (2.16), and

   $$\begin{aligned} \xi_1 &= \frac{\delta B_s(t,s)}{D(t,s)} r_t \\ \xi_2 &= \frac{\xi_1}{\frac{2}{\delta} B(s,T) D(t,s) + 1} \end{aligned}$$

   ■

2. **European option on zero-coupon bond**

   Consider a European call option maturing at time s with strike K, written on a zero-coupon bond that matures at time $T > s$. Let $c_t(r_t, s, T, K)$ denote the price at time t of an European call option. Then, the boundary condition of the PDE (2.12) is given by

   $$c_s(r_s, s, T, K) = \max\{P(r_s, s, T) - K, 0\}$$

   Under the risk-neutral measure $\widetilde{P}$, the price at time t of this call option is given by

   $$c_t(r_t, s, T, K) = \widetilde{E} \left[e^{-\int_t^s r_u du} \left(P(r_s, s, T) - K \right)^+ | r_t \right]$$

   Then, using Proposition 16, we price this option as follows.

Proposition 18 *The price at time t of a European call option with maturity s written on a zero-coupon bond expiring at time T and \$1 face value is given by*

$$\begin{aligned} c_t(r_t,s,T,K) &= P(r_t,t,s)E^s\left[\left(A(s,T)e^{-B(s,T)r_s}-K\right)^+|r_t\right] \\ &= P(r_t,t,s)F(r_t,t,s,T)\chi^2\left(\rho_2,\delta,\xi_2\right)-P(r_t,t,s)K\chi^2\left(\rho_1,\delta,\xi_1\right) \end{aligned}$$

where $\chi^2(\cdot)$ denotes the non-central chi-square distribution function and

$$\begin{aligned} \rho_1 &= \frac{\delta}{B(s,T)D(t,s)}\ln\left(\frac{A(s,T)}{K}\right) \\ \rho_2 &= \rho_1\left(\frac{2}{\delta}B(s,T)D(t,s)+1\right) \\ \xi_1 &= \frac{\delta B_s(t,s)}{D(t,s)}r_t \\ \xi_2 &= \frac{\rho_1}{\rho_2}\xi_1 \end{aligned}$$

with $P(r_t,t,s)$, $A(\cdot,\cdot)$, and $B(\cdot,\cdot)$ as given in Proposition 14, $F(r_t,t,s,T)$ as given by Proposition 17, and $D(t,s)$ as given by equation (2.16). ■

Proof. See the Appendix. ■

3. **European option on coupon bond**

Consider a European call option that matures at time s and strike K. The underlying asset is a coupon bond maturing at time T paying N coupons α_i at times j_i, $i=1,2,\cdots,N$ where $j_1>s$, $j_N=T$. The price of this coupon bond at time s is given as the sum of the corresponding zero-coupon bonds, that is,

$$P(r_s,s,T)=\sum_{i=1}^{N}\alpha_i P(r_s,s,j_i) \tag{2.22}$$

where $P(r_s,s,j_i)$, $i=1,2\cdots,N$ is given by Proposition 14.

Let $c_t\left(r_t,s,\{j_i\}_{i=1}^N,K\right)$ denote the price at time t of this call option. Using (2.22), the boundary condition of the PDE (2.12) becomes now

$$c_s\left(r_s,s,\{j_i\}_{i=1}^N,K\right)=\max\left\{\sum_{i=1}^{N}\alpha_i P(r_s,s,j_i)-K,0\right\}$$

Applying Proposition 16, the call option price is given as

$$\begin{aligned} c_t\left(r_t,s,\{j_i\}_{i=1}^N,K\right) &= P(r_t,t,s)E^s\left[c_s\left(\varpi,s,\{j_i\}_{i=1}^N,K\right)|r_t\right] \\ &= P(r_t,t,s)E^s\left[\max\left\{\sum_{i=1}^{N}\alpha_i P(\varpi,s,j_i)-K,0\right\}|r_t\right] \end{aligned}$$

In line with Jamshidian (1989), we find $K_i,\ i = 1, 2, \cdots, N$ such that

$$\max\left\{\sum_{i=1}^{N} \alpha_i P(\varpi, s, j_i) - K, 0\right\} = \sum_{i=1}^{N} \alpha_i \max\left\{P(\varpi, s, j_i) - K_i, 0\right\} \tag{2.23}$$

where $K_i = P(\kappa, s, j_i)$ and κ is the solution of $\sum_{i=1}^{N} \alpha_i P(\kappa, s, j_i) = K$.[3]

Hence, this option can be interpreted as a portfolio of European call options on zero-coupon bonds with "appropriate" strikes K_i as stated in the following Proposition.

Proposition 19 *The price at time t of a European call option with maturity s on a coupon bond expiring at T, paying coupons α_i at times $j_i,\ i = 1, 2, \cdots, N$ is given by*

$$c_t\left(r_t, s, \{j_i\}_{i=1}^{N}, K\right) = \sum_{i=1}^{N} \alpha_i\ c_t\left(r_t, s, j_i, K_i\right)$$

where $c_t\left(r_t, s, j_i, K_i\right)$ is given by Proposition 18. ∎

4. **European bond forward option**

Consider a European bond forward call option maturing at time s with strike K, where the underlying asset is a bond forward contract with expiration date T_f written on a zero-coupon bond that matures at time $T_b > T_f > s$ and \$1 face value.

Let $c_t(r_t, s, T_f, T_b, K)$ denote the price at time t of this call option.

Then, the boundary condition for the PDE (2.12) is given by

$$c_s(r_s, s, T_f, T_b, K) = \max\left\{F(r_s, s, T_f, T_b) - K, 0\right\}$$

Under the risk-neutral measure $\widetilde{P}$, the price at time t of this option is given as

$$c_t(r_t, s, T_f, T_b, K) = \widetilde{E}\left[e^{-\int_t^s r_u du}\left(F(r_s, s, T_f, T_b) - K\right)^+ | r_t\right]$$

Applying Proposition 16, the price of this option is given by the following Proposition.

Proposition 20 *The price at time t of a European bond forward call option that matures at time s on a forward contract expiring at time T_f written on a zero-coupon bond maturing at time T_b and \$1 face value is given by*

$$\begin{aligned} c_t(r_t, s, T_f, T_b, K) &= P(r_t, t, s) E^s\left[\left(F(r_s, s, T_f, T_b) - K\right)^+ | r_t\right] \\ &= P(r_t, t, s)\Theta(r_t, t, s, T_f, T_b)\chi^2\left(\rho_2, \delta, \xi_2\right) - P(r_t, t, s) K \chi^2\left(\rho_1, \delta, \xi_1\right) \end{aligned}$$

[3]Note that the existence of strikes K_i such that (2.23) has a solution is guaranteed as the bond price decreases with the instantaneous interest rate.

where $\chi^2(\cdot)$ denotes the non-central chi-square distribution function and

$$\Theta(r_t,t,s,T_f,T_b) = \frac{A(T_f,T_b)e^{-\frac{1}{2}(\xi_1-\xi_2)}}{\left(\left(\frac{2}{\delta}B(T_f,T_b)D(s,T_f)+1\right)\left(\frac{D(t,s)}{\delta}H(s,T_f,T_b)+1\right)\right)^{\frac{\delta}{2}}}$$

$$\begin{aligned}
\rho_1 &= \frac{2\delta \ln\left(\frac{A(T_f,T_b)}{K\left(\frac{2}{\delta}B(T_f,T_b)D(s,T_f)+1\right)^{\frac{\delta}{2}}}\right)}{H(s,T_f,T_b)D(t,s)} \\
\rho_2 &= \rho_1\left(\frac{D(t,s)}{\delta}H(s,T_f,T_b)+1\right) \\
\xi_1 &= \frac{\delta B_s(t,s)}{D(t,s)}r_t \\
\xi_2 &= \frac{\rho_1}{\rho_2}\xi_1 \\
H(s,T_f,T_b) &= \frac{2\delta B(T_f,T_b)B_{T_f}(s,T_f)}{2B(T_f,T_b)D(s,T_f)+\delta}
\end{aligned}$$

where $P(r_t,t,s)$, $A(\cdot,\cdot)$, and $B(\cdot,\cdot)$ as given in Proposition 14 and $D(\cdot,\cdot)$ as in (2.16). ∎

Remark 3 *Note that $P(r_t,t,s)\Theta(r_t,t,s,T_f,T_b)$ can be interpreted not as the forward price at time t, but as the price at time t of an asset paying the forward price at time s.* ∎

Corollary 8 *For all the above cases, put option prices arise directly from put-call parity.* ∎

2.3.3 Interest Rate Derivatives

In this subsection we focus our attention on pricing "pure" interest rate derivatives, that is, derivatives whose underlying is directly the interest rate. We start pricing FRA's, and then, we move to more complicated products such as swaps, caps, floors, and collars.

1. **Forward Rate Agreement**

   Consider a FRA with \$1 notional value and maturity s, where the investor agrees to pay a fixed interest rate K and receive a floating rate with tenor $T_s - s$. The floating rate is set at time s and the net cash-flow is received at time $T_r > s$.

   Then, under the risk-neutral measure $\widetilde{P}$, the FRA value at time t is given by

   $$FRA_t(r_t,s,T_r,T_s,K) = \widetilde{E}\left[e^{-\int_t^{T_r} r_u du}\left(R(r_s,s,T_s)-K\right)|r_t\right]$$

   Applying Proposition 16, the value of this FRA is given by the following Proposition.

Proposition 21 *The value at time t of a FRA with \$1 notional value and maturity s, paying a fixed rate K and receiving a floating rate with tenor $T_s - s$, is given by*

$$\begin{aligned} FRA_t(r_t, s, T_r, T_s, K) &= P(r_t, t, T_r) E^s \left[R(r_s, s, T_s) - K | r_t \right] \\ &= P(r_t, t, T_r) \left[\frac{B(s, T_s)}{T_s - s} D(t, s) \left(1 + \frac{\xi}{\delta} \right) - \frac{\ln(A(s, T_s))}{T_s - s} - K \right] \end{aligned}$$

where

$$\xi = \frac{\delta B_s(t, s)}{D(t, s)} r_t$$

with $P(r_t, t, T_r)$ and $B(t, s)$ as given in Proposition 14 and $D(t, s)$ as given by (2.16). ∎

2. **Interest rate swap and swaption**

An interest rate swap can be interpreted as either the difference between two coupon bonds or a portfolio of FRA's. Hence, swap valuation is a straightforward application of Proposition 14 or 21. Moreover, swaptions can be valued applying Proposition 19.

3. **Cap, floor, and collar**

A cap (floor) contract guarantees to its holder a pay-off if a certain floating interest rate is above (below) a specified rate, the cap (floor) level. Similarly to swaps, caps and floors involve a series of regular payments, usually referred as caplets or floorlets. Therefore, a cap (floor) can be interpreted as a portfolio of caplets (floorlets).

Consider a caplet written on a floating rate with \$1 face value and maturity s. If the caplet is exercised, the investor pays a fixed interest rate K and receives a floating rate with tenor $T_s - s$. The floating rate is set at time s and the net cash-flow is received at time $T_r > s$.

Under the risk-neutral measure $\widetilde{P}$, the price at time t of this caplet is given by

$$Caplet_t(r_t, s, T_r, T_s, K) = \widetilde{E} \left[e^{-\int_t^{T_r} r_u du} \left(R(r_s, s, T_s) - K \right)^+ | r_t \right]$$

Under the s-forward measure P^s, the caplet price is given by the following Proposition.

Proposition 22 *The price at time t of a caplet written on the floating rate with \$1 face value and tenor $T_s - s$ is given as*

$$\begin{aligned} Caplet_t(r_t, s, T_r, T_s K) &= P(r_t, t, T_r) E^s \left[\left(R(r_s, s, T_s) - K \right)^+ | r_t \right] \\ &= P(r_t, t, T_r) \frac{D(t, s) B(s, T_s)}{\delta (T_s - s)} \left[\delta + \xi - 2 e^{-\frac{\xi}{2}} \sum_{n=0}^{\infty} \left(\frac{\xi}{2} \right)^n \frac{\Gamma\left(\frac{\delta}{2} + n + 1, \frac{\rho}{2} \right)}{n! \, \Gamma\left(\frac{\delta}{2} + n \right)} \right] \\ &\quad - \left(\frac{\ln(A(s, T_s))}{T_s - s} + K \right) P(r_t, t, T_r) \left[1 - \chi^2 (\rho, \delta, \xi) \right] \end{aligned}$$

where $\chi^2(\cdot)$ denotes the non-central chi-square distribution function, $\Gamma(\cdot)$ represents the Gamma function, and

$$\begin{aligned} \xi &= \frac{\delta B_s(t,s)}{D(t,s)} r_t \\ \rho &= \left(K + \frac{\ln(A(s,T_s))}{T_s - s} \right) \frac{\delta(T_s - s)}{B(s,T_s) D(t,s)} \end{aligned}$$

with $P(r_t, t, T_r)$ and $B(t,s)$ as given in Proposition 14 and $D(t,s)$ as given by (2.16). ∎

In order to price a floorlet, same type of calculations as in this Proposition can be used. Alternatively, we can use the caplet-floorlet parity.

Cap, floor, and collar prices are a straightforward application of these results.

2.4 Conclusions

This chapter has presented a new continuous-time model for the term structure of interest rates assuming that the mean reversion level of interest rates and the spot rate volatility follow a cyclic behaviour modelled by an harmonic oscillator functional form. Under this specification, the model incorporates a lot of flexibility, allowing it to capture a variety of different shapes of the term structure. In more detail, considering the possibility of a cyclical long-term level in interest rates, this model allows us to capture a number of changes in the level, slope, and curvature of the term structure. Hence, several humps can be easily achieved choosing the appropriate parameters affecting the mean reversion level, that is, the amplitude of the wave, the temporal frequency, and the offset phase.

Our model nests the original one presented in Cox it et al. (1985), keeping the same analytical tractability of the CIR model. Consequently, we can value any contingent claim in a much more flexible framework while still maintaining the analytical tractability. Under these assumptions, we have computed closed-form expressions for prices of bonds and several fixed income and interest rate derivatives. We have also computed some risk management measures for bonds.

The results obtained have strong practical applications for pricing and risk management purposes and should be of special interest for traders, financial institutions, and risk managers.

Appendix of Proofs

Proof of Proposition 14

To solve equation (2.12), we guess an exponential-affine functional form for the bond price

$$P(r_t, t, T) = A(t, T)e^{-B(t,T)r_t}$$

with terminal conditions $A(T, T) = 1,\ B(T, T) = 0$. Then,

$$P_t = \frac{A_t}{A}P - B_t r_t P, \quad P_r = -BP, \quad P_{rr} = B^2 P$$

where arguments have been omitted and subscripts in functions $P,\ A$, and B denote partial derivatives. Replacing these expressions into (2.12), we get

$$\frac{A_t}{A} - B_t r_t - B\left[\kappa(\theta_t - r_t) - \lambda_t r_t\right] + \frac{1}{2}\sigma_t^2 r_t B^2 - r_t = 0$$

with boundary condition $A(T, T) = 1,\ B(T, T) = 0$. Since this equation is linear in r_t, we obtain the following system of ordinary differential equations (ODEs)

$$B_t - (\lambda_t + \kappa)\, B - \frac{1}{2}\sigma_t^2 B^2 + 1 = 0 \tag{2.24}$$

$$A_t - k\theta_t AB = 0 \tag{2.25}$$

Applying standard theory for Ricatti-type equations and defining $\tau = T - t$, the solution of (2.24) is given as $B(\tau) = \frac{v(\tau)}{u(\tau)}$ where $v(\tau)$ and $u(\tau)$ are solutions of the system

$$-v'(\tau) + u(\tau) - \kappa v(\tau) = 0 \tag{2.26}$$

$$-u'(\tau) + \lambda_t u(\tau) + \frac{1}{2}\sigma_t^2 v(\tau) = 0 \tag{2.27}$$

Replacing the derivative of (2.26) into (2.27), we obtain the second-order ODE

$$v''(\tau) + bv'(\tau) + e(\tau)v(\tau) = 0 \tag{2.28}$$

where $b = \kappa - \lambda_t$ and

$$e(\tau) = -\lambda_t\kappa - \frac{1}{2}A_\sigma \sin^2(\varphi - \omega T + \omega\tau)$$

Setting $v(\tau) = g(\tau)M(\tau)$, expression (2.28) becomes

$$g(\tau)M''(\tau) + (2g'(\tau) + bg(\tau))M'(\tau) + (g''(\tau) + bg'(\tau) + e(\tau)g(\tau))M(\tau) = 0$$

that represents a Mathieu's differential equation if $2g'(\tau) + bg(\tau) = 0$. Then, we get

$$g(\tau) = ce^{\frac{1}{2}(\lambda-\kappa)\tau}$$

with arbitrary constant c. Then, we obtain

$$v(\tau) = e^{\frac{1}{2}(\lambda-\kappa)\tau}\left(c_1 MC(a,q,x) + c_2 MS(a,q,x)\right) \tag{2.29}$$

where MC and MS represent the Mathieu cosine and sine functions, respectively, and

$$a = -\frac{A_\sigma + (\lambda+\kappa)^2}{4\omega^2},\ q = -\frac{A_\sigma}{8\omega^2},\ x = \varphi - \omega T + \omega\tau$$

The boundary condition $B(0) = 0$ implies $v(0) = 0$. Then, choosing $c_2 = 1$ in (2.29) implies

$$c_1 = -\frac{MS(a,q,\varphi-\omega T)}{MC(a,q,\varphi-\omega T)}$$

Substituting (2.29) and its derivative into (2.26), we get

$$u(\tau) = e^{\frac{1}{2}(\lambda-\kappa)\tau}\left[\frac{1}{2}(\lambda+\kappa)\left(c_1 MC(a,q,x) + MS(a,q,x)\right) + \omega\left(c_1 MCP(a,q,x) + MSP(a,q,x)\right)\right] \tag{2.30}$$

where MCP and MSP represent the derivatives with respect to x of the Mathieu cosine and sine functions, respectively. Therefore, using expressions (2.29)-(2.30),we get $B(\tau)$.

Finally, equation (2.25) immediately provides $A(t,T) = \exp\left\{-\int_t^T \kappa\theta_t B(t,T)dt\right\}$. ∎

Proof of Proposition 18

From Proposition 16, we know

$$c_t(r_t,s,T,K) = P(r_t,t,s)E^s\left[\left(A(s,T)e^{-\frac{1}{\delta}B(s,T)D(t,s)\varpi} - K\right)^+ | r_t\right]$$

where E^s represents expectation with respect to the s-forward measure P^s. Hence,

$$\begin{aligned} c_t(r_t,s,T,K) &= P(r_t,t,s)\int_0^\infty \left(A(s,T)e^{-\frac{1}{\delta}B(s,T)D(t,s)\varpi} - K\right)^+ d\chi^2\left(\varpi,\delta,\xi_1\right) \\ &= P(r_t,t,s)\int_0^{\rho_1} A(s,T)e^{-\frac{1}{\delta}B(s,T)D(t,s)\varpi} d\chi^2\left(\varpi,\delta,\xi_1\right) - KP(r_t,t,s)\chi^2\left(\rho_1,\delta,\xi_1\right) \end{aligned}$$

where $\chi^2(\cdot)$ denotes the non-central chi-square distribution function and

$$\begin{aligned} \xi_1 &= \frac{\delta B_s(t,s)}{D(t,s)} r_t \\ \rho_1 &= \frac{\delta}{B(s,T)D(t,s)} \ln\left(\frac{A(s,T)}{K}\right) \end{aligned}$$

Using the expression for the density function of a non-central chi-square distribution, the integral becomes

$$P(r_t,t,s)A(s,T)\int_0^{\rho_1} e^{-\frac{1}{\delta}B(s,T)D(t,s)\varpi}\left[2^{-\frac{\delta}{2}}\varpi^{\frac{\delta}{2}-1}e^{-(\varpi+\xi_1)/2}\sum_{n=0}^{\infty}\frac{\varpi^n\left(\xi_1\right)^n}{n!4^n\Gamma(\frac{\delta}{2}+n)}\right]d\varpi$$

Considering the change of variable $y = \left(\frac{2}{\delta}B(s,T)D(t,s)+1\right)\varpi$ and defining

$$\begin{aligned}\rho_2 &= \rho_1\left(\frac{2}{\delta}B(s,T)D(t,s)+1\right)\\ \xi_2 &= \frac{\rho_1}{\rho_2}\xi_1\end{aligned}$$

we get

$$P(r_t,t,s)F(r_t,t,s,T)\chi^2\left(\rho_2,\delta,\xi_2\right)$$

with $F(r_t,t,s,T)$ as given by Proposition 17. ∎

Proof of Proposition 22

From Proposition 16, we know

$$\begin{aligned}&Caplet_t(r_t,s,T_r,T_s,K) = P(r_t,t,T_r)E^s\left[\left(R(r_s,s,T_s)-K\right)^+|r_t\right]\\ =\;& P(r_t,t,T_r)\int_\rho^\infty \frac{B(s,T_s)D(t,s)}{\delta(T_s-s)}\varpi d\chi^2(\varpi,\delta,\xi) - \left(\frac{\ln(A(s,T_s))}{T_s-s}+K\right)P(r_t,t,T_r)\left[1-\chi^2(\rho,\delta,\xi)\right]\end{aligned}$$

where E^s represents expectation with respect to the s-forward measure P^s, $\chi^2(\cdot)$ denotes the non-central chi-square distribution function, and

$$\begin{aligned}\xi &= \frac{\delta B_s(t,s)}{D(t,s)}r_t\\ \rho &= \left(K+\frac{\ln(A(s,T_s))}{T_s-s}\right)\frac{\delta(T_s-s)}{B(s,T_s)D(t,s)}\end{aligned}$$

Using the expression for the density function of a non-central chi-square distribution, the integral becomes

$$\frac{B(s,T_s)D(t,s)}{\delta(T_s-s)}2^{-\frac{\delta}{2}}e^{-\frac{\xi}{2}}\sum_{n=0}^\infty\frac{\xi^n}{n!4^n\Gamma(\frac{\delta}{2}+n)}\int_\rho^\infty \varpi^{\frac{\delta}{2}+n}e^{-\frac{1}{2}\varpi}d\varpi \tag{2.31}$$

Note that

$$\int_\rho^\infty \varpi^{\frac{\delta}{2}+n}e^{-\frac{1}{2}\varpi}d\varpi = 2^{\frac{\delta}{2}+n+1}\left[\Gamma\left(\frac{\delta}{2}+n+1\right)-\Gamma\left(\frac{\delta}{2}+n+1,\frac{\rho}{2}\right)\right]$$

where $\Gamma(\alpha,\varrho)=\int_0^\varrho e^{-t}t^{\alpha-1}dt$ and $\Gamma(\alpha)\equiv\Gamma(\alpha,\infty)$. Using the Taylor expansion of the exponential function and straightforward algebra, (2.31) becomes

$$\frac{B(s,T_s)D(t,s)}{\delta(T_s-s)}\left[\delta+\xi-2e^{-\frac{\xi}{2}}\sum_{n=0}^\infty\left(\frac{\xi}{2}\right)^n\frac{\Gamma\left(\frac{\delta}{2}+n+1,\frac{\rho}{2}\right)}{n!\;\Gamma\left(\frac{\delta}{2}+n\right)}\right]$$

∎

2.5 Appendix of Figures

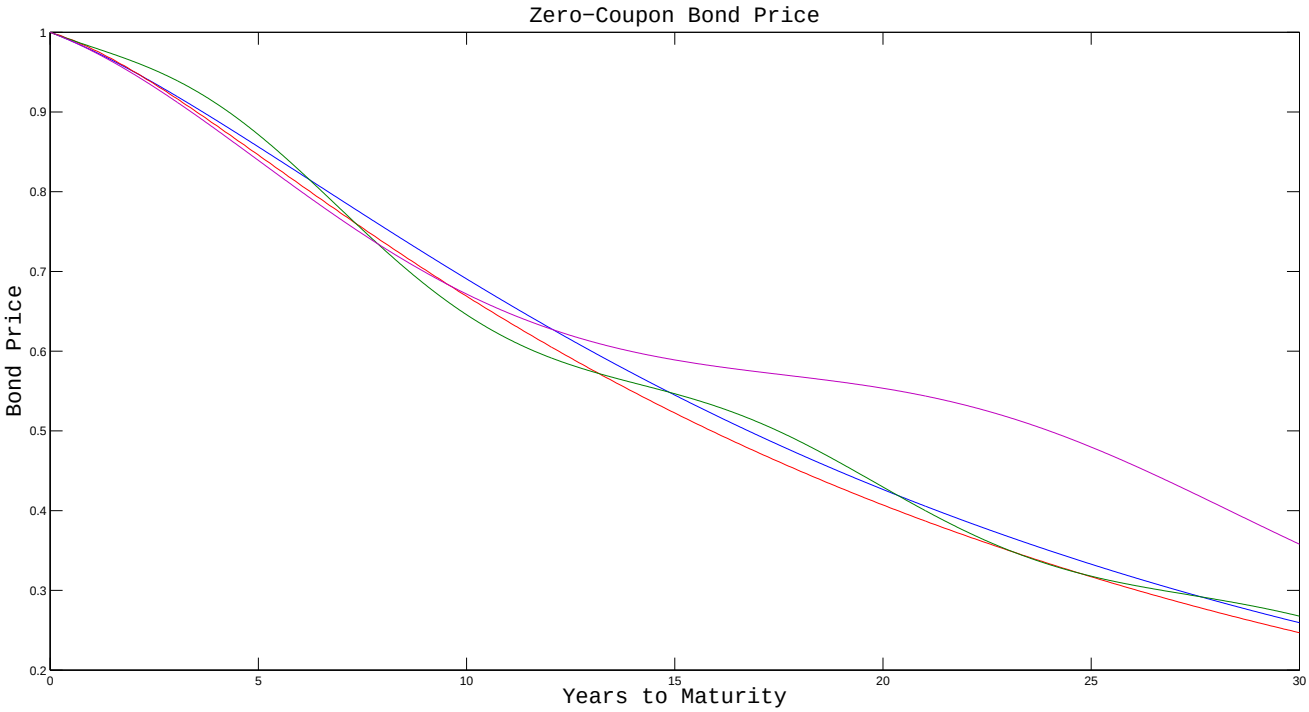

Figure 2.1: Simulation of the Zero-coupon bond price term structure for an arbitrary set of parameters.
Parameter Values CIR Model:
Lightblue line: $r_0 = 0.015,\ \theta = 0.1,\ \sigma = 0.005,\ \kappa = 0.1.$
Parameter Values Cyclic Model :
Blue line: $r_0 = 0.015,\ A_\theta = 0.2,\ A_\sigma = 0.001,\ \kappa = 0.1, \omega = 0.08, \varphi = \pi,\ \lambda = 0.$
Red line: $r_0 = 0.015,\ A_\theta = 0.1,\ A_\sigma = 0.005,\ \kappa = 0.15, \omega = 0.2, \varphi = \frac{\pi}{2},\ \lambda = 0.$
Black line: $r_0 = 0.015,\ A_\theta = 0.08,\ A_\sigma = 0.002,\ \kappa = 0.15, \omega = 0.15, \varphi = \frac{\pi}{4},\ \lambda = 0.$
Green line: $r_0 = 0.015,\ A_\theta = 0.1,\ A_\sigma = 0.002,\ \kappa = 0.3, \omega = 0.10, \varphi = \pi,\ \lambda = 0.$

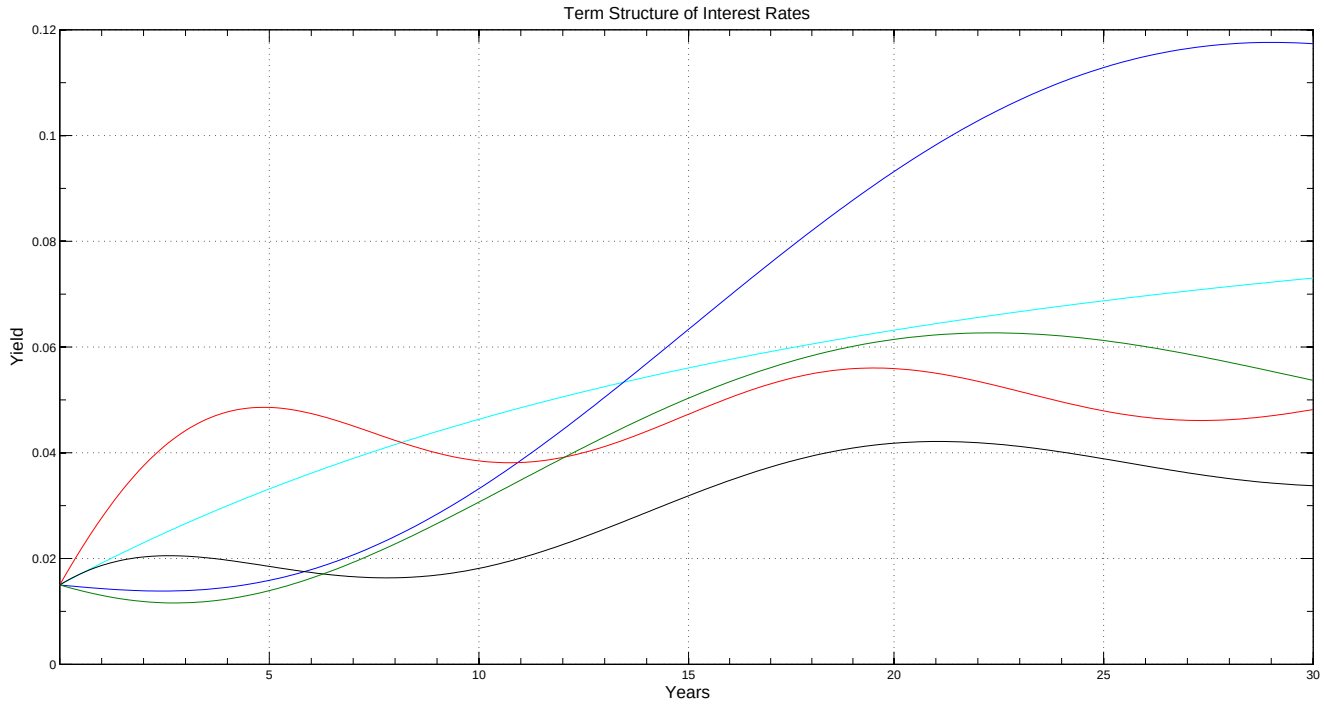

Figure 2.2: Term Structure of Interest Rates for an arbitrary set of parameters.
Parameter Values CIR Model:
Lightblue line: $r_0 = 0.015,\ \theta = 0.1,\ \sigma = 0.005,\ \kappa = 0.1.$
Parameter Values Cyclic Model :
Blue line: $r_0 = 0.015,\ A_\theta = 0.2,\ A_\sigma = 0.001,\ \kappa = 0.1, \omega = 0.08, \varphi = \pi,\ \lambda = 0.$
Red line: $r_0 = 0.015,\ A_\theta = 0.1,\ A_\sigma = 0.005,\ \kappa = 0.15, \omega = 0.2, \varphi = \frac{\pi}{2},\ \lambda = 0.$
Black line: $r_0 = 0.015,\ A_\theta = 0.08,\ A_\sigma = 0.002,\ \kappa = 0.15, \omega = 0.15, \varphi = \frac{\pi}{4},\ \lambda = 0.$
Green line: $r_0 = 0.015,\ A_\theta = 0.1,\ A_\sigma = 0.002,\ \kappa = 0.3, \omega = 0.10, \varphi = \pi,\ \lambda = 0.$

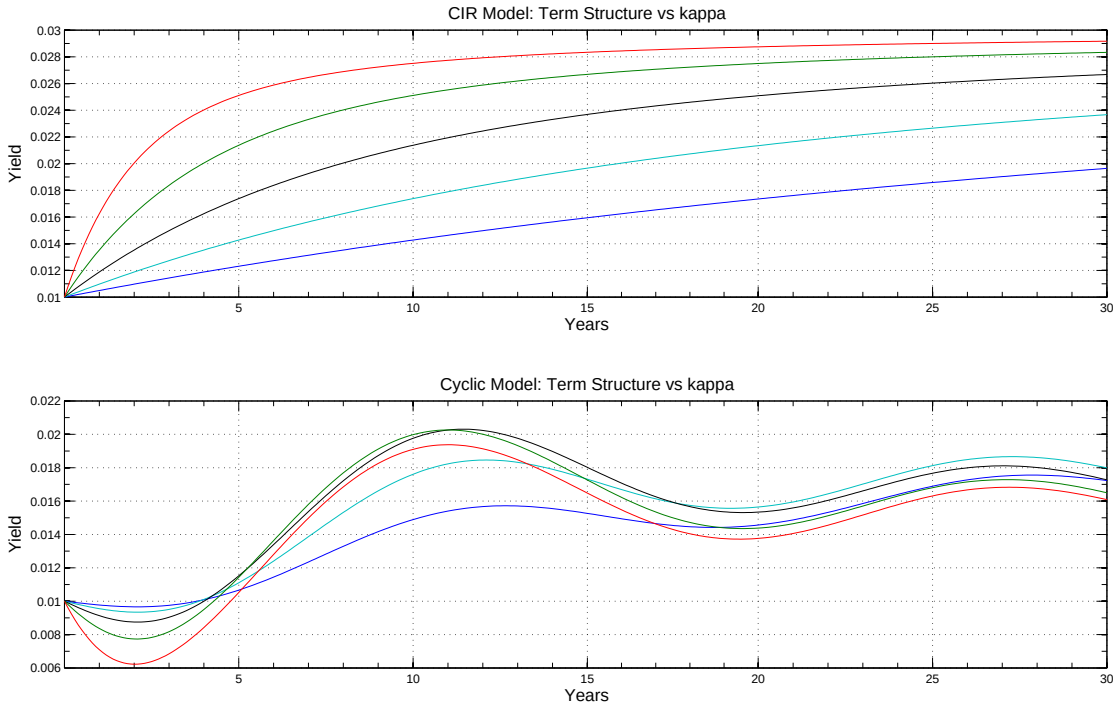

Figure 2.3: Term structure of interest rates for different values of the speed of mean reversion κ. In both models, the values of κ are: Blue Line: $= 0.05$, Lightblue Line: $= 0.1$, Black Line: $= 0.2$, Green Line: $= 0.4$, and Red Line:$= 0.8$;

Parameter Values CIR Model: $r_0 = 0.01,\ \theta = 0.03,\ \sigma = 0.0002$.

Parameter Values Cyclic Model: $r_0 = 0.01,\ A_\theta = 0.03,\ A_\sigma = 0.0002,\ \omega = 0.20,\ \varphi = 0,\ \lambda = 0$.

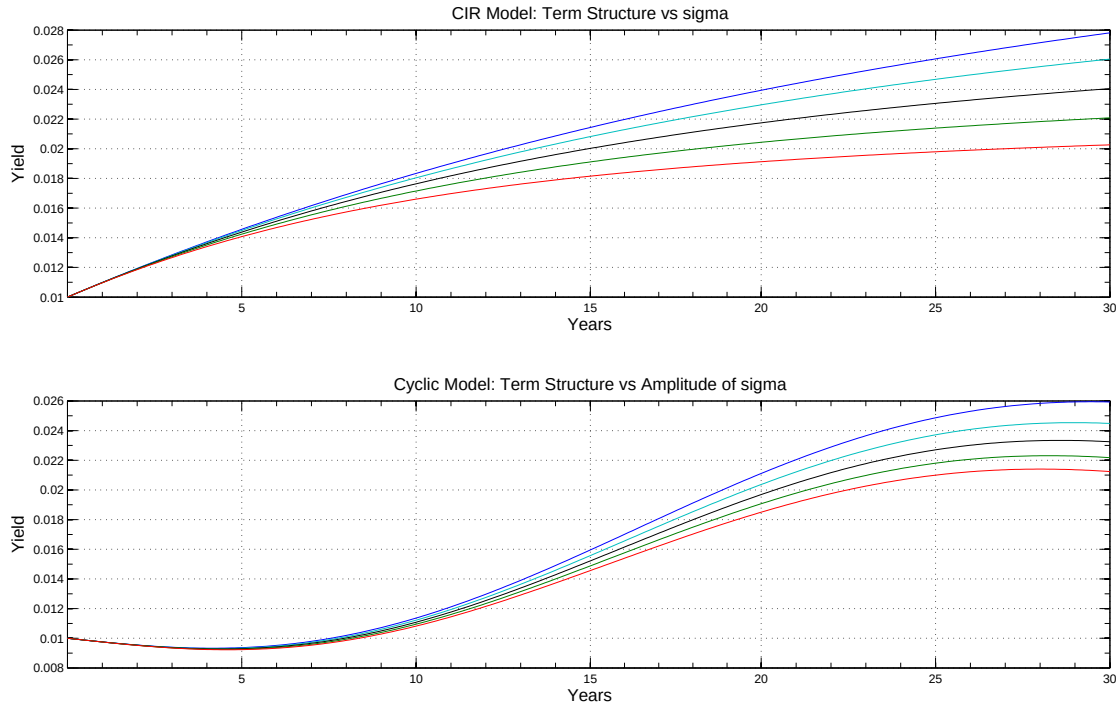

Figure 2.4: Term structure of interest rates for different values of the volatility parameter. The values of σ and A_σ corresponding to CIR and the Cyclic model, respectively, are: Blue Line: $= 0.003$, Lightblue Line: $= 0.005$, Black Line: $= 0.007$, Green Line: $= 0.009$, and Red Line:$= 0.011$;

Parameter Values CIR Model: $r_0 = 0.01,\ \theta = 0.05,\ \kappa = 0.05$.

Parameter Values Cyclic Model: $r_0 = 0.01,\ A_\theta = 0.05,\ \kappa = 0.05,\ \omega = 0.08,\ \varphi = 0,\ \lambda = 0$.

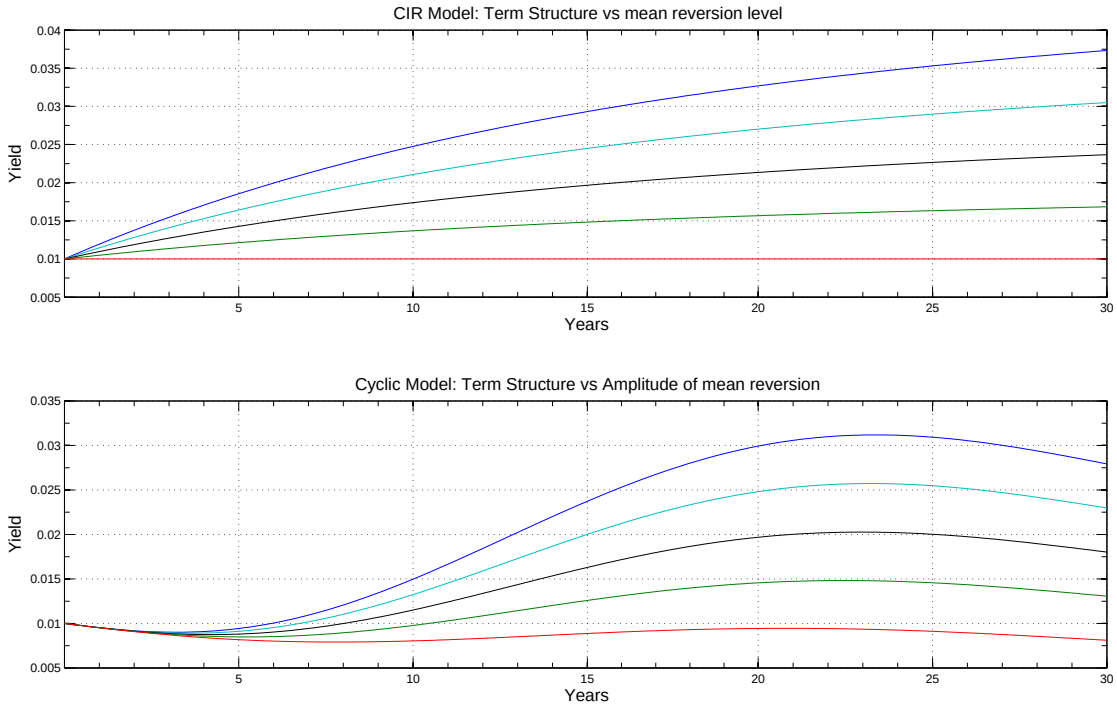

Figure 2.5: Term structure of interest rates for different values of the mean reversion level. The values of θ and A_θ corresponding to CIR and the Cyclic model, respectively, are: Blue Line: $= 0.05$, Lightblue Line: $= 0.04$, Black Line: $= 0.03$, Green Line: $= 0.02$, and Red Line:$= 0.01$;
Parameter Values CIR Model: $r_0 = 0.01,\ \sigma = 0.0002,\ \kappa = 0.1$.
Parameter Values Cyclic Model: $r_0 = 0.01,\ A_\sigma = 0.0002,\ \kappa = 0.1,\ \omega = 0.1,\ \varphi = 0,\ \lambda = 0$.

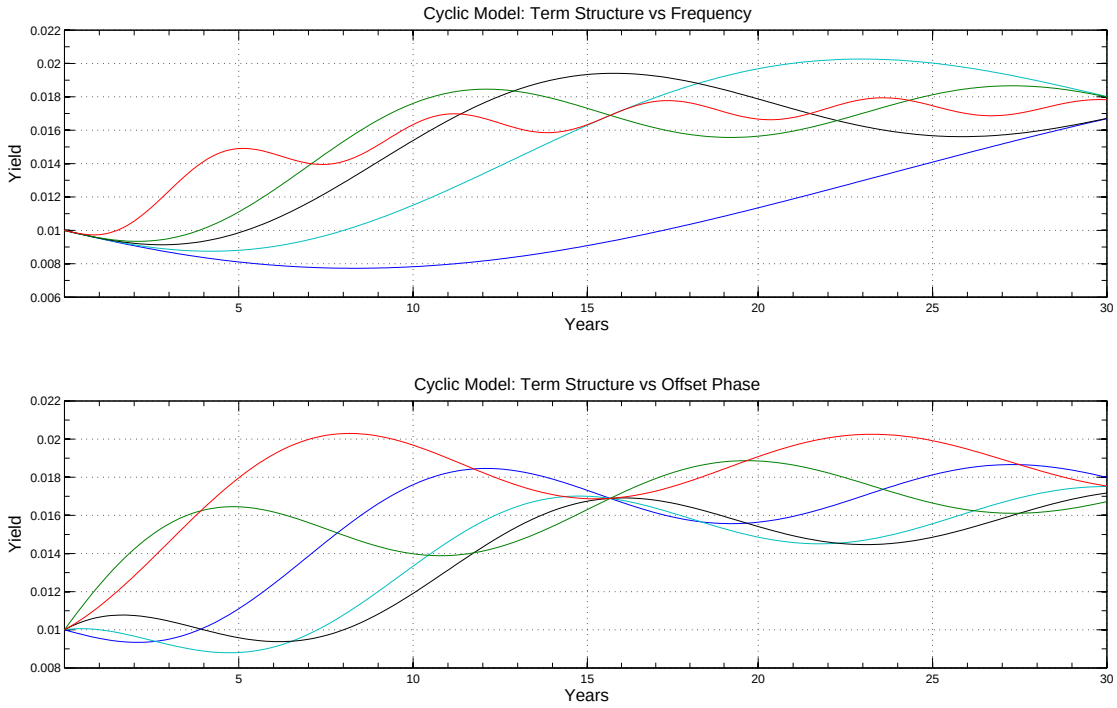

Figure 2.6: Term structure of interest rates for different values of the frequency and offset phase.
The values of ω in the first graph are: Blue Line: $= 0.05$, Lightblue Line: $= 0.1$, Black Line: $= 0.15$, Green Line: $= 0.2$, and Red Line:$= 0.5$. And $r_0 = 0.01,\ A_\theta = 0.03,\ A_\sigma = 0.0002,\ \kappa = 0.1, \varphi = 0,\ \lambda = 0$.
The values of φ in the second graph are: Blue Line: $= 0$, Lightblue Line: $= \frac{\pi}{6}$, Black Line: $= \frac{\pi}{4}$, Green Line: $= \frac{\pi}{2}$, and Red Line:$= \frac{3\pi}{4}$. And $r_0 = 0.01,\ A_\theta = 0.03,\ A_\sigma = 0.0002,\ \kappa = 0.1,\ \omega = 0.2,\ \lambda = 0$.

Bibliography

[1] Black, F., E. Dermand and W. Toy (1990). A One-Factor Model of Interest Rates and its Application to Treasury Bond Options. *Financial Analysts Journal*, 46, 33–39.

[2] Black, F. and P. Karasinski (1991). Bond and Option Pricing when Short Rates are Lognormal. *Financial Analysts Journal*, 47, 52-59.

[3] Brennan, M.J. and E.S. Schwartz (1980). Analyzing Convertible Bonds. *Journal of Financial and Quantitative Analysis*, 15, 4, 907-929.

[4] Brigo, D. and F. Mercurio (2006). *Interest Rate Models Theory and Practice*, Springer-Verlag Berlin Heidelberg.

[5] Chan, K.C., G.A. Karolyi, F.A. Longstaff, and A.B. Sanders (1992). An Empirical Comparison of Alternative Models of the Short-Term Interest Rate. *Journal of Finance*, 47, 3, 1209-1227.

[6] Chen, L. (1996). *Interest Rate Dynamics, Derivatives Pricing, and Risk Management*. Springer-Verlag, Berlin.

[7] Cox, J.C., J.E. Ingersoll, and S.A. Ross (1985). A Theory of the Term Structure of Interest Rates. *Econometrica*, 53, 2, 385-408.

[8] Duffie, D. and R. Kan (1996). A Yield-Factor Model of Interest Rates. *Mathematical Finance*, 6, 4, 379-406.

[9] Feller, W. (1951). Two Singular Diffusion Problems. *Ann. Math.*, 54, 173-182.

[10] Filipović, D. (2009). *Term Structure Models A Graduate Course*, Springer-Verlag Berlin Heidelberg.

[11] Heath, D., R. Jarrow, and A. Morton (1992). Bond Pricing and the Term Structure of Interest Rates: A New Methodology for Contingent Claims Valuation. *Econometrica*, 60, 77-105.

[12] Ho, T.S.Y. and S. Lee (1986). Term Structure Movements and Pricing Interest Rate Contingent Claims. *Journal of Finance*, 41, 5, 1011-1029.

[13] Hull, J. and A. White (1990). Pricing Interest-Rate-Derivative Securities. *Review of Financial Studies*, 3, 4, 573–592.

[14] Hull, J. and A. White (1993). One-Factor Interest-Rate Models and the Valuation of Interest-Rate Derivative Securities, *Journal of Financial and Quantitative Analysis*, 28, 2, 235-254.

[15] Jamshidian, F. (1989). An Exact Bond Option Formula. *Journal of Finance*, 44, 1, 205-209.

[16] Karatzas, I. and S. E. Shreve (1988). Brownian Motion and Stochastic Calculus, New York, Berlin, Heidelberg. Springer-Verlag.

[17] Longstaff, F.A. and E.S. Schwartz (1992). Interest Rate Volatility and The Term Structure: A Two-Factor General Equilibrium Model. *Journal of Finance*, 47, 4, 1259-1282.

[18] Merton, R.C. (1973). Theory of Rational Option Pricing. *Bell Journal of Economics and Management Science*, 4, 1, 141-183.

[19] Mercurio, F. and J.M. Moraleda (2000). An Analytically Tractable Interest Rate Model with Humped Volatility. *European Journal of Operational Research*, 120, 205-214.

[20] Schaefer, S.M. and E.S. Schwartz (1984). A Two-Factor Model of the Term Structure: An Approximate Analytical Solution. *Journal of Financial and Quantitative Analysis*, 19, 4, 413-424.

[21] Vasicek, O. (1977). An Equilibrium Characterization of the Term Structure. *Journal of Financial Economics*, 5, 2, 177-188.

[22] Webber, N. and J. James (2001). *Interest Rate Modelling: Financial Engineering*, John Wiley & Sons, Ltd, England.

Chapter 3

Valuation of commodity derivatives when spot prices revert to a cyclical mean

3.1 Introduction

Characterizing the stochastic behaviour of commodity prices constitutes an issue of special relevance for practitioners in financial markets and it has been deeply analysed in many academic papers throughout the years. That is hardly surprising, since some commodity markets are very liquid and they move every day a huge amount of financial investments. Furthermore, many financial contingent claims such as futures, options and options on futures use some commodity as the underlying asset. Given the seasonal behaviour exhibited by most commodities, this chapter introduces a new continuous-time model based on an Ornstein-Uhlenbeck process for the logarithm of the commodity spot price, with a reversion to a time dependent long-run level, the time variation of the long-run price level being characterized by a Fourier series. The underlying idea behind this assumption is that the pricing process is driven by market forces and dominated by a strong seasonal component. Intuitively, some commodity prices are pulled back to a lower mean reversion level whenever the supply is high or the demand is low, while this reversion level tends to be higher whenever the supply is low or the demand is high. In other cases, a given commodity may be perceived as a refuge against bad economic times, and the cyclical behaviour in its price may reflect in part the evolution of the business cycle in some major economy. Under this framework, we compute closed-form expressions for the prices of futures, European options and European options on futures.[1]

In the academic literature we can find a significant number of papers addressing empirically and theoretically the commodity valuation problem. A pioneer contribution can be found in Schwartz (1997), who compares three mean-reverting models for the stochastic behaviour of commodity. The first model is a simple one-factor model based on the logarithm of the commodity spot price, constituting the starting point of our posited model. The second is the two-factor model proposed in Gibson and Schwartz (1990), where the second factor accounts for the convenience yield of the commodity. Finally, the third model is an extension of the Gibson and Schwartz (1990) model that incorporates the stochastic behaviour of interest rates as in Vasicek (1977). An interesting twist of the two-factor model is presented in Schwartz and Smith (2000), where the log-spot price is described as the sum of two state variables referred to as the short-term deviation in prices and the equilibrium price level, respectively. In more detail, short-run deviations are assumed to revert toward zero and the equilibrium level is assumed to follow a Brownian motion process.

Addressing the possible seasonal behaviour of the commodity price, a simple and clever contribution can be found in Lucia and Schwartz (2002). In this paper the authors use the Scandinavian electricity market to compare a number of models based on the spot price and the logarithm of the spot price, where the seasonal component is arbitrary added in the spot (log-spot) price and modelled by a deterministic trigonometric function with annual frequency. An interesting extension of

[1] In this chapter we make no distinction between futures and forward agreements.

the one-factor log-spot price model presented in Lucia and Schwartz (2002) can be found in Cartea and Figueroa (2005), where the stochastic process follows a zero level mean-reverting jump-diffusion process for the underlying log-spot price and the exponential of the trigonometric function is replaced by a Fourier series of order five. For a thorough description of some commodity models see, for instance, Pilipović (1998).

Energy and power markets present a perfect framework to analyse the suitability of this kind of models with a seasonal component. By its own nature, any source of energy is difficult to store or transport. For instance, natural gas low density makes highly impractical its storability and transportation, and has a deep impact on its price, specially in those periods of high demand or production shortages. Additionally, there is a bunch of seasonal variables driving the commodity price, such as business activity, weather conditions, market regulations, etc. There is a rich academic literature focused on energy markets and the corresponding pricing issues. Some interesting contributions on this area can be found in Clewlow and Strickland (2000), Eydeland and Wolyniec (2003), Geman (2005), Burger, Graeber, and Schindlmayr (2007), Forsythe (2007), Weron (2007), and Carmona and Coulon (2012), among many others.

In this chapter, we focus our analysis on natural gas as a source of energy, taking Henry Hub as the pricing point for natural gas futures contracts. We compare the fitting ability of our model to market data against two alternative benchmarks. In particular, we use the one-factor models proposed in Schwartz (1997) and Lucia and Schwartz (2002) for the logarithm of the commodity spot price. Since the seasonal component varies among commodities and it could even be different for the same commodity at different maturities, it will be crucial to identify those underlying periods driving the market forces. We use spectral analysis to identify such frequencies, and in particular, the fundamental frequency.

This chapter is organized as follows. Section 3.2 presents the benchmark models and their main features. Section 3.3 derives the posited model and the futures pricing formula. Section 3.4 provides closed-form expressions for prices of different derivatives. Section 3.5 presents the empirical analysis. Finally, Section 3.6 summarizes the main findings and provides some concluding remarks.

3.2 Benchmark models

This Section introduces the benchmark models presented by Schwartz (1997) and Lucia and Schwartz (2002), Model 1 and Model 2, respectively.

3.2.1 Model 1

This model assumes that the commodity spot price S_t follows a stochastic process given by,

$$dS_t = \kappa\left(\mu - \ln(S_t)\right) S_t dt + \sigma S_t dW_t$$

where κ, μ, and σ are constant parameters, and W_t is a standard Wiener process.

Moreover, defining $X_t = \ln(S_t)$, assuming a constant market price of risk λ, and applying Ito's Lemma, the log price can be represented by the following risk-neutral process

$$dX_t = \kappa\left(\widetilde{\alpha} - X_t\right) dt + \sigma d\widetilde{W}_t$$

where

$$\widetilde{\alpha} = \mu - \frac{\sigma^2}{2\kappa} - \frac{\lambda\sigma}{\kappa}$$

where $\widetilde{\alpha}$, κ and σ are constant parameters and $\widetilde{W}_t = W_t + \lambda t$ is a standard Wiener process under the risk-neutral measure $\widetilde{P}$. In addition, under this measure, the solution to equation (3.2.1) is given as

$$X_s = e^{-\kappa(s-t)} X_t + \left(1 - e^{-\kappa(s-t)}\right)\widetilde{\alpha} + \sigma \int_t^s e^{-\kappa(s-u)} d\widetilde{W}_u$$

which is normally distributed with mean and variance at time T as follows

$$\begin{aligned}
\widetilde{E}[X_T|F_t] &= e^{-\kappa(T-t)} X_t + \left(1 - e^{-\kappa(T-t)}\right)\widetilde{\alpha} \\
\widetilde{V}[X_T|F_t] &= \frac{\sigma^2}{2\kappa}\left(1 - e^{-2\kappa(T-t)}\right)
\end{aligned}$$

Since the spot price of the commodity at time T is log-normally distributed, the forward price of the commodity is given as

$$\begin{aligned}
F(S_t, t, T) &= \widetilde{E}\left[S_T|F_t\right] = \exp\left\{\widetilde{E}\left[X_T|F_t\right] + \frac{1}{2}\widetilde{V}\left[X_T|F_t\right]\right\} \\
&= \exp\left\{e^{-\kappa(T-t)}\ln(S_t) + \left(1 - e^{-\kappa(T-t)}\right)\widetilde{\alpha} + \frac{\sigma^2}{4\kappa}\left(1 - e^{-2\kappa(T-t)}\right)\right\}
\end{aligned}$$

Alternatively,

$$\ln(F(S_t, t, T)) = e^{-\kappa(T-t)}\ln(S_t) + \left(1 - e^{-\kappa(T-t)}\right)\widetilde{\alpha} + \frac{\sigma^2}{4\kappa}\left(1 - e^{-2\kappa(T-t)}\right) \tag{3.1}$$

3.2.2 Model 2

Proposed by Lucia and Schwartz (2002), we find another one factor model based on the log spot price. However, this model incorporates an interesting feature to capture the seasonal effect in the

pricing process. Particularly, model 2 incorporates a deterministic function of time, $f(t)$, in more detail

$$\begin{aligned} \ln S_t &= f(t) + Y_t \\ f(t) &= \alpha + \vartheta D_t + \gamma \cos\left((t+\varphi)\cdot\frac{2\pi}{365}\right) \end{aligned}$$

where α, ϑ, γ, and φ are constant parameters, $D_t = 1$ if date t is holiday or weekend, $D_t = 0$ otherwise, and Y_t is a zero level mean-reverting stochastic process given as

$$dY_t = -\kappa Y_t dt + \sigma dW$$

where κ and σ are positive and constant parameters. Under the risk-neutral measure, that is, defining a constant market price of risk $\Lambda(t) = \lambda$, the risk-neutral process is given as

$$dY_t = \kappa(\alpha^* - Y_t)dt + \sigma d\widetilde{W}$$

where $\alpha^* = -\lambda\sigma/\kappa$ is a constant parameter.

In addition, defining $X_t = \ln(S_t)$ and applying some basic algebra we find that the solution for X_s under the risk-neutral measure is given as

$$X_s = f(s) + Y_t e^{-\kappa(s-t)} + \left(1 - e^{-\kappa(s-t)}\right)\alpha^* + \sigma\int_t^s e^{-\kappa(s-u)}d\widetilde{W}$$

Again, since the spot price of the commodity at time T is log-normally distributed, the forward price of the commodity is given as

$$\begin{aligned} F(S_t,t,T) &= \widetilde{E}\left[S_T|F_t\right] = \exp\left\{\widetilde{E}\left[X_T|F_t\right] + \frac{1}{2}\widetilde{V}\left[X_T|F_t\right]\right\} \qquad (3.2) \\ &= \exp\left\{f(T) + e^{-\kappa(T-t)}(\ln(S_t) - f(t)) + \left(1 - e^{-\kappa(T-t)}\right)\alpha^* + \frac{\sigma^2}{4\kappa}\left(1 - e^{-2\kappa(T-t)}\right)\right\} \end{aligned}$$

with $\alpha^* = -\lambda\sigma/\kappa$

3.3 A New Model for the Commodity Price

This section introduces the new valuation model of commodity prices and develops the corresponding expression for pricing futures contracts.

3.3.1 The New Model

Let S_t denote the commodity spot price available at time t. Then, the evolution of the commodity spot price, S_t, is given by the stochastic differential equation

$$dS_t = \kappa\left(f(t) - \ln(S_t)\right)S_t dt + \sigma S_t dW_t \qquad (3.3)$$

where $\kappa,\ \sigma \in \mathbb{R}^+$ and W_t is a standard Wiener process. The main assumption made in this model is that the mean reversion level, $f(t)$, follows a time-dependent periodic function characterized by a Fourier series, in more detail

$$f(t) = \sum_{n=0}^{\infty} Re\left[A_n e^{inwt}\right]$$

where it is only considered the real part of the series since it is the part that makes economic sense. Note that, $\forall n \mid A_n \in \mathbb{C}$, so that there is a phase factor contained in A_n. In more detail, consider $A_n = A_{x,n} + iA_{y,n}$ where $A_{x,n}, A_{y,n} \in \mathbb{R}$. Hence, $A_{x,n}$ and $A_{y,n}$ denote the amplitude and phase of each term in the Fourier expansion, respectively. Note that this model nests model 1 presented in Schwartz (1997) by taking $A_n = 0,\ \forall n \in \mathbb{N} - \{0\}$.

Moreover, defining $X_t = \ln(S_t)$, assuming a constant market price of risk, that is $\Lambda(S_t, t) = \lambda$, and applying Ito's Lemma, the log price can be represented by the following risk-neutral process

$$dX_t = \mu_t dt + \sigma d\widetilde{W}_t \tag{3.4}$$

where

$$\mu_t = \kappa\left(\widetilde{\alpha} + g(t) - X_t\right) \tag{3.5}$$

$$\widetilde{\alpha} = A_0 - \frac{\sigma^2}{2\kappa} - \frac{\lambda\sigma}{\kappa} \tag{3.6}$$

$$g(t) = \sum_{n=1}^{\infty} Re\left[A_n e^{inwt}\right] \tag{3.7}$$

where $A_0 \in \mathbb{R}$ and $\widetilde{W}_t = W_t + \lambda t$ is a standard Wiener process under the risk-neutral measure $\widetilde{P}$.

The following Proposition establishes the solution of the stochastic differential equation (3.4).

Proposition 23 *The solution of the risk-neutral process followed by the logarithm of the commodity spot price is given as*

$$X_s = e^{-\kappa(s-t)}X_t + \left(1 - e^{-\kappa(s-t)}\right)\widetilde{\alpha} + \sum_{n=1}^{\infty} Re\left[\frac{\kappa A_n}{\kappa + inw}\left(e^{inws} - e^{-\kappa(s-t)+inwt}\right)\right] + \sigma\int_t^s e^{-\kappa(s-u)}d\widetilde{W}_u$$

■

Figure 3.1 presents the evolution of the spot price time series for four different set of parameters. In the first graph we only consider the drift process, that is $\sigma = 0$. We can see how flexible this model is, in fact, any scenario can be replicated increasing the number of terms in the Fourier expansion. The second graph considers the drift and diffusion process, this representation presents a simulated spot price walk considering each underlying scenario. For illustrative purposes, Figures 3.2 and 3.3 show how the spot price responds to different values of $\widetilde{\alpha},\ \kappa,\ A_{n,x},\ A_{n,y},$ and ω with $n = 1,\ \sigma = 0$.

From Proposition 23, it is clear that the conditional distribution of the logarithm of the commodity spot price at time T follows a normal distribution where the mean and variance under the risk-neutral probability measure $\widetilde{P}$ are given as

$$\begin{aligned}
\widetilde{E}\left[X_T|F_t\right] &= e^{-\kappa(s-t)}X_t + \left(1-e^{-\kappa(s-t)}\right)\widetilde{\alpha} + \sum_{n=1}^{\infty} Re\left[\frac{\kappa A_n}{\kappa+inw}\left(e^{inws} - e^{-\kappa(s-t)+inwt}\right)\right] \quad (3.8)\\
\widetilde{V}\left[X_T|F_t\right] &= \widetilde{V}\left[\sigma\int_t^T e^{-\kappa(T-u)}d\widetilde{W}_u\right] = \left(\sigma\int_t^T e^{-\kappa(T-u)}d\widetilde{W}_u\right)^2 = \sigma^2\int_t^T e^{-2\kappa(T-u)}du\\
&= \frac{\sigma^2}{2\kappa}\left(1-e^{-2\kappa(T-t)}\right) \quad (3.9)
\end{aligned}$$

where we have applied the isometry property for stochastic integrals in the variance.

Since $X_t = \ln(S_t)$, the forward price of a commodity maturing at time T is a straightforward application of the properties of the log-normal distribution under the risk-neutral measure. Hence, the following proposition arises

Proposition 24 *Assuming a constant interest rate, the forward price of a commodity maturing at time T is given by*

$$\begin{aligned}
F(S_t,t,T) &= \widetilde{E}\left[S_T|F_t\right] = \exp\left\{\widetilde{E}\left[X_T|F_t\right] + \frac{1}{2}\widetilde{V}\left[X_T|F_t\right]\right\}\\
&= \exp\left\{e^{-\kappa(T-t)}\ln(S_t) + \left(1-e^{-\kappa(T-t)}\right)\widetilde{\alpha} + \frac{\sigma^2}{4\kappa}\left(1-e^{-2\kappa(T-t)}\right)\right.\\
&\quad \left. + \sum_{n=1}^{\infty} Re\left[\frac{\kappa A_n}{\kappa+inw}\left(e^{inws} - e^{-\kappa(s-t)+inwt}\right)\right]\right\}
\end{aligned}$$

Alternatively,

$$\begin{aligned}
\ln(F(S_t,t,T)) &= e^{-\kappa(T-t)}\ln(S_t) + \left(1-e^{-\kappa(T-t)}\right)\widetilde{\alpha} + \frac{\sigma^2}{4\kappa}\left(1-e^{-2\kappa(T-t)}\right)\\
&\quad + \sum_{n=1}^{\infty} Re\left[\frac{\kappa A_n}{\kappa+inw}\left(e^{inws} - e^{-\kappa(s-t)+inwt}\right)\right] \quad (3.10)
\end{aligned}$$

■

3.4 Option Pricing

This section focuses on option pricing. In more detail, we compute closed-form expressions for the prices of European options written on the commodity and the forward commodity price under the new model framework.

- **European option on the commodity**

  Consider a call option maturing at time T with strike K, written on a commodity. Let $c_t(S_t;t;T;K)$ denote the price at time t of this call option. Then, the terminal condition to this call option is given by

$$c_T(S_T;T;T;K) = \max\{F(S_T;T;T) - K;0\}$$

  Hence, under the risk-neutral measure $\widetilde{P}$, the price at time t of this option will be given by

$$c_t(S_t;t;T;K) = \widetilde{E}\left[e^{-r(T-t)}(F(S_t;t;T) - K)^+|F_t\right]$$

  The call option price is given by the following Proposition.

  Proposition 25 *The price at time t of a European call option with maturity T written on a commodity is given by*

$$\begin{aligned} c_t(S_t,t,T,K) &= \widetilde{E}\left[e^{-r(T-t)}(S_T - K)^+|F_t\right] \\ &= e^{-r(T-t)}\int_{-\infty}^{\infty}(S_T - K)^+\rho(\mu,\Sigma)dX_T \\ &= e^{-r(T-t)}\left[e^{\mu+\frac{1}{2}\Sigma^2}\Phi(d_1) - K\Phi(d_2)\right] \end{aligned}$$

  where $\rho(\mu,\Sigma)$ defines the normal density function and

$$\begin{aligned} \mu &= \widetilde{E}[X_T|F_t] \\ \Sigma &= \widetilde{V}[X_T|F_t] \\ d_1 &= \frac{\mu + \Sigma^2 - \ln(K)}{\Sigma} \\ d_2 &= d_1 - \Sigma \end{aligned}$$

  with $\widetilde{E}[X_T|F_t]$ and $\widetilde{V}[X_T|F_t]$ given by equation (3.8) and (3.9), respectively.

- **European option on the commodity forward**

  Consider a European forward call option that matures at time T with strike K. If this option is exercised, the call-holder pays K and receives a forward maturing at time s on a commodity. Let $c_t(S_t;t;T;s;K)$ denote the price at time t of this option. The terminal condition of this option is given as

$$c_T(S_T;T;s;K) = max\{F(S_T;T;s) - K,0\}$$

Under the risk-neutral measure $\widetilde{P}$, the price at time t of this option is given as

$$c_t(S_t;t;T;s;K) = \widetilde{E}\left[e^{-r(T-t)}(F(S_T;T;s)-K)^+|F_t\right]$$

Hence, the following proposition arises.

Proposition 26 *The price at time t of a European forward call option with maturity T on a forward contract expiring at time s written on a commodity is given by*

$$\begin{aligned} c(S_t,t,T,s,K) &= \widetilde{E}\left[e^{-r(T-t)}(F(S_T,T,s)-K)^+|F_t\right] \\ &= e^{-r(T-t)}\int_{-\infty}^{\infty}(F(S_T,T,s)-K)^+\rho(\mu,\Sigma)dX_T \\ &= e^{-r(T-t)}\left[\exp\left\{\Omega+\mu e^{-\kappa(s-T)}+\frac{1}{2}\Sigma^2e^{-2\kappa(s-T)}\right\}\Phi(d_1)-K\Phi(d_2)\right] \end{aligned}$$

where $\rho(\mu,\Sigma)$ denotes the normal density function and

$$\begin{aligned} \mu &= \widetilde{E}\left[X_T|F_t\right] \\ \Sigma^2 &= \widetilde{V}\left[X_T|F_t\right] \\ \Omega &= \left(1-e^{-\kappa(s-T)}\right)\widetilde{\alpha}+\left(1-e^{-2\kappa(s-T)}\right)\frac{\sigma^2}{4\kappa}+\sum_{n=1}^{\infty}Re\left[\frac{\kappa A_n}{\kappa+inw}\left(e^{inws}-e^{-\kappa(s-T)+inwT}\right)\right] \\ \nu &= \left(\ln(K)-\Omega\right)e^{\kappa(s-T)} \\ d_1 &= \frac{\mu+\Sigma^2e^{-\kappa(s-T)}-\nu}{\Sigma} \\ d_2 &= \frac{\mu-\nu}{\Sigma} \end{aligned}$$

with $\widetilde{E}[X_T|F_t]$ and $\widetilde{V}[X_T|F_t]$ given by equation (3.8) and (3.9), respectively.

3.5 Empirical Analysis

3.5.1 Data

The data set used for the empirical study consist of daily observations of futures contracts written on natural gas. In more detail, we take Henry Hub as the pricing point for natural gas futures contracts, which is traded on the New York Mercantile Exchange (NYMEX). We have complete data for the spot prices and the twelve contracts closest to maturity from 02/02/1998 to 07/03/2011. In this analysis we are going to take into consideration the Ng5, Ng8 and Ng12, where Ng5 is the fifth contract closest to maturity, and so on.

Since the models for the forward price have the form given as in the previous Sections, we estimate the structural parameters by minimizing the fitting error of each model as:

$$Y_t = \sum_{i=1}^{6} \beta_i z_{it} + u_t$$

where u_t can be interpreted either as a measurement or as an approximation error in the pricing formula. For every model we follow a non-weighted least-squares approach to obtain the parameter estimates.

Model 1

We hope to identify the values of the structural parameters: $\theta = (\widetilde{\alpha}, \kappa, \sigma)$.

$$\begin{aligned} Y_t &= \ln(F(S_t,t,T)) - e^{-\kappa(T-t)} \ln(S_t) \\ z_{1t} &= 1 - e^{-\kappa(T-t)} \\ z_{2t} &= \left(1 - e^{-2\kappa(T-t)}\right)/4\kappa \\ \beta_1 &= \widetilde{\alpha};\ \beta_2 = \sigma^2;\ \beta_3 = \beta_4 = \beta_5 = \beta_6 = 0 \end{aligned}$$

Model 2

Neglecting ϑ, considering trading days and with some basic algebra we reorganized model 2. In this case, we hope to identify the values of the structural parameters: $\theta = (\widetilde{\alpha}, \kappa, \sigma, \gamma, \varphi)$.

$$\begin{aligned} Y_t &= \ln(F(S_t,t,T)) - e^{-\kappa(T-t)} \ln(S_t) \\ z_{1t} &= 1 - e^{-\kappa(T-t)} \\ z_{2t} &= \left(1 - e^{-2\kappa(T-t)}\right)/4\kappa \\ \beta_1 &= \widetilde{\alpha} = \alpha + \alpha^*;\ \beta_2 = \sigma^2;\ \beta_3 = \gamma;\ \beta_4 = 0 \\ f_1(t,T) &= \cos\left((T+\varphi)\cdot 2\pi\right) - e^{-\kappa(T-t)} \cos\left((t+\varphi)\cdot 2\pi\right) \end{aligned}$$

Model 3

This model assumes only one term in the Fourier expansion, hence we hope to identify the values of the structural parameters $\theta = \left(\widetilde{\alpha}, \kappa, \sigma, A_{(x,n_1)}, A_{(y,n_1)}, \omega\right)$.

$$\begin{aligned} Y_t &= \ln(F(S_t,t,T)) - e^{-\kappa(T-t)} \ln(S_t) \\ z_{1t} &= 1 - e^{-\kappa(T-t)} \\ z_{2t} &= \left(1 - e^{-2\kappa(T-t)}\right)/4\kappa \\ \beta_1 &= \widetilde{\alpha};\ \beta_2 = \sigma^2 \end{aligned}$$

and $Re\left[(A_{(x,n_1)} + iA_{(y,n_1)})\dfrac{\kappa}{\kappa + inw}\left(e^{inws} - e^{-\kappa(s-t)+inwt}\right)\right]$ derives in $\beta_3 z_{3t} + \beta_4 z_{4t}$.

Model 4

In this case we assume two terms in the Fourier expansion, which leads us to identify the values of the structural parameters $\theta = \left(\widetilde{\alpha}, \kappa, \sigma, A_{(x,n_1)}, A_{(y,n_1)}, A_{(x,n_2)}, A_{(y,n_2)}, \omega\right)$.

$$\begin{aligned} Y_t &= \ln(F(S_t,t,T)) - e^{-\kappa(T-t)}\ln(S_t) \\ z_{1t} &= 1 - e^{-\kappa(T-t)} \\ z_{2t} &= \left(1 - e^{-2\kappa(T-t)}\right)/4\kappa \\ \beta_1 &= \widetilde{\alpha};\ \beta_2 = \sigma^2 \end{aligned}$$

where $\sum_{n=n_1,n_2} Re\left[(A_{(x,n)} + iA_{(y,n)})\frac{\kappa}{\kappa + inw}\left(e^{inws} - e^{-\kappa(s-t)+inwt}\right)\right]$ derives in $\sum_{i=3}^{6}\beta_i z_{it}$.

3.5.2 In-Sample Analysis

The key assumption in this chapter is that there is a seasonal pattern in futures prices, besides being non-stationary. Table 3.1 presents the Augmented Dickey-Fuller (ADF) test for the time series for the log-spot price as well as for the log-price of each of the futures contracts considered, and the first differences of each of these series. Clearly, the existence hypothesis that a unit root exists cannot be rejected in any case, meaning that both, the spot and futures price series are non-stationary. On the other hand, the presence of a unit root is rejected when considering the first difference of each price. Figures 3.4 to 3.7 present the autocorrelation and partial autocorrelation function for each time series.

Table 3.2 shows the estimation results for the long-run relationship between the futures and the spot price:

$$\ln F_t(\tau) = \alpha + \beta \ln S_t + a_t$$

where τ corresponds to each futures tenor, Ng 5, 8, and 12, respectively. Table 3.3 presents the Augmented Dickey-Fuller test for each residual time series and its first difference. In every case we reject the existence of a unit root. Figures 3.8 to 3.10 present the residual and its first difference time series corresponding to the estimation of Ng 5, 8, and 12. Figures 3.11 to 3.13 present the autocorrelation and partial autocorrelation function for each residual time series and its first difference time series. Hence, the logarithm of each futures price is cointegrated with the logarithm of the spot price, as it is usually the case in most liquid futures markets.

The expected seasonal pattern suggests that it is reasonable to study the spectral density of futures prices, bearing in mind that for any such time series the spectral density should be expected to have a maximum at the zero frequency, due to the presence of a unit root. Figures 3.14 to 3.16 present the logarithm of the price of gas natural for Ng 5, Ng 8 and Ng 12 futures contracts, and the

associate spectral density, where $f(Hz) = \frac{\omega}{2\pi}$. These figures confirm that intuition, the maximum spectral density corresponding to the zero frequency. However, an additional interesting result arises in these spectra: for the three time series of futures prices the maximum spectral density, other than the global maximum at the zero frequency, is found for a rather low frequency, which should be interpreted as the fundamental frequency. The fundamental frequency is indicating that there is an underlying long-run period driving the behaviour of futures prices, of about 15 to 16 years.

This result is quite interesting for our purposes. However, since the three models we consider are driven by the commodity spot price, we are specifically interested in the spectral component which is not explained by the spot price. The reason is that we are interested in the seasonal period that is specific to futures prices and hence, on the seasonal component that it is not inherited through the dependence of futures prices from the spot price. This is a not trivial endeavour because, according to our model, the relationship between spot and futures prices is not very straightforward. In fact, it depends on the reversion parameter κ, which should be estimated for each model. In addition, we should remember that our proposed model has been developed under the assumption that the mean reversion level follows over time an evolution characterized by a Fourier series. Alternatively, the model posited by Lucia and Schwartz (2002) assumes a zero level mean-reverting process and arbitrarily adds a trigonometric function with an annual frequency. Therefore, relaxing the annual frequency assumption will not collapse Lucia and Schwartz model into our model.

The estimated spectra are precisely very important to conduct the specification of our model for estimation purposes. We need to truncate the infinite Fourier series, and it is important to have some idea about how many terms may be needed to fit the futures price data, and which frequencies should be incorporated into the chosen terms of the Fourier expansion. At this point, we already know that to appropriately capture the dynamics in natural gas futures prices it is necessary to include in the model the detected fundamental frequency.

To detect the frequencies that are relevant to explain the dynamics in futures prices, we create a grid of frequencies and fit our model to the observed time series for each value of ω in the grid. These estimations will provide us with a measure of the fitting errors for each frequency, thereby exposing the cyclical component not captured by the spot price. Figure 3.17 shows the residual sum of squares of estimating our model for a fixed value of ω in $(0, 2\pi)$. The results are quite conclusive: there is a well defined minimum fitting error at a point very close to the fundamental frequency obtained in estimated spectrum, indicating an underlying long run period of 15 to 16 years. This analysis reveals another interesting feature: the second relevant term in the Fourier series for the Ng 5 and Ng 8 is the annual frequency, which of course is a multiple of the fundamental frequency $(n \cdot \omega = 2\pi n \cdot f(Hz))$. However, the importance of the annual frequency decreases with maturity, completely disappearing beyond the futures expiring in one year, Ng 12. This may be reasonable:

since the Ng 12 expiration date is exactly one wavelength of the annual frequency, then it makes sense that the annual frequency has a negligible effect on the Ng 12 time series. Since the analysis considers the relation between the spot and futures prices, it is fair to say that this frequency is indicating a cyclical behaviour in the futures price which is not captured by the spot price.

To obtain the spectrum of the component of futures prices which is not explained by spot prices, we use the estimated parameters associated with this fundamental frequency to compute the function $\hat{s}(F_t, S_t)$, given as

$$\hat{s}(F_t, S_t) = \ln(F(S_t, t, T)) - e^{-\hat{\kappa}(T-t)} \ln(S_t) - \hat{\tilde{\alpha}} \left(1 - e^{-\hat{\kappa}(T-t)}\right) - \frac{\hat{\sigma}^2}{4\hat{\kappa}} \left(1 - e^{-2\hat{\kappa}(T-t)}\right)$$

The spectrum of this function will expose the underlying component that is not fully explained by the spot price or by any trend. Figures 3.18 to 3.20 present the spectrum of the $\hat{s}$-function for each futures price, suggesting that at most three terms in the Fourier expansion should be enough to attain a good fit of the $\hat{s}$-function. As expected, the frequencies identified in each spectrum match exactly the frequencies detected in the graphs of the residual sum of squares for fixed values of ω, confirming that we certainly have spotted the frequencies we need to obtain accurate estimates.

Tables 3.4 to 3.6 present the estimated parameters and the corresponding standard deviation for each chosen futures price and for the whole sample, as well as goodness of fit measures for each model. For the whole period we present the minimized value of the function $\sum_{i,t} \min \mathrm{SR}(\hat{\theta}_{i,t})$ and $\sum_{i,t} |\hat{u}_{i,t}|$, the sum of the absolute value of pricing errors for the whole period, to represent how well each model fits the observed futures prices. In addition, Figures 3.21 to 3.23 present the Ng 5, 8 and 12 adjustment error time series for Model 2, 3, and 4. To keep the graphs as clear as possible we have intentionally excluded Model 1. On February 25, 2003 every model shows a particularly poor fit. That day, United States, Britain and Spain presented to the UN Security Council a resolution stating that Iraq "has failed to take the final opportunity" to disarm. Rumors of an imminent war plunged stock markets all over the world, while many commodities prices raised till historical maximums. Henry Hub spot price has closed at 19.38$, when average spot price oscillated at 5$.

Regarding the goodness of fit the results are conclusive. Compared with the benchmark models, both representations of our model dramatically improve the in-sample fit of every observed futures time series. Model 3, the model with just one term in the Fourier expansion, reduces the aggregate sum of squares of Model 2 by 28%, 54% and 79%, for Ng 5, 8 and 12, respectively. Comparing Model 3 with Model 1, the improvement is of 48%, 61% and 79% for Ng 5, 8 and 12, respectively. It is encouraging to know that we do not need to go farther away in the Fourier expansion to achieve a good fitting, even though increasing the number of terms in the Fourier expansion would eventually allow for fitting arbitrarily well the observed time series. On this regard, it is interesting to point out that the annual frequency proposed by the Schwartz and Lucia model has little impact by itself.

In fact, for the futures contract expiring in one year, Model 2 provides no further improvement from the model with no seasonal component. In fact, there is an annual frequency in the process driving the futures price, but that annual fluctuation is mostly explained by the spot price. On the other hand, the long run frequency, between 15 and 16 years, explains the seasonality in futures prices that is not captured by the spot price. This frequency might well be related to the business cycle.

Although the main improvement comes with the incorporation of the fundamental frequency, adding a second term in the model still provides further improvements. Comparing Model 4 against Model 3, i.e., the models with two and one term in the Fourier expansion, the relative improvement is given as 45%, 40% and 27% for Ng 5, 8 and 12, respectively. For contracts Ng 5 and Ng 8, the second term incorporates the annual frequency, while the second term for the Ng 12 futures contract suggests a period of 4 years.

Figures 3.24 to 3.26 show Models 3 and 4 fitting error spectra of each futures estimation. As it should be, the fundamental frequency has been completely removed from the spectrum. Model 3 fitting error of futures series Ng 5 and 8 is dominated by the annual frequency, and it is completely eliminated from the model 4 fitting error spectra. Model 4 fitting error spectra reveals no dominating frequency, although we can spot some frequencies standing from the noise which could be incorporated in further term of the Fourier expansion. On this respect, adding a third term in the Fourier expansion provides a relative improvement over the model with two term of 11.5%, 20.5% and 20% for the estimation of Ng 5, 8, and 12, respectively.

3.6 Conclusions

This chapter has introduced a continuous-time model for the logarithm of the commodity spot price, assuming that it reverts to a mean level that follows a cyclical behaviour over time that is characterized by a Fourier series. Under this assumption, our model nests the original one-factor model presented in Schwartz (1997), while allowing for a more flexible evolution of the commodity spot price and preserving the analytical tractability of the Schwartz model. Under this framework, we have obtained analytical expressions for the prices of futures, European option on the commodity and European options on commodity futures.

Considering Natural gas as the underlying asset of the futures contract, we have also analysed the empirical performance of two versions of our model against two different one-factor benchmarks, those proposed in Schwartz (1997) and Lucia and Schwartz (2002). In order to identify the fundamental frequency and the underlying period driving the futures contract price, we have conducted a spectral analysis of three futures with different tenors, in particular Ng 5, Ng 8 and Ng 12. The spectrum revealed that there is a short frequency driving the futures price behaviour of about 15

to 16 years. Although the annual frequency has some relevance in Ng 5 and Ng 8, it tends to decrease with maturity. Considering the effect of the fundamental frequency, even in its simplest representation based on a single term of the Fourier expansion, our model outperforms both benchmark models, providing a better and more reliable in-sample fitting of the commodity futures price. Adding a second term in the Fourier expansion provides an improvement relative to the one term representation, although the improvement tends to be lower for longer maturities. On this respect, it is worth poniting out that increasing the number of terms in the Fourier expansion would eventually allow for fitting the observed time series arbitrarily well. These results are very relevant, suggesting that our proposed Fourier model provides a simple and powerful tool for portfolio management, risk management and derivative pricing on commodities.

3.7 Appendix of Tables

Table 3.1: Augmented Dickey-Fuller test

		ADF(Level)		ADF(First Difference)
	Lags	t-stat (p-value)	Lags	t-stat (p-value)
Spot	26	-2.2492(0.189)	25	-13.0611(3.833e-29)
Ng 5	25	-2.0527(0.264)	24	-10.5281(6.566e-21)
Ng 8	23	-1.9750(0.298)	22	-9.7038(2.933e-18)
Ng 12	19	-1.6753(0.444)	25	-12.3007(1.096e-26)

Note: Augmented Dickey-Fuller test for the log spot and futures price, and the first differences of each of these series.

Table 3.2: Estimation results

	Ng 5	Ng 8	Ng 12
α	0.2311(0.0089)	0.2703(0.0101)	0.3046(0.0109)
β	0.9095(0.0056)	0.8945(0.0063)	0.8721(0.0068)
Log-likelihood function	1422.346	1024.496	775.8086
R^2	0.890935	0.860997	0.834877

Note: Estimation results for the long-run relationship between the futures and the spot price given by process 3.5.2. Standard errors in parentheses

Table 3.3: Augmented Dickey-Fuller test

		ADF(Level)		ADF(First Difference)
	Lags	t-stat (p-value)	Lags	t-stat (p-value)
a_t(Ng 5)	30	-4.6453(1.025e-4)	29	-11.2560(2.803e-23)
a_t(Ng 8)	30	-3.8854(2.156e-3)	26	-13.6307(5.906e-31)
a_t(Ng 12)	27	-3.1480(2.323e-2)	26	-14.3477(3.446e-33)

Note: Augmented Dickey-Fuller test for each residual time series and its first difference.

Table 3.4: Parameters estimates. In-Sample Estimation Ng 5

Parameter	Model 1	Model 2	Model 3	Model 4
$\hat{\beta}_1$	-14.7756(7.0527)	2.4228(0.0337)	0.4320(0.3487)	1.4190(0.2193)
$\hat{\beta}_2$	9.2165(10.2398)	0.1134(0.0271)	3.8248(1.0256)	0.8830(0.5870)
$\hat{\kappa}$	0.2539(0.1846)	0.2309(0.0079)	1.2085(0.0210)	1.1148(0.0129)
$\hat{\beta}_3$	-	0.0661(0.0085)	-	-
$\hat{\varphi}$	-	0.0607(0.0032)	-	-
$\hat{A}_{(x,n_1=1)}$	-	-	-0.2224(0.0279)	-0.1561(0.0107)
$\hat{A}_{(y,n_1=1)}$	-	-	0.4984(0.0228)	0.5529(0.0087)
$\hat{A}_{(x,n_2=15)}$	-	-	-	-0.3117(0.0109)
$\hat{A}_{(x,n_2=15)}$	-	-	-	-0.3839(0.0092)
$\hat{\omega_0}$	-	$2 \cdot \pi$	0.4152(0.0032)	0.4175(0.0003)
$\sum_{i,t} \min \mathrm{SR}(\hat{\theta}_{i,t})$	80.0594	57.9226	41.7740	22.9802
$\sum_{i,t} \lvert\hat{u}_{i,t}\rvert$	346.6403	309.4022	291.4021	205.9710

Note:$\sum_{i,t} \min \mathrm{SR}(\hat{\theta}_{i,t})$ represents the least squares pricing error, $\sum_{i,t} |\hat{u}_{i,t}|$ shows the pricing errors in absolute value.

Table 3.5: Parameters estimates. In-Sample Estimation Ng 8

Parameter	Model 1	Model 2	Model 3	Model 4
$\hat{\beta}_1$	-7.1126(6.5074)	2.5991(0.1140)	0.9698(0.4022)	1.6985(0.0039)
$\hat{\beta}_2$	3.6508(2.7470)	0.0000(0.0000)	1.7696(0.9716)	0.0000(0.0000)
$\hat{\kappa}$	0.1787(0.0219)	0.1721(0.0209)	0.9308(0.0152)	0.9223(0.0132)
$\hat{\beta}_3$	-	-0.0557(0.0284)	-	-
$\hat{\varphi}$	-	0.5826(0.0827)	-	-
$\hat{A}_{(x,n_1=1)}$	-	-	-0.0928(0.0313)	-0.1979(0.0116)
$\hat{A}_{(y,n_1=1)}$	-	-	0.6017(0.0250)	0.5228(0.0101)
$\hat{A}_{(x,n_2=16)}$	-	-	-	-0.4101(0.0124)
$\hat{A}_{(x,n_2=16)}$	-	-	-	-0.3657(0.0130)
$\hat{\omega_0}$	-	$2 \cdot \pi$	0.4020(0.0027)	0.3901(0.0003)
$\sum_{i,t} \min \mathrm{SR}(\hat{\theta}_{i,t})$	102.1405	86.6176	39.8256	23.9565
$\sum_{i,t} \lvert\hat{u}_{i,t}\rvert$	406.3963	390.8210	285.4515	205.1990

Note:$\sum_{i,t} \min \mathrm{SR}(\hat{\theta}_{i,t})$ represents the least squares pricing error, $\sum_{i,t} |\hat{u}_{i,t}|$ shows the pricing errors in absolute value.

Table 3.6: Parameters estimates. In-Sample Estimation Ng 12

Parameter	Model 1	Model 2	Model 3	Model 4
$\hat{\beta}_1$	2.3811(0.8887)	1.8400(0.0839)	1.3963(0.5728)	1.1713(0.2376)
$\hat{\beta}_2$	0.0000(0.0000)	0.1640(0.0179)	0.5359(1.2134)	1.1805(0.5932)
$\hat{\kappa}$	0.1431(0.4613)	0.1464(0.0051)	0.7846(0.0120)	0.8904(0.0085)
$\hat{\beta}_3$	-	0.0858(0.0101)	-	-
$\hat{\varphi}$	-	0.3240(0.0179)	-	-
$\hat{A}_{(x,n_1=1)}$	-	-	-0.1175(0.0299)	-0.1913(0.0224)
$\hat{A}_{(y,n_1=1)}$	-	-	0.5820(0.0253)	0.5116(0.0178)
$\hat{A}_{(x,n_2=3)}$	-	-	-	-0.4965(0.0206)
$\hat{A}_{(x,n_2=3)}$	-	-	-	-0.4196(0.0206)
$\hat{\omega_0}$	-	$2 \cdot \pi$	0.3758(0.0031)	0.3723(0.0021)
$\sum_{i,t} \min \mathrm{SR}(\hat{\theta}_{i,t})$	118.9080	117.6984	24.4762	17.7831
$\sum_{i,t} \lvert\hat{u}_{i,t}\rvert$	490.5892	480.9532	217.4176	188.5439

Note:$\sum_{i,t} \min \mathrm{SR}(\hat{\theta}_{i,t})$ represents the least squares pricing error, $\sum_{i,t} |\hat{u}_{i,t}|$ shows the pricing errors in absolute value.

3.8 Appendix of Figures

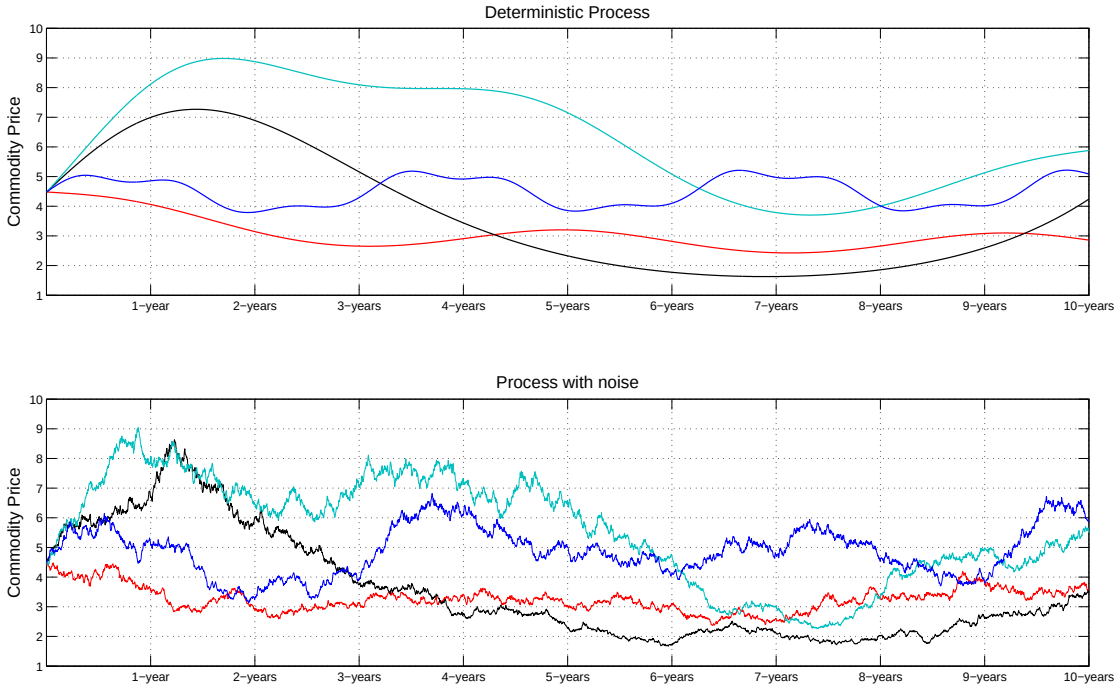

Figure 3.1: Spot price time series simulation for an arbitrary set of parameters. The first graph represents the drift process, that is setting $\sigma = 0$. The second graph represents the whole process with $\sigma = 0.2$

Red line: $\widetilde{\alpha} = 1,\ \kappa = 0.5,\ A_{n=1,x} = 0.4,\ A_{n=1,y} = 0,\ A_{n=3,x} = 0,\ A_{n=3,y} = 0,\ \omega = 1.5.$

Black line: $\widetilde{\alpha} = 2,\ \kappa = 0.5,\ A_{n=1,x} = 1,\ A_{n=1,y} = \frac{\pi}{2},\ A_{n=3,x} = 0,\ A_{n=3,y} = 0,\ \omega = 0.4.$

Lightblue line: $\widetilde{\alpha} = 2,\ \kappa = 0.5,\ A_{n=1,x} = 0.8,\ A_{n=1,y} = 0,\ A_{n=3,x} = 0.4,\ A_{n=3,y} = 0,\ \omega = 0.5.$

Blue line: $\widetilde{\alpha} = 1.5,\ \kappa = 0.5,\ A_{n=1,x} = 0.6,\ A_{n=1,y} = 0,\ A_{n=3,x} = 0.5,\ A_{n=3,y} = 0,\ \omega = 2$

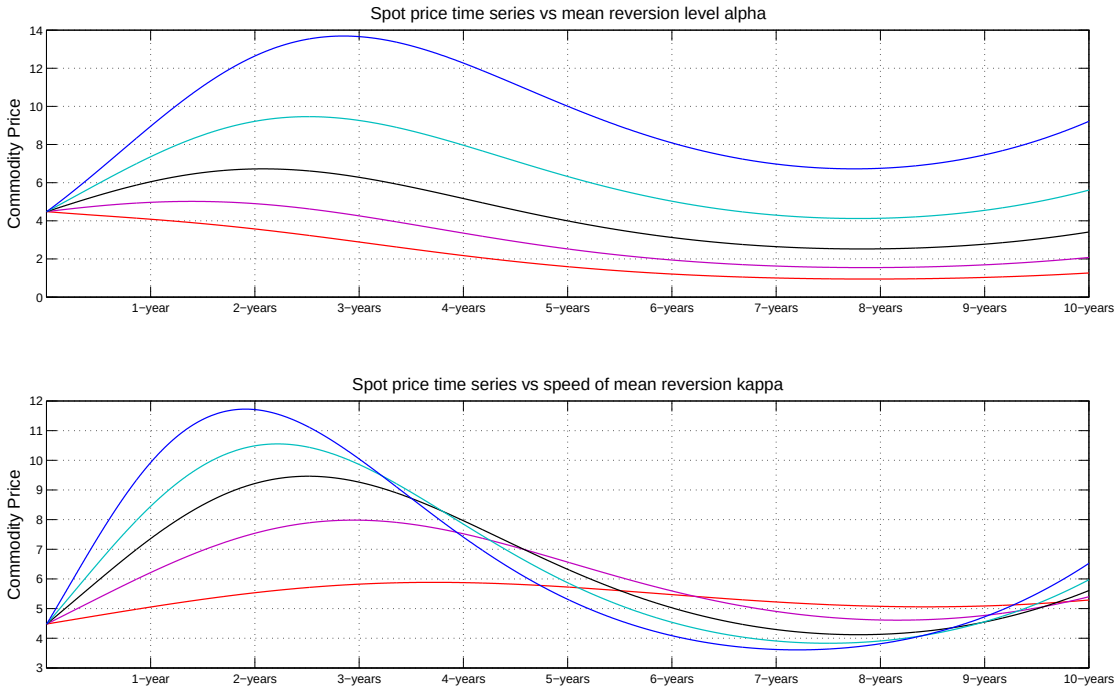

Figure 3.2: Spot price time series simulation for an arbitrary set of parameters and no diffusion process, $\sigma = 0$. For both graphs: $A_{n=1,x} = 0.8,\ A_{n=1,y} = 0,\ n = 1,\ \omega = 0.5$.

The first graph represents the spot price time series for $\kappa = 0.5$ and different values of $\widetilde{\alpha}$:

Red line: $\widetilde{\alpha} = 0.5$, *Violet line:* $\widetilde{\alpha} = 1$, *Black line:* $\widetilde{\alpha} = 1.5$, *Lightblue line:* $\widetilde{\alpha} = 2$, *Blue line:* $\widetilde{\alpha} = 2.5$.

The second graph represents the spot price time series for $\widetilde{\alpha} = 2$ and different values of κ:

Red line: $\kappa = 0.1$, *Violet line:* $\kappa = 0.3$, *Black line:* $\kappa = 0.5$, *Lightblue line:* $\kappa = 0.7$, *Blue line:* $\kappa = 1$.

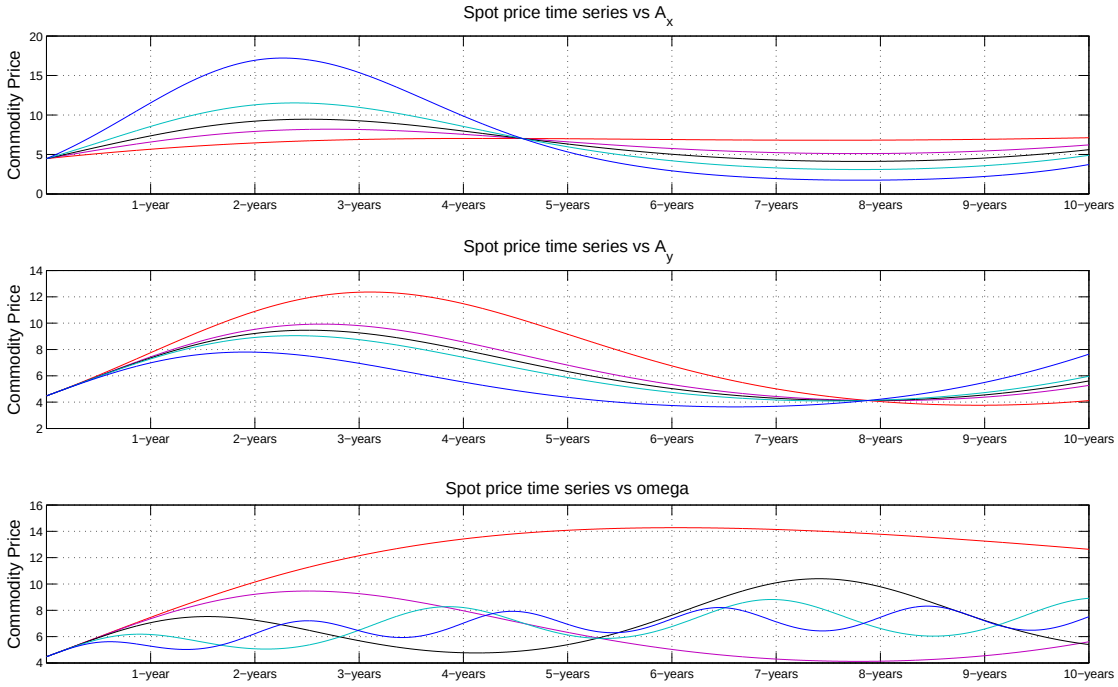

Figure 3.3: Spot price time series simulation for an arbitrary set of parameters and no diffusion process, $\sigma = 0$. For the three graphs: $\widetilde{\alpha} = 2,\ \kappa = 0.5,\ n = 1,\ \sigma = 0$.

The first graph represents the spot price time series for $A_{n=1,y} = 0,\ \omega = 0.5$ and different values of $A_{n=1,x}$: *Red line:* $A_{n=1,x} = 0.1$, *Violet line:* $A_{n=1,x} = 0.5$, *Black line:* $A_{n=1,x} = 0.8$, *Lightblue line:* $A_{n=1,x} = 1.2$, *Blue line:* $A_{n=1,x} = 2$.

The second graph represents the spot price time series for $A_{n=1,x} = 0.8,\ \omega = 0.5$ and different values of $A_{n=1,y}$:

Red line: $A_{n=1,y} = -0.5$, *Violet line:* $A_{n=1,y} = -0.1$, *Black line:* $A_{n=1,y} = 0$, *Lightblue line:* $A_{n=1,y} = 0.1$, *Blue line:* $A_{n=1,y} = 0.5$.

The third graph represents the spot price time series for $A_{n=1,x} = 0.8,\ A_{n=1,y} = 0$ and different values of ω: *Red line:* $\omega = 0.1$, *Violet line:* $\omega = 0.5$, *Black line:* $\omega = 1$, *Lightblue line:* $\omega = 2$, *Blue line:* $\omega = \pi$.

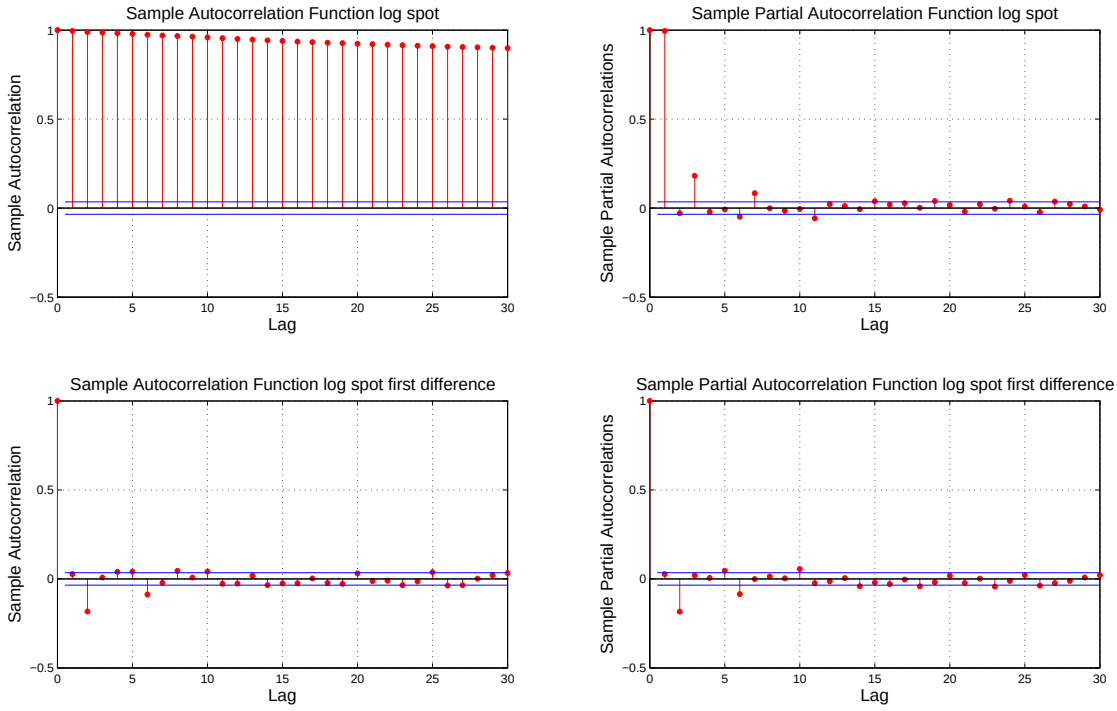

Figure 3.4: Autocorrelation and Partial autocorrelation function for the logarithm of the spot price series and its first difference series

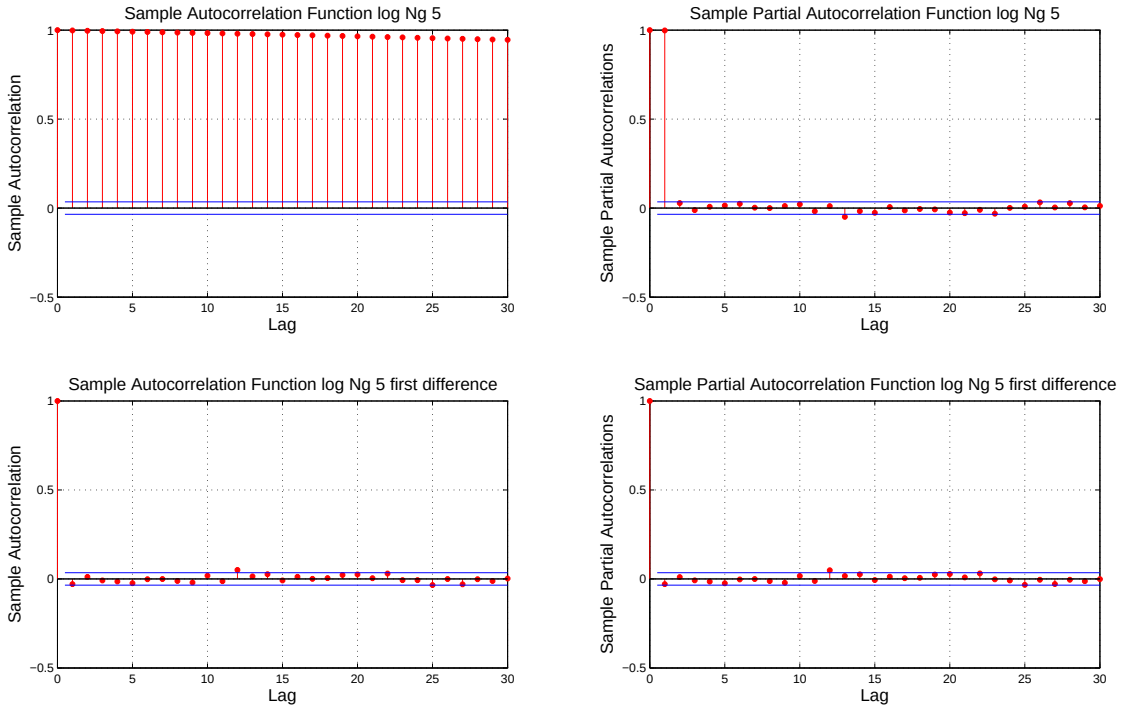

Figure 3.5: Autocorrelation and Partial autocorrelation function for the logarithm of the Ng 5 futures price series and its first difference series

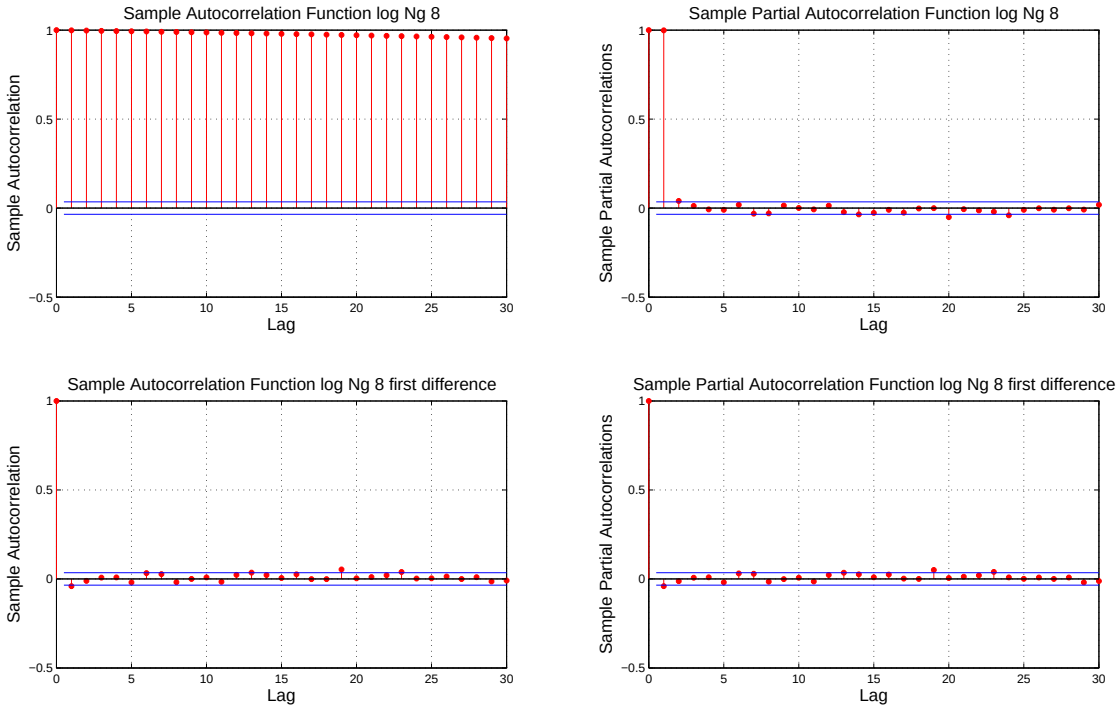

Figure 3.6: Autocorrelation and Partial autocorrelation function for the logarithm of the Ng 8 futures price series and its first difference series

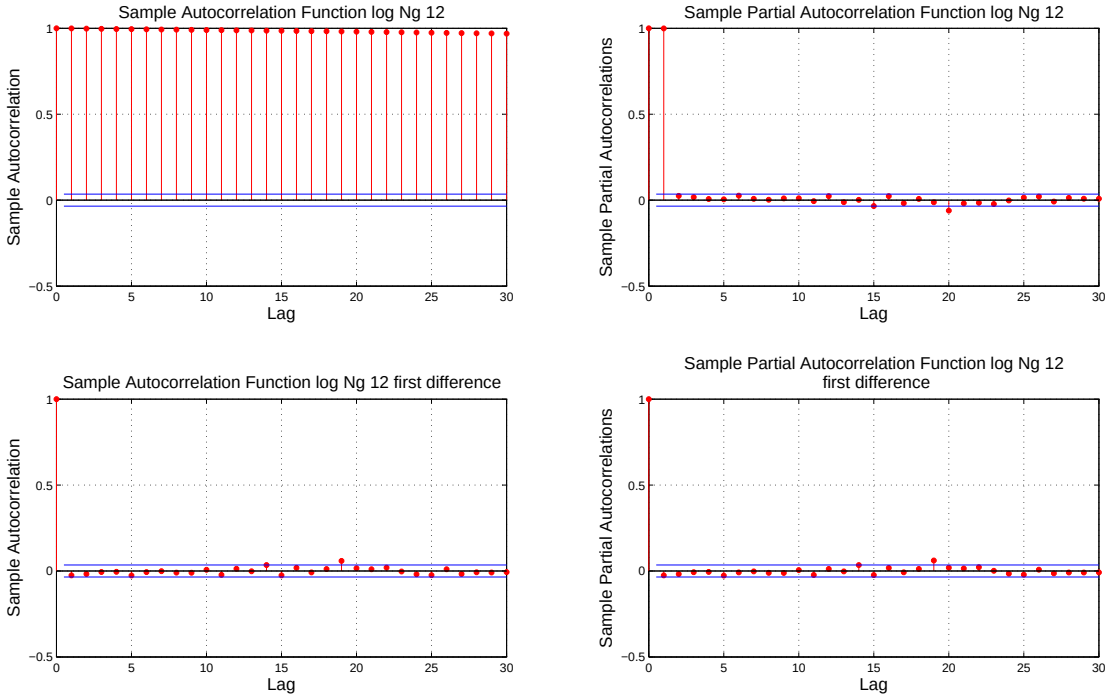

Figure 3.7: Autocorrelation and Partial autocorrelation function for the logarithm of the Ng 12 futures price series and its first difference series

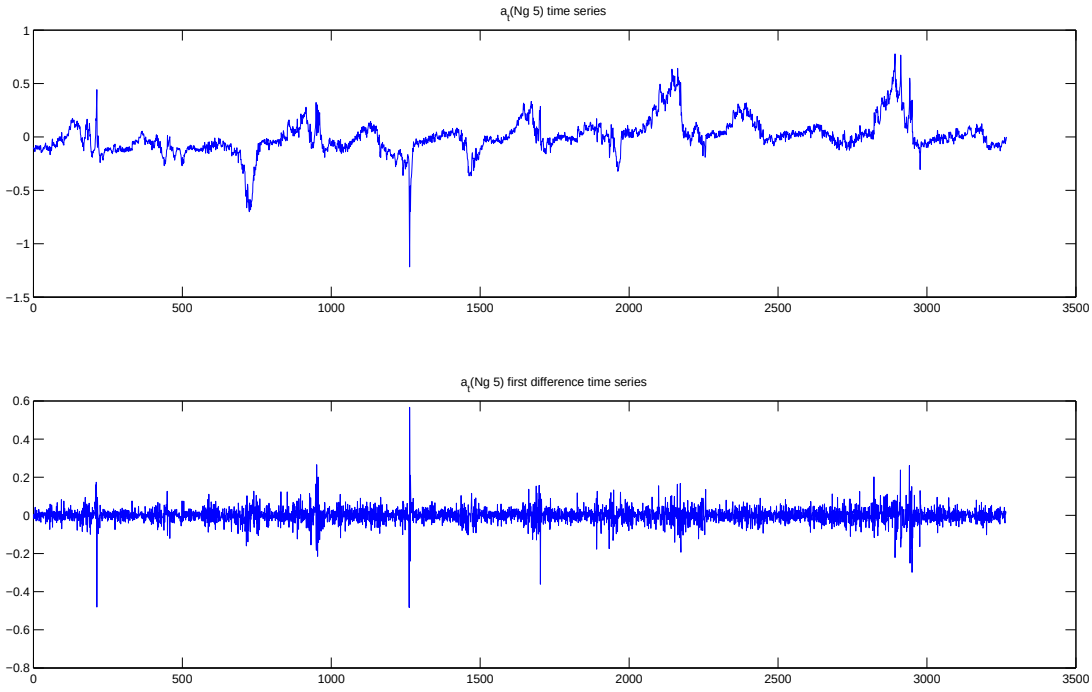

Figure 3.8: a_t(Ng 5) time series and its first difference series

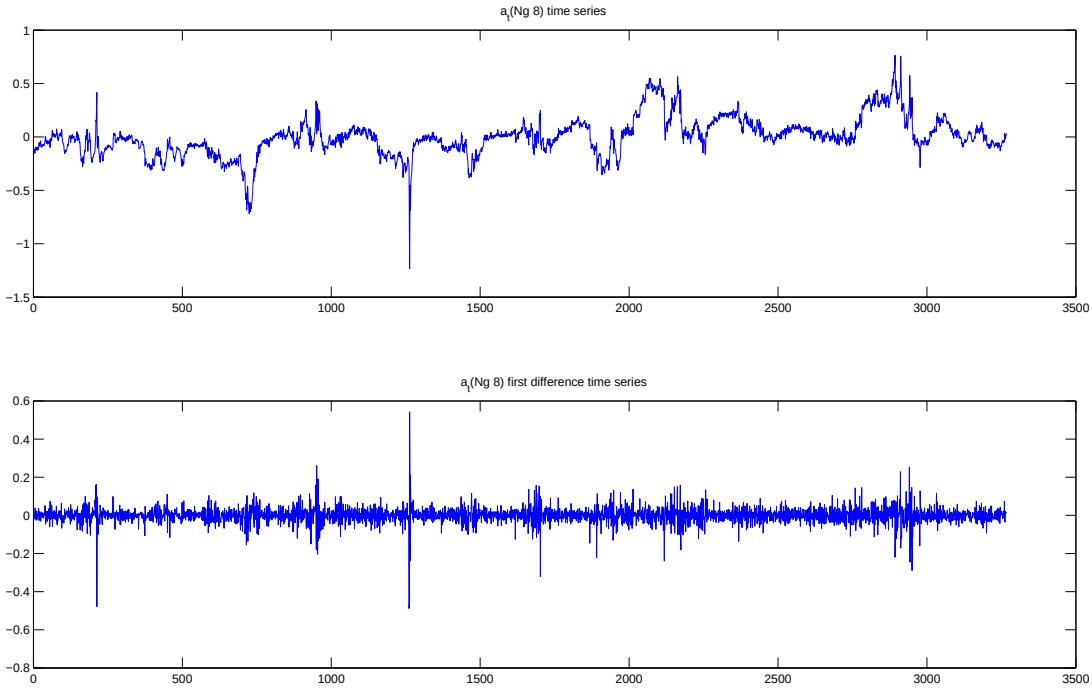

Figure 3.9: a_t(Ng 8) time series and its first difference series

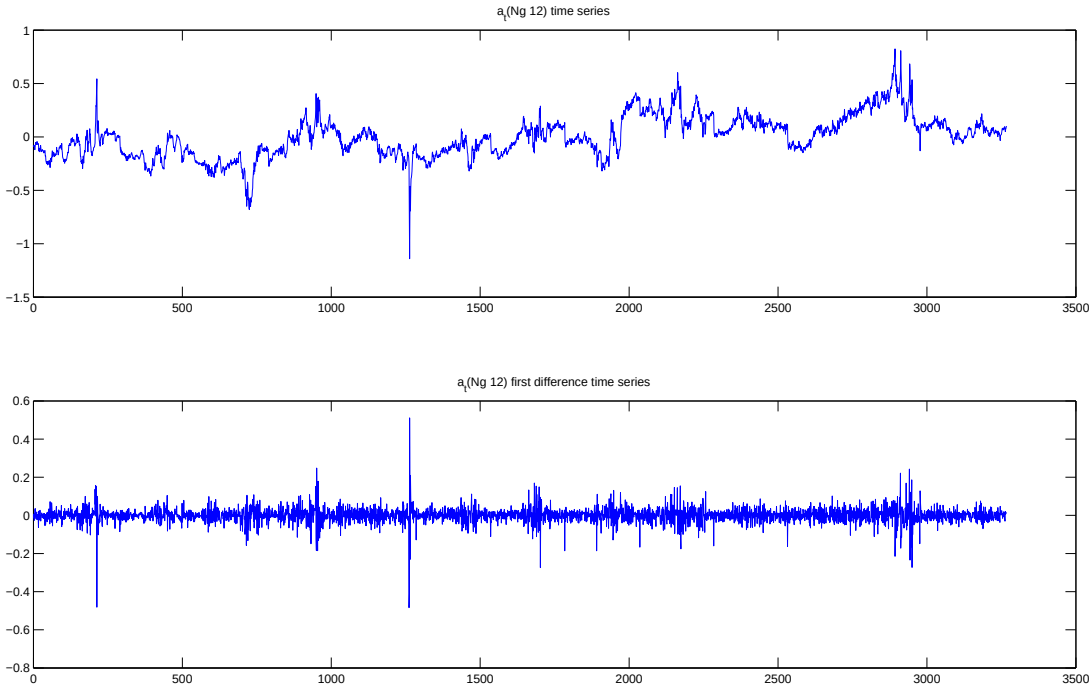

Figure 3.10: a_t(Ng 12) time series and its first difference series

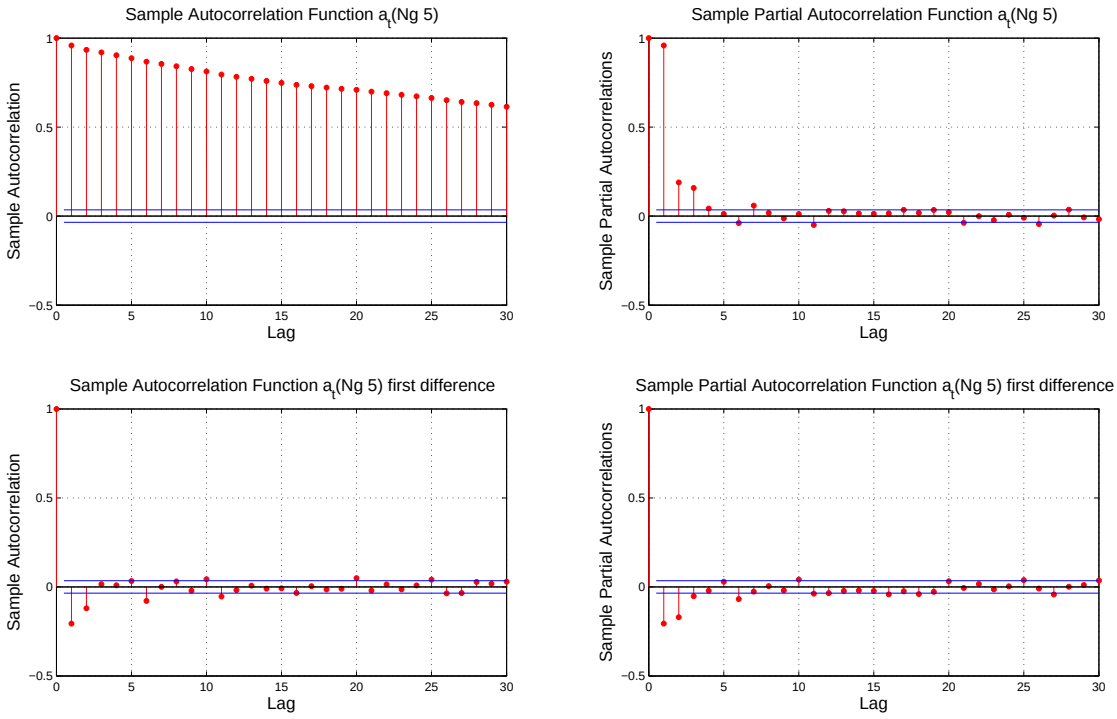

Figure 3.11: Autocorrelation and Partial autocorrelation function for the a_t(Ng 5) time series and its first difference series

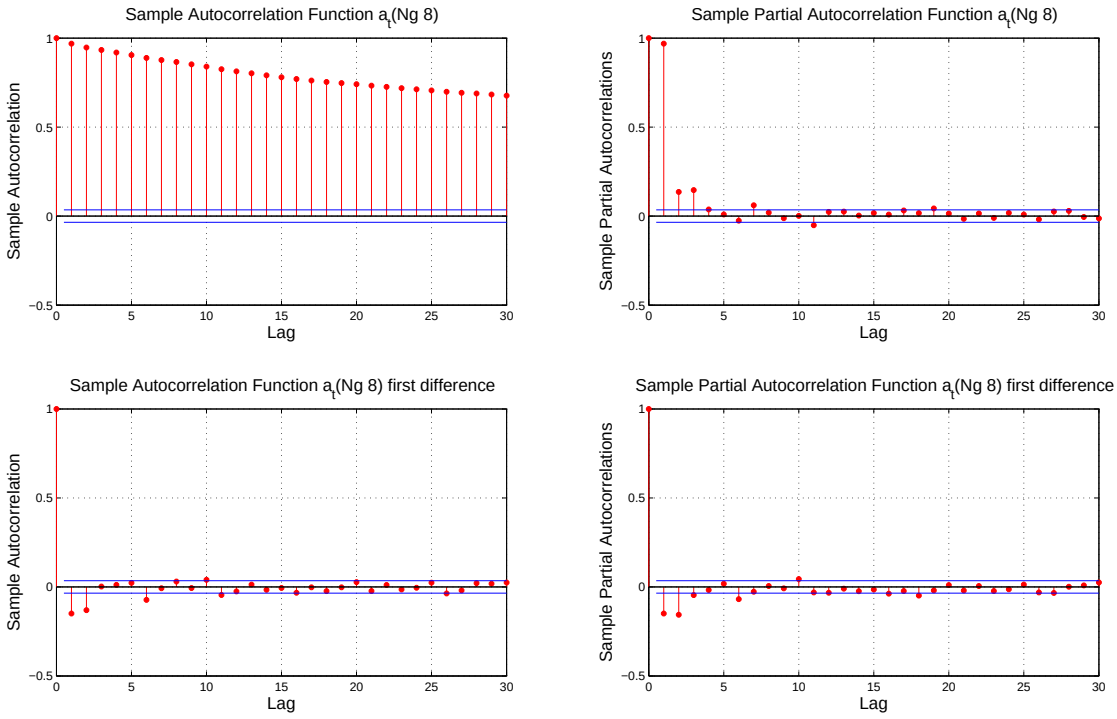

Figure 3.12: Autocorrelation and Partial autocorrelation function for the a_t(Ng 8) time series and its first difference series

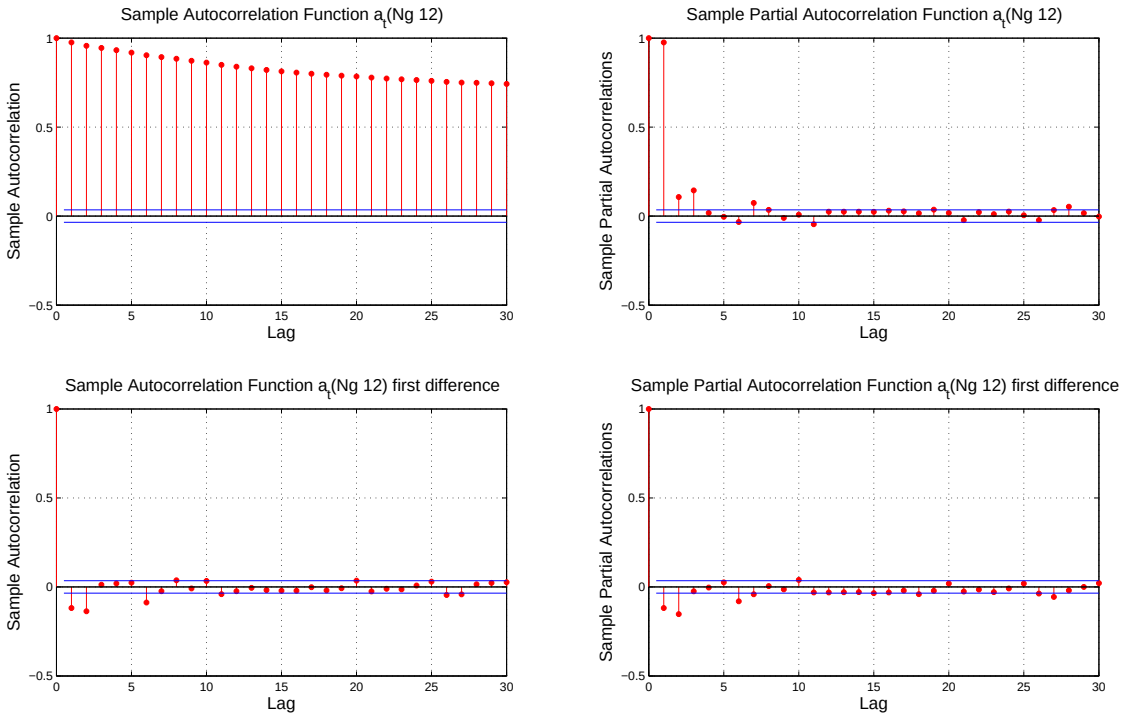

Figure 3.13: Autocorrelation and Partial autocorrelation function for the a_t(Ng 12) time series and its first difference series

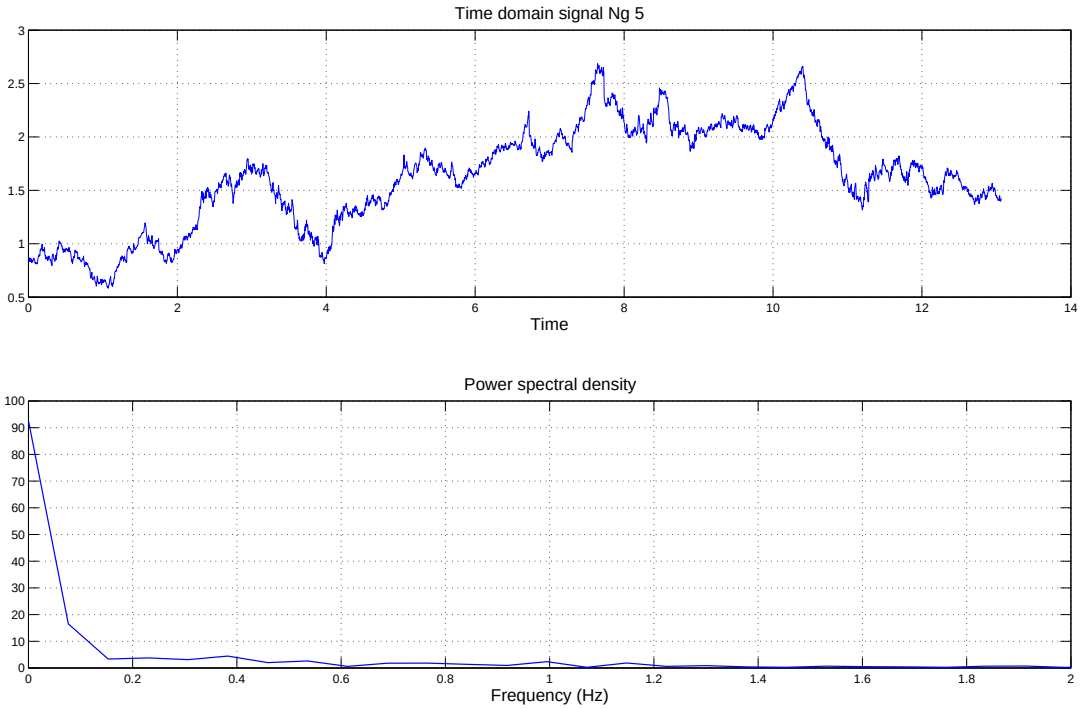

Figure 3.14: Log(Ng 5) Spectral Density

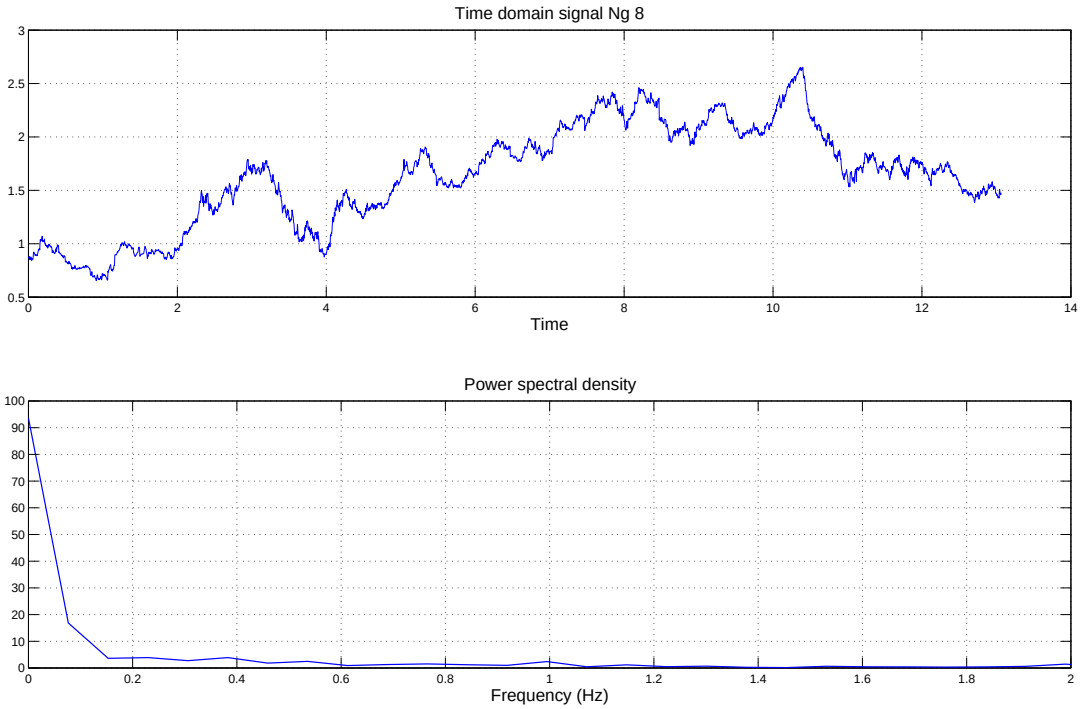

Figure 3.15: Log(Ng 8) Spectral Density

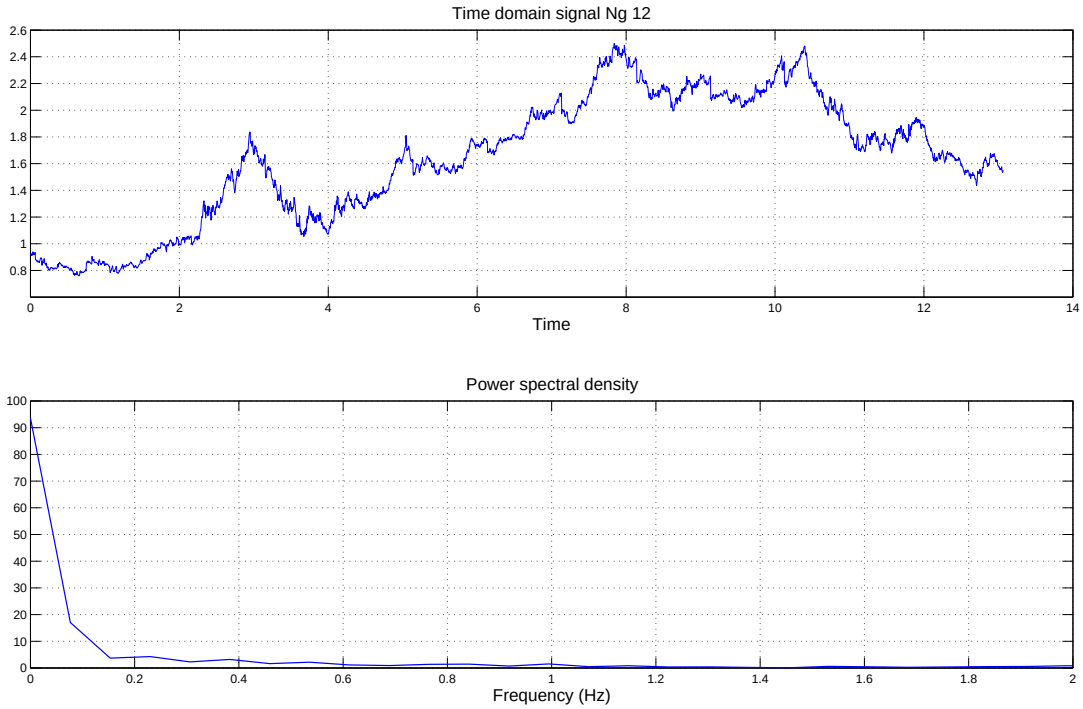

Figure 3.16: Log(Ng 12) Spectral Density

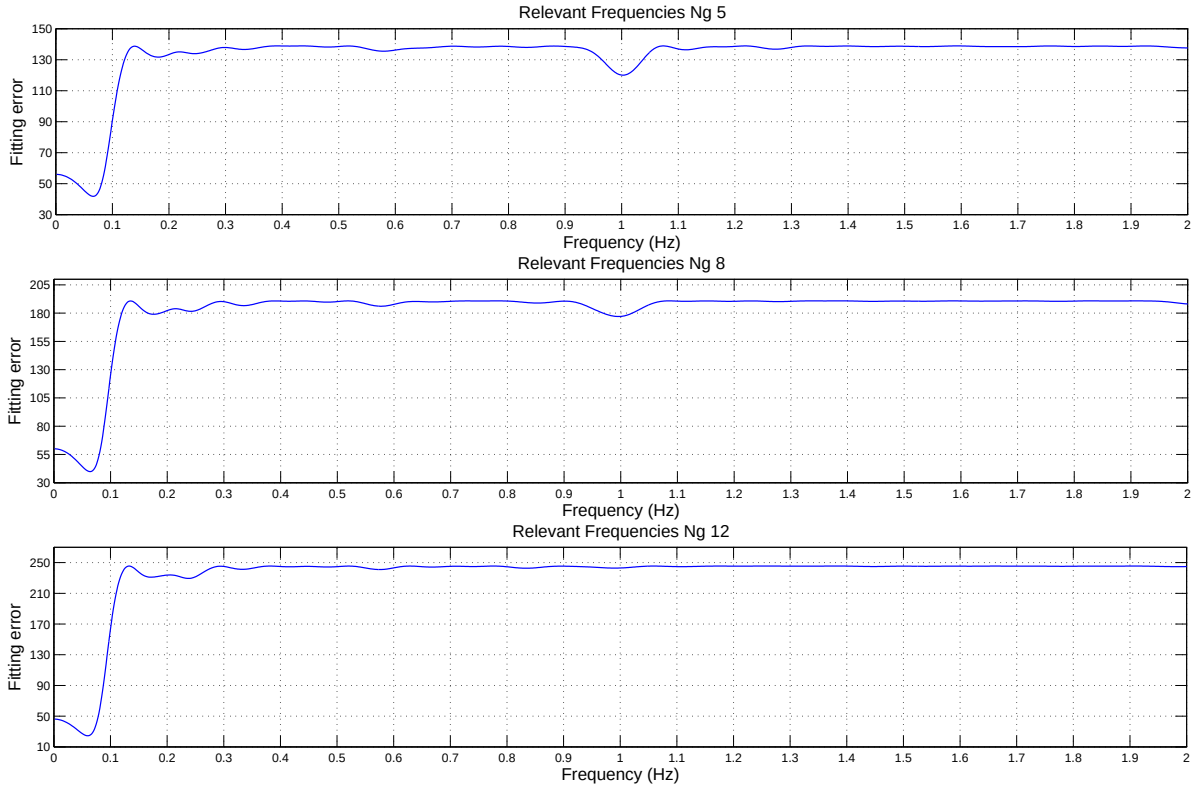

Figure 3.17: Residual sum of squares for log futures prices estimating model 3 for a fixed frequency, indicated in the horizontal axis

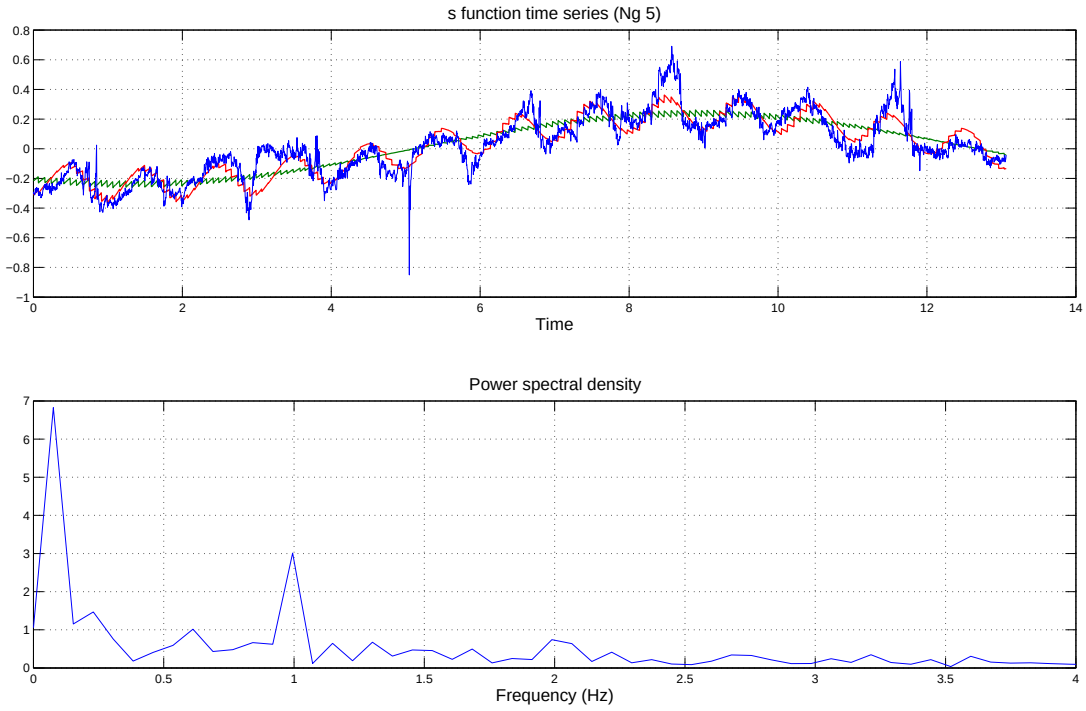

Figure 3.18: Spectral density for the $\hat{s}$ -function corresponding to Ng 5 futures contract. The green line in the first graph shows how one term in Fourier expansion fits the s-function. Similarly, the red line in the first graph shows how two term in Fourier expansion fits the s-function.

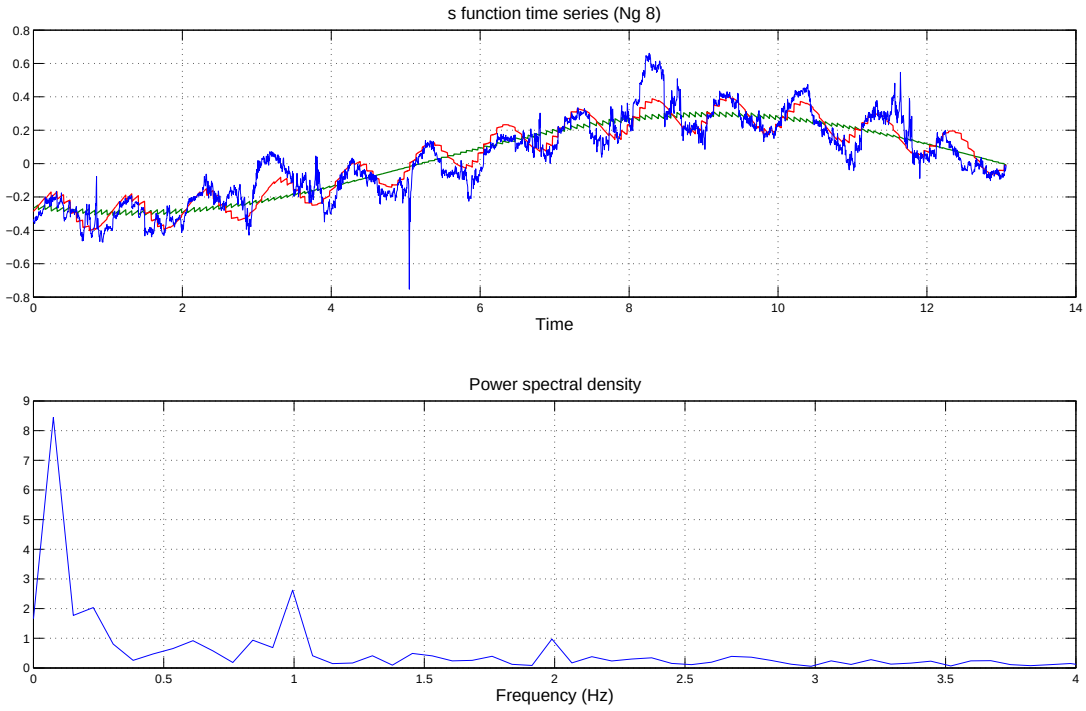

Figure 3.19: Spectral density for the $\hat{s}$ -function corresponding to Ng 8 futures contract. The green line in the first graph shows how one term in Fourier expansion fits the s-function. Similarly, the red line in the first graph shows how two term in Fourier expansion fits the s-function.

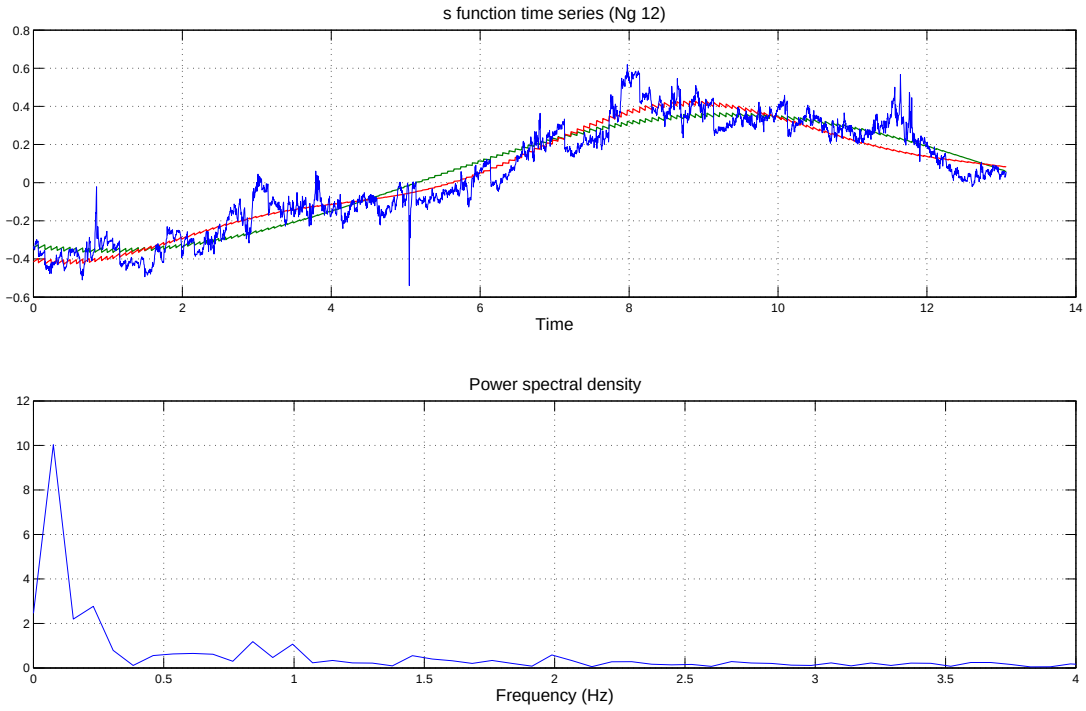

Figure 3.20: Spectral density for the $\hat{s}$ -function corresponding to Ng 12 futures contract. The green line in the first graph shows how one term in Fourier expansion fits the s-function. Similarly, the red line in the first graph shows how two term in Fourier expansion fits the s-function.

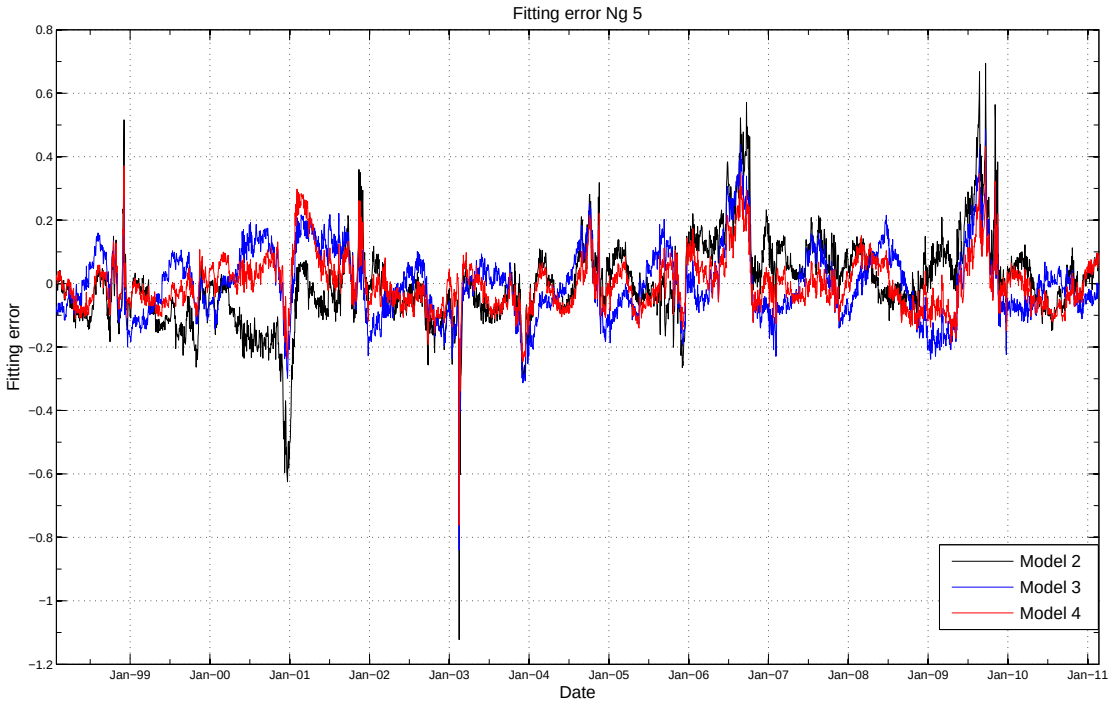

Figure 3.21: Fitting errors from Models 2, 3 and 4 for Ng 5 futures prices

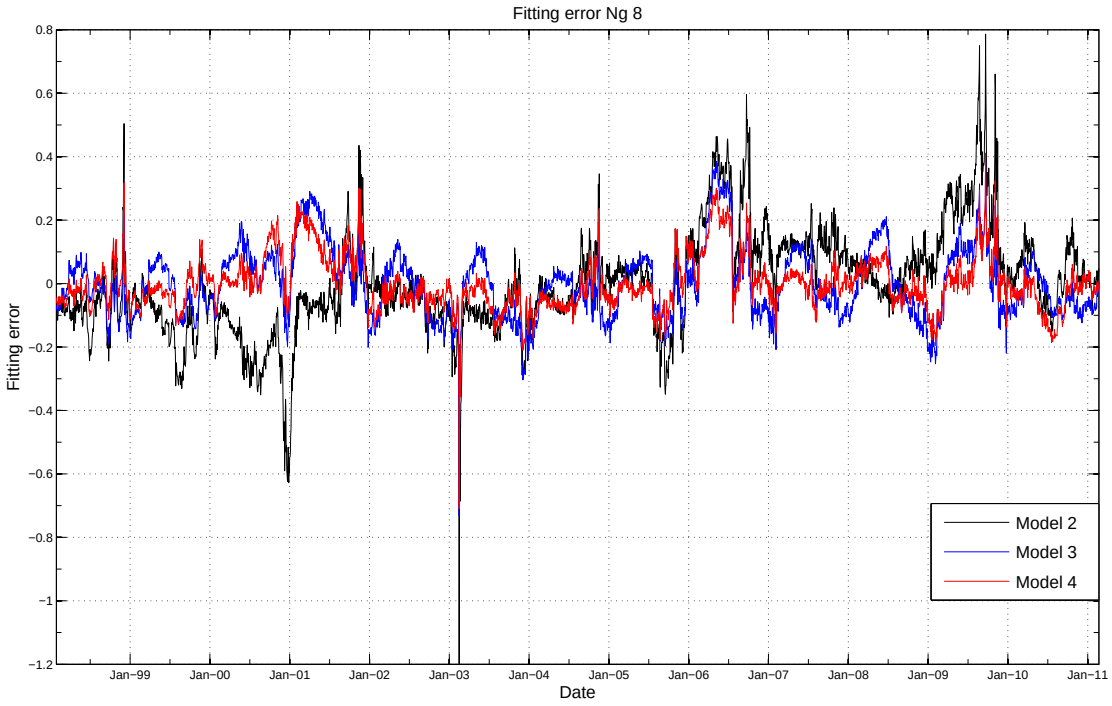

Figure 3.22: Fitting errors from Models 2, 3 and 4 for Ng 8 futures prices

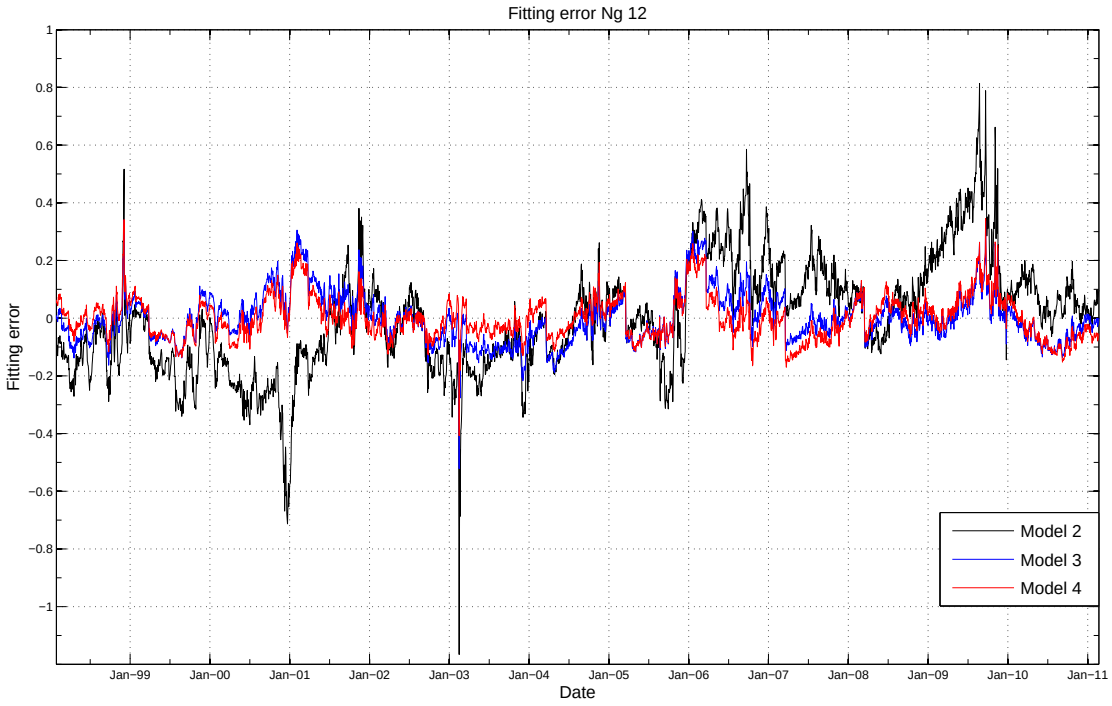

Figure 3.23: Fitting errors from Models 2, 3 and 4 for Ng 12 futures prices

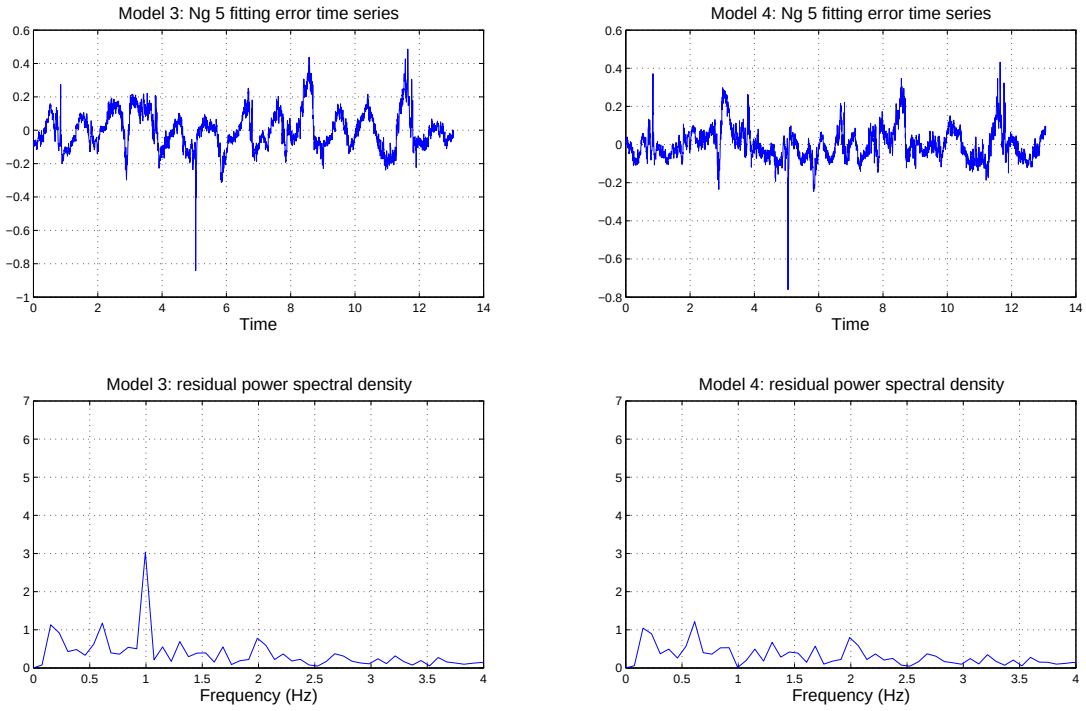

Figure 3.24: Spectral density for fitting errors for the Ng 5 futures prices from models 3 and 4

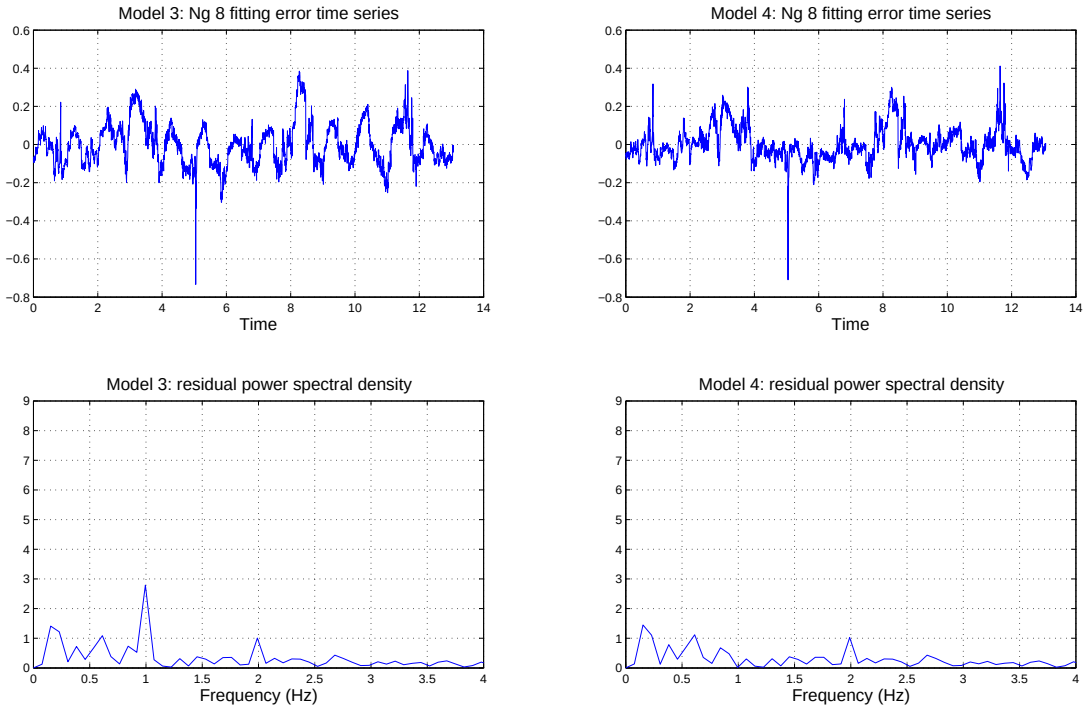

Figure 3.25: Spectral density for fitting errors for the Ng 8 futures prices from models 3 and 4

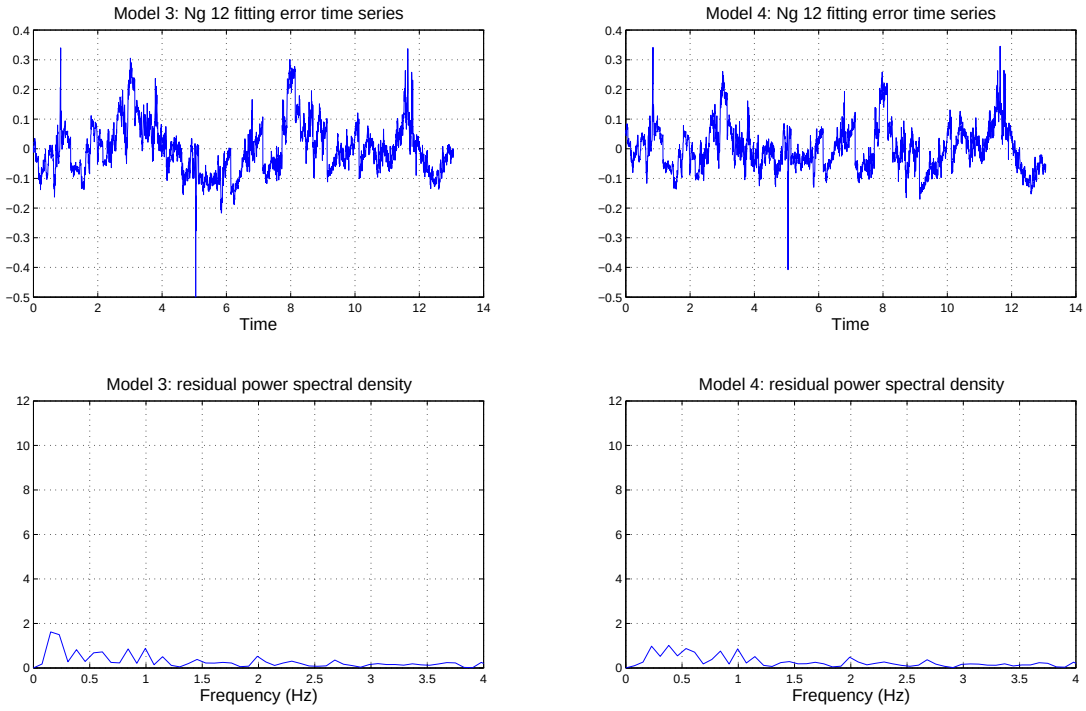

Figure 3.26: Spectral density for fitting errors for the Ng 12 futures prices from models 3 and 4

Bibliography

[1] Burger, M., B. Graeber, and G. Schindlmayr (2007). Managing Energy Risk: An Integrated View on Power and Other Energy Markets. *Finance. Wiley,* 2007.

[2] Carmona, R. and M. Coulon (2013). A Survey of Commodity Markets and Structural Models for Electricity Prices. Proceedings from the special thematic year at the Wolfgang Pauli Institute, Vienna, Editors: F.E. Benth, V. Kholodnyi, P. Laurence (2013).

[3] Cartea, A. and M.G. Figueroa (2005). Pricing in Electricity Markets: a Mean Reverting Jump Diffusion Model with Seasonality, *Applied Mathematical Finance* 12, 313-335.

[4] Clewlow, L. and C. Strickland (2000). Energy Derivatives: Pricing and Risk Management. *Lacima Productions,* 2000.

[5] Eydeland, A. and K. Wolyniec (2003). Energy and Power Risk Management: New Developments in Modeling, Pricing and Hedging. *Finance. Wiley,* 2003.

[6] Forsythe, P. (2007). A semi-lagrangian approach for natural gas valuation and optimal operation. *SIAM Journal on Scientific Computing*, 30:339-368, 2007.

[7] Geman, H. (2005). Commodities and commodity derivatives: Modeling and Pricing of Agriculturals, Metals and Energy. *Finance. Wiley,* 2005.

[8] Gibson, R., and E.S. Schwartz(1990). Stochastic Convenience Yield and the Pricing of Oil Contingent Claims. *The Journal of Finance*, 45:3, 959-976 July 1990.

[9] Lucía, J. and E.S. Schwartz (2002). Electricity prices and power derivatives: Evidence from the nordic power exchange. *Review of Derivatives Research*, 5:1 (2002), pp. 5-50.

[10] Pilipović, D. (1998). Energy Risk, Valuing and Managing Energy Derivatives. *Mc Graw-Hill*, 1998.

[11] Schwartz, E.S. The stochastic behaviour of commodity prices: Implications for valuation and hedging. *The Journal of Finance*, 52:3, 923-973, July 1997.

[12] Schwartz, E.S. and J. Smith (2000), Short-Term Variations and Long-Term Dynamics in Commodity Prices, Management Science 46, 893-911.

[13] Vasicek, O. (1977). An Equilibrium Characterization of the Term Structure. *Journal of Financial Economics*, 5, 2, 177-188.

[14] Weron, R. (2007). Modeling and Forecasting Electricity Loads and Prices: a statistical approach. *Finance. Wiley,* 2007.